Technical Report
TR-20-16
October 2020

Full-scale buffer installation test

Test of the behaviour of a segmented buffer during the installation phase

Matti Nord
Peter Eriksson
Lars-Erik Johannesson
Anni Fritzell

SVENSK KÄRNBRÄNSLEHANTERING AB

SWEDISH NUCLEAR FUEL
AND WASTE MANAGEMENT CO

Box 3091, SE-169 03 Solna
Phone +46 8 459 84 00
skb.se

SVENSK KÄRNBRÄNSLEHANTERING

ISSN 1404-0344
SKB TR-20-16
ID 1898564
October 2020

Full-scale buffer installation test

Test of the behaviour of a segmented buffer during the installation phase

Matti Nord, Peter Eriksson, Lars-Erik Johannesson,
Anni Fritzell

Svensk Kärnbränslehantering AB

Keywords: Segmented buffer, Full-scale test, THM, KBP1018.

A pdf version of this document can be downloaded from www.skb.se.

Abstract

The current reference design of the buffer consists of ring shaped blocks around the canister and cylindrical block below and above the canister. This design makes the block very large and although it has been shown that this type of blocks can be produced with good quality they require a very large press. This large press is expensive due to the large forces it has to handle. To get around this problem, one idea is to divide the block into smaller parts, so called segmented blocks, in order to be able to use smaller standard presses used for example in refractory industry. These smaller presses are also much easier to automate and would therefore reduce the manufacturing cost significantly.

Based on experiences from the production of segmented blocks for this test, the blocks held an overall high quality. They were well within specified height and weight requirements without any need of machining after compaction.

The design with segmented block means that there will be a number of slots in-between the blocks which will affect the transport of water vapour in the system. The current reference design has previous been tested (Luterkort et al. 2017) to find out how the buffer behaves with regards to water redistribution, displacement of the blocks and thermally during the installation phase.

To ensure that the segmented buffer doesn't behave totally different than the reference design, i.e. large ring shaped and cylindrical blocks, a similar test with segmented blocks was needed as well. This report describes the installation and the result from that test. The test was instrumented with approximately 100 temperature sensors and 10 relative humidity (RH) sensors.

The test was running for 90 days with a canister which had a thermal power of 1 700W. After the test period the test was dismantled and water content and density of the buffer were determined. The results suggest that the concept with segmented blocks is viable and that the difference compared to the reference design, i.e. with ring shaped and cylindrical blocks, are small in the overall performance of the buffer. However, more work is needed to better understand the system to be able to set all specifications and tolerances on the manufacturing and installation.

Sammanfattning

Den nuvarande referensutformningen på bufferten består av ringformade block runt kapseln och cylindriska block ovan och under kapseln. Denna design gör att blocken stora och även om det har visats att dessa stora block kan produceras med god kvalitet så erfordras en väldigt stor press. Denna stora press är dyr på grund av de stora krafterna den måste klara av. Ett förslag att undvika denna stora press och istället använda standardpressar från till exempel industrin för eldfast tegel är att dela upp blocken i mindre bitar, så kallade segmenterade block. Dessa mindre pressar är också lättare att automatisera vilket signifikant sänker tillverkningskostnaden.

Baserat på erfarenheter från produktionen av segmenterade block för detta test hade blocken en övergripande hög kvalitet. De låg väl inom specifika krav på höjd och vikt utan bearbetning efter kompaktering.

Designen med segmenterade block har mycket spalter emellan blocken vilket kommer påverka transporten av vattenånga i systemet. Den nuvarande referensutformningen har tidigare testats (Luterkort et al. 2017) för att ta reda på hur bufferten beter sig med hänsyn till omfördelning av vatten, blockrörelser och termiskt under installationsfasen.

För att försäkra sig om att den segmenterade bufferten inte har helt olika beteende den referensdesignen, det vill säga med ringformade och cylindriska block, så behövdes ett test liknande det som gjorts tidigare. I denna rapport beskrivs installationen och resultatet från detta test. Testet var instrumenterat med ca 100 temperaturgivare och 10 givare för relativ fuktighet (RH).

Testet utfördes under 90 dagar med en kapsel som hade en termisk effekt på 1 700W. Efter testperioden bröts testet och vattenkvoter och densiteter bestämdes. Resultatet antyder att konceptet med segmenterade block är gångbart och att skillnaden jämfört med referensutformningen, det vill säga med ringformade och cylindriska block, är små för bufferten som helhet. Dock så behövs mer arbete för att bättre förstå systemet för att kunna sätta korrekta specifikationer och toleranser på tillverkning och installation.

Contents

1 Introduction

1.1 Background

The bentonite buffer is an important part of the solution of storing nuclear waste according to the KBS-3 concept. According to current reference design the buffer consists of large disk- and ring-shaped blocks surrounding the canister with spent fuel. Furthermore, the buffer and the canister with spent fuel are installed in vertical deposition holes.

The reference design makes the blocks very large and although it has been shown that this kind of blocks can be produced with good quality they require a very large press. This large press is expensive due to the large forces it has to handle. In the technical development process for the bentonite buffer, SKB investigates a different type of buffer blocks, so called segmented blocks. By using segmented blocks instead of full-size blocks, the compaction force is reduced which facilitates for smaller and cheaper presses. It would also be possible to increase degree of automation. Furthermore, an added benefit is that losses due to manufacturing or transport damage will be reduced since it is possible to replace individual segmented block that has been damaged, rather than a full disc or a ring. An illustration of full size- and segmented blocks are presented in Figure 1-1.

However, uncertainties were identified linked to the buffer's early THM (Thermal-Hydraulic-Mechanical) development. To reduce these uncertainties a full-scale test with segmented blocks has been performed.

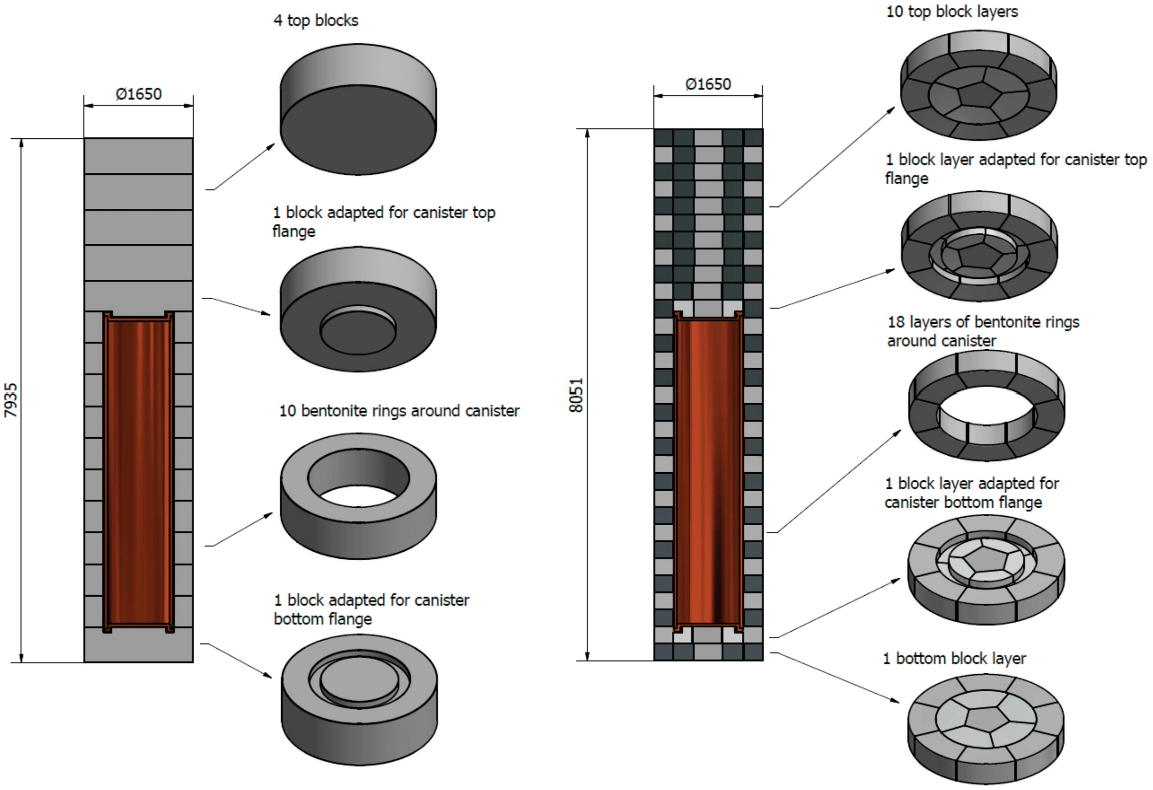

***Figure 1 1.** Left: The reference design consisting of whole blocks. Right: The suggested design with segmented blocks.*

1.2 Purpose of this report

This report presents execution and results from a full-scale test with segmented buffer blocks performed during the winter 2019/2020 at Äspö Hard Rock Laboratory. The report will be used as reference for the basis of a decision if SKB should change current reference design to involve segmented blocks. In that context, the report must present conclusions regarding the performance of the segmented buffer that may influence such decision.

Moreover, the report shall present all necessary information and data regarding the test to allow future re-examination and evaluation of the test results.

1.3 Test objectives

The main purpose of the full-scale experiment was to learn more about different aspects of Thermal Hydraulic and Mechanical (THM) processes during the installation phase. For this reason, a manual installation of the test was done since no installation equipment exists yet. An important aspect was to learn more about the prediction whether the buffer will shrink or expand during the period from the installation of the buffer and canister until it is supported by the backfill.

This new experiment is about installing segmented blocks in a so called “dry” deposition hole. In October 2015 to February 2016, a similar experiment was carried out according to the reference method and data from the two experiments are evaluated and compared in this report.

The analysed data from this experiment will be used to update the early THM models and to get a better understanding of the processes and determine if there are any major differences in behaviour between segmented and solid rings and blocks.

2 Production of segmented blocks and pellets

This chapter describes the results and the experience of designing and manufacturing of segmented bentonite blocks used in the full-scale test.

2.1 The block design

Since SKB never have tested or manufactured segmented blocks there was a need to design these blocks. In this design process both design requirements and a design philosophy were considered. A key aspect for the new block design is that it still must fulfil the same basic design requirements as the reference design with solid blocks and rings.

Basic design requirements

- Nominal diameter of the deposition hole is Ø1 750 mm.
- The outer diameter of the buffer should be Ø1 650. This diameter creates a theoretical gap of 50 mm for buffer pellets between the compacted buffer blocks and the rock wall.
- The inner diameter of buffer rings should be 1 070 mm. This diameter implies that a 10 mm slot is created between the canister and the buffer.
- Installed buffer blocks and pellets should generate a swelling pressure between 3 and 10 MPa.

Design philosophy

- Use as few blocks types as possible.
- Avoid sharp angles.
- It should be possible to use a standard press (16 000 kN, to achieve a maximum compaction pressure of 100 MPa.).
- The block height should be suitable for a standard press. Within this limitation, the size of the individual blocks should be maximized to reduce production time.
- There should be a possibility to overlap gaps between the blocks.
- No machining should be required after compaction, except for the blocks that need to be modified to create space for the top and bottom flanges of the canister.
- The buffer should be homogeneous and generate as equal swelling pressure throughout the whole deposition hole as possible.
- Buffer blocks must have sufficient strength to be handled and installed without the risk of cracking.

2.1.1 Block types

With the given design parameters, the concept for a segmented buffer ended up with a base of three different block types, as illustrated in Figure 2-1:

Because of the shape of the canister and the philosophy to generate the same swelling pressure throughout the whole deposition hole there are variations of type I and II blocks.

Type I_1: Outer block, around the canister. These blocks are of a higher density than the rest of the blocks. The philosophy behind this is further explained in Section 2.2.1.

Type I_2: Outer block, placed together with type $II_{1\ \mathrm{or}\ 2}$ and a type III to make a full block layer.

Type II_1: Inner ring.

Type II_2: Inner ring with a machined slot for the canister flange, illustrated in Figure 2-2. These blocks are placed together with block type I_2 and III to create the layers towards the bottom and the top of the canister.

Type III: Centre block.

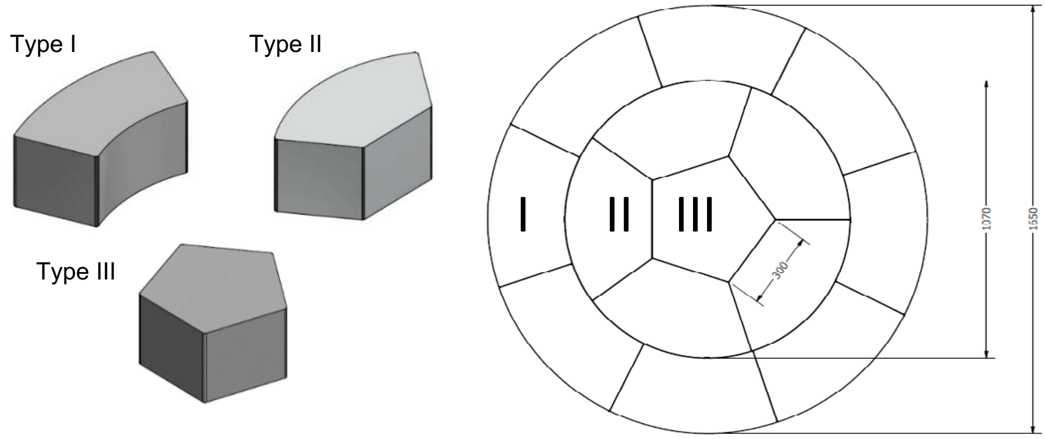

Figure 2-1. Type I Outer block, Type II Inner block and Type III Centre block.

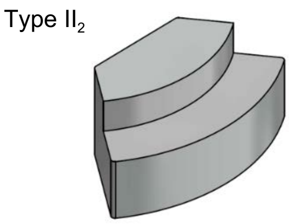

Figure 2-2. Machined slot for canister in type II block.

2.2 Material

The blocks were made from a bentonite branded in Europe under the name BARA-KADE 1002, the material has been analysed by SKB in Svensson et al. (2019). This is a natural sodium dominated bentonite from the United States (Wyoming). All the bentonite was first delivered to Äspö, where it was tested, and prepared. The bentonite was mixed with water to achieve a water content of about 17%, before it was sent to Höganäs Borgestad AB for manufacturing of the blocks.

2.2.1 Block density and water content

In the design process, the chosen buffer density shall meet a swelling pressure requirement of between 3 and 10 MPa. This design is based on small-scale compaction experiments and conducted swelling pressure measurements on the material (Kronberg et al. 2020).

Since BARA-KADE is a Wyoming bentonite similar to MX-80 the density design made on the reference design material is also used in this test (Svensson et al. 2019).

In order to get similar densities in all part of the buffer after saturation, the blocks in the ring sections around the canister must be compacted to a higher density compared to the blocks placed above and under the canister.

According to calculations made on MX-80 for the reference design, the dry density of the rings has been set to 1 735 kg/m^3 and the dry density of the solid blocks has been set to 1 700 kg/m^3. This assumes that the density of the pellet gap is 1 000 kg/m^3. Performed tests in full-scale indicate that this assumption is reasonable.

When installing segmented blocks, the amount of gaps has been estimated to be 0.8% of the buffer volume. To simplify and setting a conservative estimation for this test, 1% is used in the design. To compensate for the gaps in a conservative way, the density of the segmented blocks are increased by 1 %. The target dry density of the different blocks used in this test is presented in Table 2-1. However, as the amount of gaps is uncertain, the requirement on the achieved density is not considered to be a crucial aspect of the test. More important in this test is to have stricter requirements on dimensions than on dry density. The block tolerances are presented in Section 2.3.

It was decided to use a water content of 17% based on experiences from MX-80 which is similar to the type of bentonite used here (BARA-KADE 1002) (Kronberg et al. 2020).

Table 2-1. Recommended dry density of segmented blocks.

Type of blocks	Water content (%)	Dry density (kg/m^3)
Ring blocks around canister	17	1 752
Full block layers above and underneath the canister	17	1 717

2.3 Block tolerances

To achieve a homogeneous buffer that also is robust to install there are two parameters that are extra important in the quality control, the height and the weight of the blocks.

The given tolerances are:

- All block should have a height of 250 ±1.5 mm.
- This tolerance is critical for the installation process. The rather wide tolerance is set by the fact that the blocks should not be machined after compaction, meaning that this tolerance should cover all deviations in height including block expansion.
- Dry density tolerance was set to ± 50 kg/m^3 and given the press area for the type I and II mould the target weight for each block type was:
- Type I_1:78.05 ± 2.23 kg
- Type I_2:76.49 ± 2.23 kg
- Type $II_{1 \text{ and } 2}$: 72.53 ± 2.11 kg (before machining of Type II_2)

2.4 Construction and manufacturing of mould

Höganäs Borgestad AB designed press moulds for producing segmented blocks which were adapted to one of their hydraulic presses. In an early stage it was decided that only moulds for block type I and II should be constructed due to that very few blocks of type III were needed for the test. In the full-scale installation test, block type III was produced by cutting pieces from two pressed type II blocks as can be seen in Figure 3-7.

The manufacturing of the moulds was performed by Maskinteknik i Oskarshamn AB. Figure 2-3 shows a 3D layout of one of the moulds and manufactured inserts for both type I and type II blocks.

Before shipment from Maskinteknik i Oskarshamn AB, the moulds were inspected towards the manufacturing drawings. All manufacturing specifications given by the drawings such as dimensions, hardness of components, surface finish etc. was according to specifications.

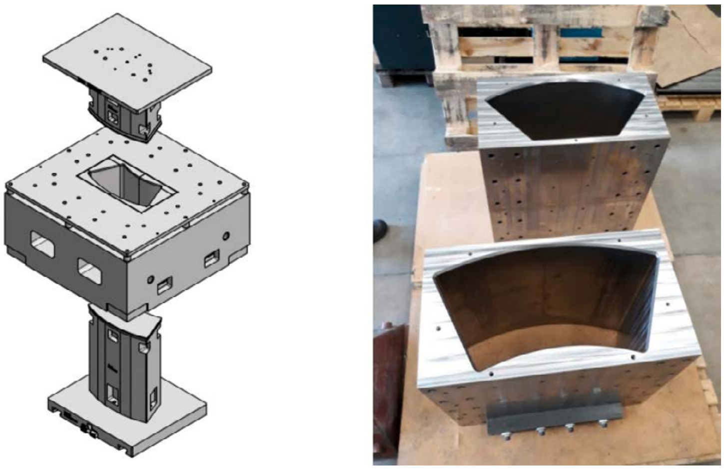

Figure 2-3. Left: 3-D model of mould for outer segments. Right: Picture from manufacturing.

2.5 Production of blocks

A total of 398 blocks, of satisfactory quality, were manufactured of the period of 6 days in June and July 2019 at Höganäs Borgestad AB.

June 25th: 91 blocks
June 26th: 53 blocks
June 27th: 84 blocks
June 28th: 48 blocks
3rd July: 48 blocks
4th July: 74 blocks

The actual compaction time for one block is fairly short, around 2 minutes. If including preparations and post press activities the time for each block increases. Furthermore, with regular cleaning of the form, as the bentonite sticks to it, the average production rate was about 8 blocks/hour.

The press

The press used was a 1 600 metric ton SACMI press, illustrated in Figure 2-4.

Block handling

As the blocks are smaller than the full-size reference blocks, the segmented blocks can be handled by an industrial robot (see Figure 2-4). The robot grabs the block from the press and places it on a scale to check the weight of each block. After the weight control the robot stacks the block on a Euro-pallet (EU standard size).

Each pallet house 6 blocks that are stacked in two layers separated with Styrofoam as protection. The block stack was then sealed with two layers of a transparent plastic film, illustrated in Figure 2-5.

Figure 2-4. *The industrial robot grabbing a finished block from the SACMI press.*

Figure 2-5. *Left: First layer of blocks on a Euro-pallet. Right: Pallet with 6 blocks separated with Styrofoam.*

2.6 Quality control

2.6.1 Hydraulic pressure and filling height

To achieve the right density of the blocks, the weight and height of the blocks must be within the given tolerances described in Section 2–3. At Höganäs Borgestad AB this was achieved by compacting test blocks of the different block types. This was done by adjusting the filling height of the mould and the hydraulic pressure generated during compaction, the desired block height could also be set in the press. By comparing these data towards the actual weight and height of the final products the press could be tuned in for each block type. When these parameters were stable, production began.

During production the filling height, hydraulic pressure and height of each block were monitored and recorded manually. Only minor adjustment of these parameters was necessary during production. Hydraulic pressure and filling height are displayed in Table 2-2.

2.6.2 Weight

After compaction an industrial robot placed the block on the scale, where a person manually recorded the value before the robot placed the block on a Euro-pallet. The average block weights are shown in Table 2-2 and 2-3.

2.6.3 Block height

The final height was recorded for each block during the compaction of the blocks. As an extra measurement, 20% of the produced blocks were checked manually by a digital caliper. The average block heights are displayed in Table 2-2.

Table 2-2. Quality control during manufacturing.

	Type I_1	Type I_2	Type II
Number of blocks produced	180	96	122
Block height, specified value (mm) Average measured by press (mm)	**250±1.5** 249.54	**250±1.5** 249.51	**250±1.5** 249.51
Standard deviation, block height measured in press (mm)	0.14	0.047	0.05
Average height measured with caliper (mm)	249.73	249.72	249.53
Standard deviation, block height measured with caliper (mm)	0.47	0.31	0.25
Block weight, specified value (kg) Average, measured during production (kg)	**78.05±2.2** 78.08	**76.49±2.2** 76.16	**72.53±2.1** 72.63
Standard deviation, block weight (kg)	0.26	0.23	0.41
Dry density, specified value (kg/m^3) Average, calculated from production data (kg/m^3)	**1752±50** 1755.88	**1717±50** 1713.05	**1717±50** 1722.78
Standard deviation, dry density (kg/m^3)	5.49	5.15	9.84
Compaction pressure (average in MPa)	44.83	32.43	34.68
Compaction pressure, standard deviation (MPa)	1.48	1.32	0.87
Filling height in mould (average in mm)	404.83	396.60	396.25
Standard deviation (filling height in mm)	3.47	2.38	2.09

2.7 Conclusions from block production

The blocks held an overall high quality, and were well within the specified requirements presented in Section 2.3:

- The final height of the blocks had a standard deviation of up to 0.47 mm (Table 2-2, block type I_1), all block types had a height tolerance of ±1.5mm which means that this deviation is within tolerance by margin.
- The mass of the blocks had a standard deviation of up to 0.41 kg (block type II). For a type II block with a nominal weight of 72.53 kg this corresponds to a standard deviation in dry density of 9.84 kg/m^3 as presented in Table 2.3. This standard deviation suggests that the requirement of ±50 kg/m^3 can be achieved during production.

The rather small deviation in the values given in Table 2-3 indicates that the material was homogenized well in aspect of water content and granule size.

Results from the block production presented in this report indicate that tolerances for block height and weight could be tightened if necessary.

2.8 Deviations observed during production of blocks

As the blocks were compacted, three main deviations were noted:

1. Contaminations in the bentonite
2. Small, shallow cracks in the finished blocks
3. Material sticking to the press

2.8.1 Contaminations in the bentonite

The delivered bentonite contained various contaminations, usually found as lumps in the big bags the bentonite was delivered in. This interrupted the automated filling of material to the press at Höganäs Borgestad AB and it affected the quality of the compacted blocks. The reason for these lumps was considered to be contamination from a poorly cleaned screw conveyor from which pieces of old bentonite has come loose and has fallen into the mixer at Äspö, see Figure 2-6.

2.8.2 Small cracks

All the blocks manufactured for this study has shown hairline cracks that run horizontally, which are located in the lower half of the block, perpendicular to the direction of compaction, see Figure 2-7. The cracks are thought to be shallow and seem not to affect the mechanical properties of the blocks. A simple test of the strength was made on a block that was discarded. The test was done by using a sledgehammer, trying to see if the micro cracks caused the block to fail along the cracks, this was not the case.

The micro cracks are believed to originate from air trapped in the bentonite which, after the pressure was released, expanded and formed the cracks.

Figure 2-6. *Bentonite lumps found during production.*

Figure 2-7. *Euro-pallet with blocks. Small horizontal cracks can be seen on the lower half of the blocks.*

2.8.3 Material sticking to the press

The bentonite blocks tended to stick to the bottom of the mould. By time the stuck material started to form small "cakes" that created imprints in the shape of pits when compacting new blocks. This meant that the press had to be stopped and cleaned.

The problem seemed to increase when a higher hydraulic pressure is used. At the beginning there was a thin film of bentonite formed on the bottom of the form, this gradually evolved into a larger aggregation in a corner of the form. The "left" corner was the most susceptible corner to form this cake as illustrated in Figure 2-8.

This problem has been observed in previous projects when compaction blocks with other bentonite materials.

2.8.4 Areas of improvement regarding negative deviations

The blocks produced held a high quality, both regarding dimensions and density, but there are improvements to be made regarding the negative deviations found during production.

Contaminations in the bentonite

To avoid this problem the bentonite should be controlled for lumps and other kind of contaminates. This could be achieved by letting the material pass through a sieve before it is used in the press.

Micro cracks

There was micro crack observed in the bottom of the compacted blocks. Even though these are shallow and do not seem to affect the strength of the blocks, these types of visual defects should be avoided if possible since it is difficult to distinguish this type of micro cracks from deeper cracks that could degrade the strength of the blocks. The micro cracks could possibly be avoided if the air in the material is evacuated by a vacuum system during compaction. This type of press was not available at Höganäs Borgestad AB.

Material sticking to the press

The problem with materials sticking to the bottom of the press mould is thought to occur due to one or several issues such as; lumps of wetter bentonite, uneven loads, or poor surface finish on the horizontal compaction plates of the mould. This could potentially be rectified by avoiding contaminations in the bentonite, changing the water content of the material or the compaction force used. If the deviation is caused by poor surface finish on the compaction plates, the solution could be to reducing the adhesiveness of the bentonite to the compaction plates by thoroughly polishing the mould or to plate the metal with a harder metal, such as chrome. Another plausible solution is adding a thin film such as Teflon or similar to the compaction plates to reduce friction and adhesion.

***Figure 2-8.** Bottom mould plate with material that got stuck.*

2.9 Production of pellets

The pellets used for the filling of the outer slot between the buffer blocks and the wall of the deposition hole was manufactured using roller-compaction, in accordance with the reference design, at a test site at Sahut Conreur, La Sentinelle, France. Test equipment was used for the manufacturing and is thus not constructed for full-scale production of bentonite pellets for a repository. However, the judgement is that the performed test production can be scaled up and adapted for a larger production.

For the chosen production technique, i.e. roller compaction, the bentonite is poured into the equipment consisting of two wheels and is compacted to pillow shaped pellets between them, see Figure 2-9.

The bentonite used for the production of the pellets is the same as for the production of the buffer blocks i.e. BARA-KADE with a water content of about 12%. The dimensions of the pellets are 15.8 × 15 × 7 mm. After production, the pellets were tested in the laboratory where the density of the pellets, both individual pellets and the average density of a filling, the strength of the pellets and its water content were determined. This data is reported in detail in Lundgren and Johannesson (2020) and summarized in Table 2-3.

Table 2-3. The pellets used at the large-scale test.

Material	BARA-KADE
Type	Roller compacted
Water content	12%
Density individual pellets*)	2000–2060 kg/m^3
Bulk density*)	1100–1150 kg/m^3

*) In the densities the water is included

Figure 2-9. *The press used for producing pellets, a) the filling of the bentonite between the two wheels and b) the perforating of the wheel filled with compacted bentonite.*

3 Full-scale test

A full-scale test with segmented blocks has been performed at Äspö Hard Rock Laboratory in the deposition hole DD0092G01 (often called the CRT-hole). The test was running for 90 days during October 2019 to January 2020. In this test, a new buffer concept of segmented bentonite blocks was tested. Furthermore, the test was carried out with a pellet-filled outer gap and a heated canister with a thermal power corresponding to the power expected from a canister with spent nuclear fuel, about 1 700 W.

As buffer material, both for the blocks and the pellets, a Wyoming bentonite with the trade name BARA_KADE 1002 was used, see also Section 2.2.

3.1 Test design, instrumentation and basic equipment

3.1.1 Adjustments on the test setup compared with the reference design

The geometry of this test was based on the reference design described in SKB (2010) but there were some modifications, for example, in this test the concept with segmented blocks was installed by SKB for the first time.

Below the most important differences between the reference design and the design used in this test with segmented block, see Figure 1-1, are listed:

- The test hole at Äspö is 8 624 mm deep. To fill up the extra space 4 extra layers were installed, making it a total of 14 block layers above the canister.
- The average diameter of the selected deposition hole is 1 762 m. This causes the pellet-filled outer gap to be nominally 6 mm wider than the reference design.
- The test deposition hole lacks the bevel in the upper part.
- The canister has an extra lid on the top of the canister that protects the heater cables. This means that the canister in the experiment is about 150 mm higher than the reference design. This also means that the buffer blocks around the canister are correspondingly 150 mm higher to match the height of the canister.

3.1.2 Layout and coordinate system for installed blocks, sensor and sampling

For the positions of the various instruments to be traceable in the buffer a layout and marking system for segmented blocks has been introduced for this test, illustrated in Figure 3-1. The full bentonite layers underneath and above the canister are referred to as C blocks and block layers around the canister (ring segments) are referred to as R blocks. For example: first layer that was installed in the bottom of the deposition hole was C1. The individual blocks of layer C1 are marked as in Figure 3-1 (right).

Also, a coordinate system for the deposition hole has been developed at Äspö and used in many full-scale tests during the years. The layout and the coordinate system are also used when placing the outer blocks and determining positions for the different samples taken from the buffer. The inner- and centre blocks are placed at random directions but always so that gaps between different block layers were avoided. Each position in the buffer can be determined by three coordinates as illustrated in Figure 3-2:

1. r-coordinates determine the horizontal distance from the centre of the deposition hole.
2. z-coordinates determine at what height from the bottom of the deposition hole the position is located.
3. α-coordinates determine the angle from the horizontal direction A (0° = end of the tunnel).

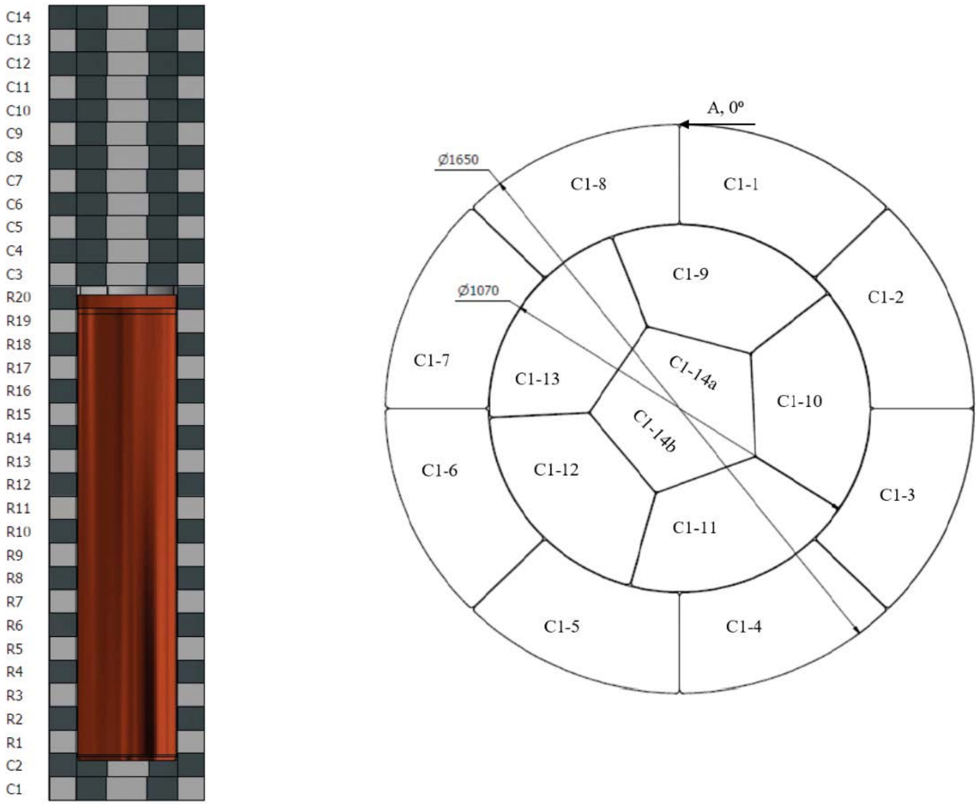

Figure 3-1. *left) Block layer layout, right) Example of numbering of individual blocks in one block layer.*

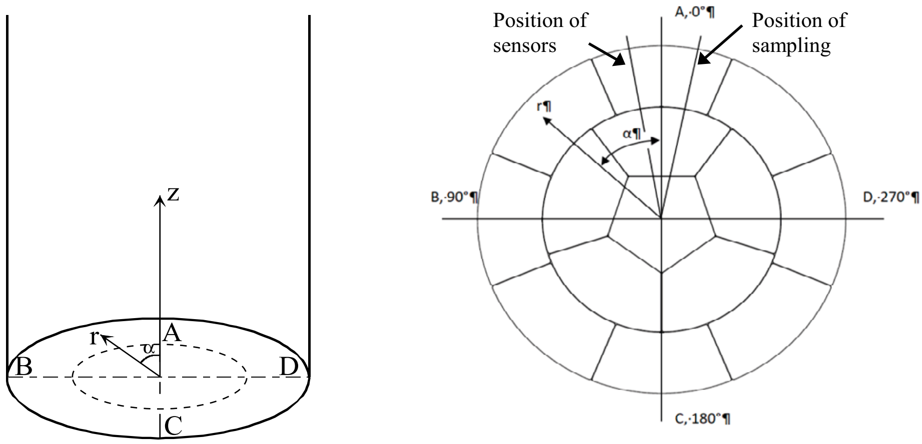

Figure 3-2. *Coordinate system used when describing the positions of the installed sensors or samples. A, 0 degrees are pointing towards the end of the tunnel and C, 180 degrees towards the tunnel mouth.*

3.1.3 Instrumentation and monitoring of the test

The installation of the sensors was adapted so that no sensors were installed in or near gaps between the segmented blocks. It was also important to avoid sections with sensors at the sampling of the buffer after the test. Since the outer ring segments are placed in a "brick wall pattern" and each block covers 45°, there are gaps in every 22.5° if looking axially through the entire buffer. The same principle applies to sampling. Therefore, the sensors are placed theoretically 11.25° counter clockwise the directions of A, B, C and D and the sampling is made in 11.25° clockwise A, B, C and D, see Appendix 1 and Figure 3-2.

About 100 temperature sensors and10 humidity-sensors (RH-sensors) were installed in the buffer, on the canister surface and in the surrounding rock. Positions for the sensors are displayed in Appendix 1.

The RH sensors were much larger than the thermocouples, which gives a great risk of condensation if placed incorrectly. All sensors were therefore installed in the blocks by making groves with the same dimensions as the sensor. In some cases, the tip of the transducer, in which the electronics for the measurement of RH is placed, was directed towards the outer pellet-filled gap. The cables for both the RH sensors and the heaters are routed according to the same principle as the thermal sensors in the buffer, through the buffer blocks and along the outside of the buffer stack.

Some of the installed buffer blocks did not contain any sensors at all, so that any influence of the installed sensors on the test results can be studied. All machining of the buffer blocks needed to be able to install sensors and pull cables from them as well as cables from the heaters in the canister was done when the buffer blocks were in place in the deposition hole. This was done to minimize the risk of losing a block when handling them. In order to make an assessment of the size of movements, measurements of the vertical position of the buffer blocks and the canister were made both during installation and during dismantling. During the course of the experiment, the displacements of the upper surface of the top layer of blocks was measured at least twice a week. The first week measurements were made every weekday.

These measurements were given by comparing the difference in height between a fix point in the tunnel wall next to the test and the height of installed blocks, using a levelling instrument and a measuring rod.

3.2 Basic equipment

All practical work was done manually using basic equipment, listed in Table 3-1.

Table 3-1. List of basic equipment used during the test.

Type of equipment	Function
Lift basket for segmented buffer blocks	The basket is operated by an electrical telpher. It is used to lift the blocks into the deposition hole. The lift basket is designed to be able to lift 4 blocks at a time. (New equipment for this test)
Vacuum lifting tool for segmented buffer blocks	Lift single buffer blocks. The tool is mainly used to lift the blocks from the lift basket and fine position them when stacking the buffer. (New equipment for this test)
Scale	For measuring the weight of each block before installation.
Caliper	For measuring the height of each block before installation.
Levelling instrument.	Measurement of the height of every other block layer.
Vertical guide lasers	Three self-levelling vertical point lasers were installed on aluminium arms at the top of the deposition hole as a guide when stacking blocks. (New equipment for this test)
Lift basket for personal lift	The basket is used to transport staff down into the deposition hole. The basket has a diameter smaller than the inner diameter of the outer block ring so it can be used to transport people and equipment down into the deposition hole even when the outer block rings are in place. (Existing equipment)
Gantry crane incl. telpher	Crane on wheels that can be rolled over the hole. Mainly used for the lift basket. (Existing equipment)
Personal lifting system with harness	Health and security were an important factor when planning the full-scale test. There was extra focus on risks of fall injuries associated with manual work in the deposition hole. To prevent this risk a flexible system for personal lifting was implemented. The system consisted of a swivel telpher beam mounted at the tunnel floor next to the deposition hole, a telpher approved for personal lifting and a harness allowing the worker to travel up and down the 8.6 m deep deposition hole while still being able to work without detaching the harness. For the system to be approved the harness must be connected to a second safety function in form of a fall arrest block. The arrest block was fastened in an approved lifting eye in the tunnel ceiling. Before use, the complete lifting system were inspected and approved by an external authorised company.
Heated canister	The canister is designed to deliver the same power as a real canister filled with nuclear waste. The heat from the canister is an important parameter to get an as realistic (according to the actual situation in the spent fuel repository) test as possible. The canister had earlier been used as a heater in other tests. To reduce the risk of malfunctioning, all heat elements were replaced. The canister has four heaters installed with a total power of 4000 watts. To simulate the heat generated from one canister 1700–1750 watts is used during the test.
Deposition Machine	The machine is used to place the canister in the deposition hole. The machine is transported to a position above the deposition hole using the Liftec-trailer. (Existing equipment)
Liftec-trailer	Used when transporting the Deposition Machine. (Existing equipment)
Sensors with associated measuring equipment	Over 100 temperature sensors and 10 were installed to monitor the test during 90 days of operation time. About 15 RH sensors are installed to monitor the installation and operation time The canister is equipped with power monitoring (Mainly existing equipment, sensors supplemented if necessary)

3.3 Preparations at test site before installation

Before installation there were some activities related to the test hole. For example: gathering data of the test hole, doing new measurements of water inflow and preparing installation equipment.

3.3.1 Characterization of the deposition hole

A characterization of the deposition hole has been made after it was drilled. This work is reported in Hardenby (2002). The mapping shows that there are some cracks near the tunnel floor.

3.3.2 Geometry of the deposition hole

Measurement of the deposition hole diameter was made shortly after the hole was drilled (Andersson and Johansson 2002). The average diameter of the deposition hole was determined to be 1 762 m.

Since this test hole has been used in several tests and there has been modifications made to the bottom plate it was decided to do a new depth measurement of the hole. The tunnel floor is not perfectly horizontal but the average depth between the tunnel floor and the bottom plate is 8 624 mm.

3.3.3 Natural water inflow

It was decided that the test should be performed with only natural water inflow. The inflow was measured for 30th days before the installation started, the average water inflow during this period was 8.8E−04 litres per minute (1.27 litres per day).

To see if there had been any big changes of water inflow during the operation phase, a new measurement for 36th days was done after dismantling the test and the average water inflow during this period was 7.2E−04 litres per minute (1.03 litres per day).

Historical inflow is presented in Table 3-2.

Table 3-2. Measured water inflow to deposition hole CRT.

	Uppmätta inflöden (l/min)		
	2002	**2015**	**2018**
CRT **DD0092G01**	2.05E−4	8.3E−04	8.8E−04

3.3.4 Checking the bottom levelling of the deposition hole

To be able to install a straight block stack, the bottom plate of the deposition hole needs to be flat and horizontal. Before installation the bottom was measured to be within 1–2 mm of the horizontal plane and the surface was approved for installation without any further action.

3.3.5 Protecting the buffer during installation

Since there is a natural inflow of water from the rock into the deposition hole the humidity (RH) can reach 100 % in the bottom of the hole. Such high humidity would damage the installed bentonite blocks. In the final repository for spent fuel, there will be a bottom plate made of copper protecting the bottom buffer blocks. In this test, a plate made of aluminum was used instead. Aluminum will not be allowed in the final repository due to corrosion but since the test period was only 90 days, this does not affect the results. During the initial phase of the installation, a plastic sheet shaped as a tube was attached to the aluminium plate, illustrated in Figure 3-3. This type of plastic cover has been successfully used before, for example in Luterkort et al. (2017), and the purpose is to prevent water to reach and thereby damage the buffer during installation. The plastic cover is attached with a release system that allows for removing the plastic from the surface.

Inflowing water was collected in the bottom of the hole between the plastic cover and the rock and is pumped out through a preinstalled hose. (The hose can be seen in the right bottom corner in Figure 3-3).

Figure 3-3. *Plastic tube attached to the aluminium plate in the bottom of the test hole.*

3.3.6 Installing extra pump in the upper part of the test hole

In the top of the test hole there are vertical slots that have been used in previous tests. Some of these slots tend to lead water and are therefore sealed with sheet metal and sealing foam to prevent water to enter the test. The slots can be seen in Figure 3-12 (b) below. It was decided to install an extra pump to collect the water from these sealed slots.

3.3.7 Vertical guide lasers

Three self-levelling vertical point lasers were installed on aluminium arms at the top of the deposition hole as a guide when stacking blocks, illustrated in Figure 3-4. The lasers served as a vertical reference by pointing on the top surface of every installed block layer. During installation the blocks were adjusted when placed by keeping the same distance between the laser dots and the inner radius of the outer ring blocks. The aluminium arms could be moved to the side to clear the hole when needed.

Besides these lasers, conventional measuring equipment was used, such as spirit-level and scale.

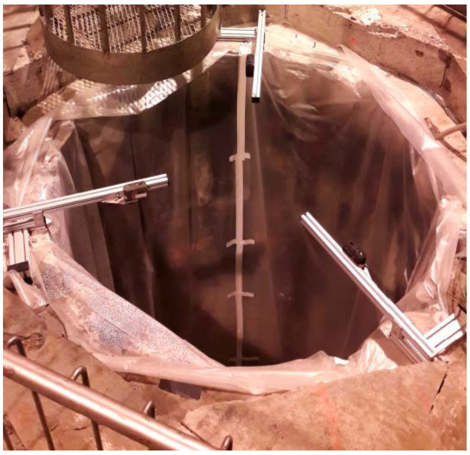

Figure 3-4. *Vertical guide lasers mounted on aluminium arms.*

3.4 Installation

The installation, starting with placing first bottom block until turning on the canister heaters, were performed in 31 calendar days from 2019-09-17 to 2020-10-18. The majority of the work was performed by two persons during normal working hours Monday to Friday.

The main sequences of the installation are presented below.

2019-09-17 – 2019-09-19. Xx Installation of bottom blocks, C1 and C2

The installation began by placing layer C1 in the centre of the hole. The first layer was placed with one joint between two blocks facing straight downstream the tunnel towards the "A" direction illustrated in Figure 3-2. The blocks were stacked with a brickwork pattern, illustrated in Figure 3-5. As seen in Figure 3-6 there was a gap between the centre block halves that was cut by hand. These joints were left as they were and the judgement was that they would not influence the test results. If segmented blocks are to be used in the final repository for spent fuel the centre block is manufactured in one piece and there will be no big gap between the blocks.

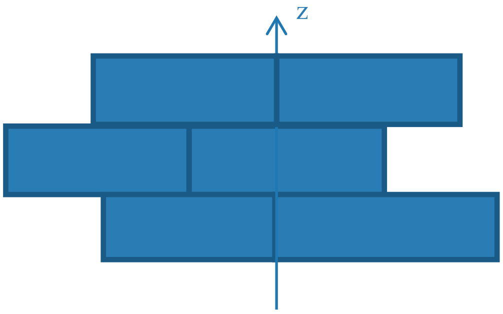

Figure 3-5. *Principle how the block joints are displaced relative each other.*

Figure 3-6. *Installation of bottom layers. Left: layer C1, right: layer C2.*

2019-09-20 Cutting a slot for the canister flange in C2

To make room for the canister bottom flange, a slot was created in bottom layer C2, like the Type II_2 illustrated in Section 2.1.1. In this test the slot was done manually by core drilling. When the cores were removed all surfaces of the slot needed to be smoothened by hand. The canister flange and pictures of the slot are illustrated in Figure 3-7 and 3-8.

2019-09-24 – 2019-10-07 Installation of segmented rings R1–R20

The ring segments were stacked carefully and by using folding rule, spirit-level and the vertical lasers, illustrated in Figure 3-4, it was possible to get a circular and vertical block stack, some pictures from the installation are shown in Figure 3-9.

When stacking the blocks manually there was a tendency that the largest gap between the blocks on every layer was found between the last block stacked and the one placed first.

After installing R1–R20 the gap between every block on every layer were measured by inserting tall metal strips with different thicknesses between the blocks. A measuring interval of 0.5 mm was used, if a metal stripe with thickness 0.5 mm couldn't fit between two blocks the width of the gap were considered as 0 mm, measurements are documented in Appendix 2. This is a rough measuring method but the results can be used as an indication for analysing the THM models used in this test and for indicating an area of improvement when constructing the block handling equipment.

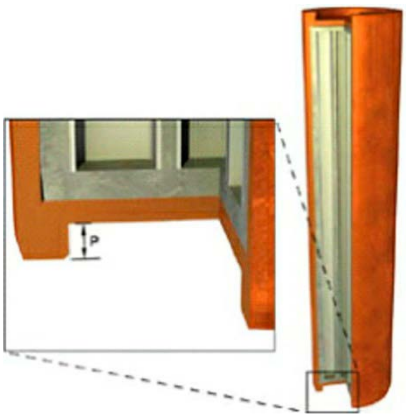

Figure 3-7. *Cross section of canister showing the bottom flange.*

Figure 3-8. *Left: Core drilling of slot in layer C2, right: Finished slot.*

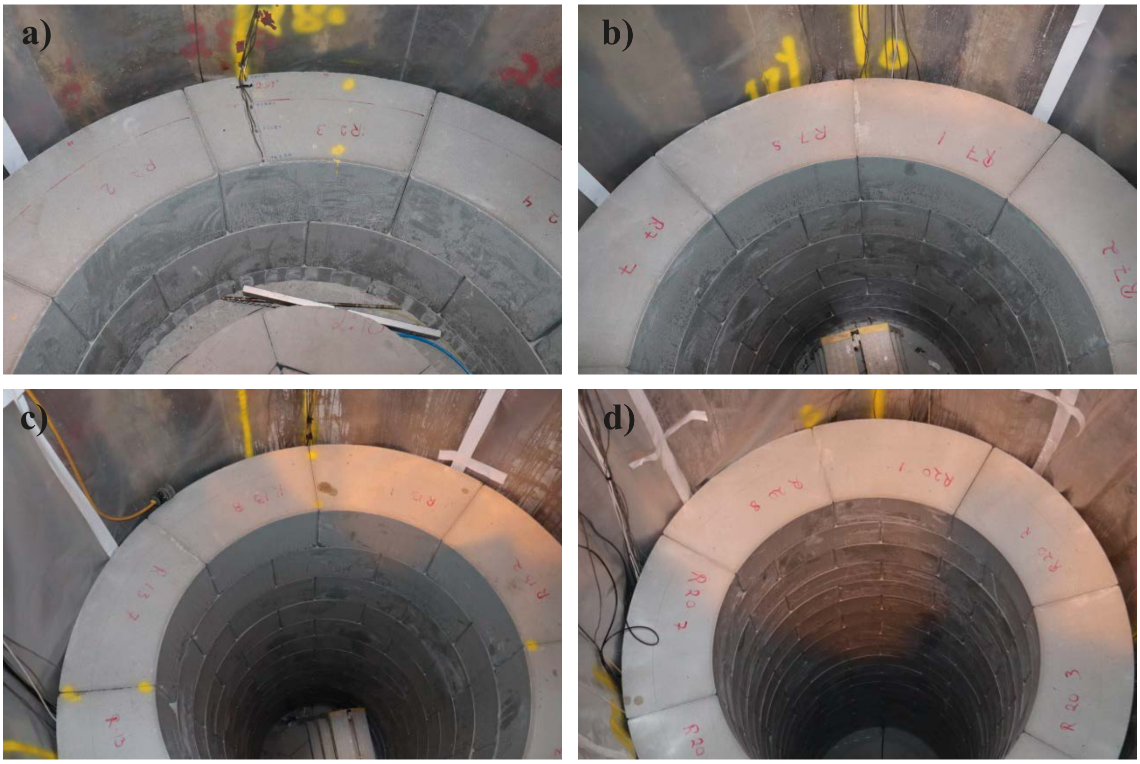

Figure 3-9. *Installation of ring layers . a) R2, b) R7, c) R13, d) R20.*

2020-10-09 Installation of pellets up to R20 before installation of canister

Before installing pellets, the plastic tube was removed. Under ideal conditions the tube should be kept for protecting the blocks until all blocks were placed. However, the risk of touching and thereby moving some blocks when installing the canister was considered too high. Therefore, it was decided to stabilize the block stack by installing pellets up to R20 before installing the canister. Installation of pellets is illustrated in Figure 3-10.

Figure 3-10. *Left: Bag of pellets. Right: Pellets installed up to R20.*

2020-10-09 – 2020-10-10 Installation of canister

A deposition machine loaded with the canister was transported down to the test site and positioned over the deposition hole as can be seen in Figure 3-11. The deposition machine is an early prototype used only for tests like this.

The installation sequence with this prototype machine is a slow process which takes several hours. Figure 3-12 shows two pictures from the installation. During installation there were some problems with a computer box on the deposition machine but these problems were solved in less than half a day. Besides of these problems the installation went as planned.

2019-10-14 Replacement of three blocks from R20

During a weekend there had been a minor leakage of natural water into the upper part of the deposition hole due to failure of the pump described in Section 3.3.6. The leakage had led to that three bentonite blocks from layer R20 had been damaged and had to be replaced together with the surrounding pellets. After having repaired the pump and replaced the blocks and pellets the installation was resumed without any deviations. Removal of damaged blocks is illustrated in Figure 3-13.

2019-10-15 Filling out the centre of R20 above the canister

To fill the gap between the top of the canister and the upper surface of R20, a modified centre layer which consisted of approximately 100 mm high type II and type III blocks were added to R20.

Figure 3-11. *Deposition machine.*

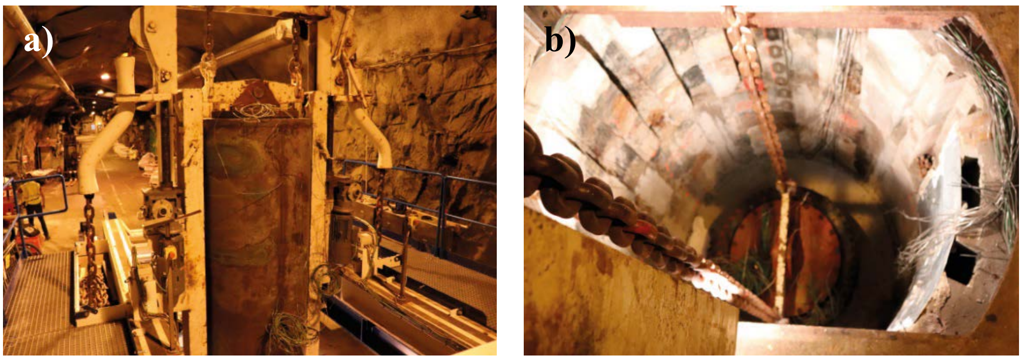

Figure 3-12. *a) Canister in position for installation, b) End of installation.*

***Figure 3-13.** Removal of three damaged bentonite blocks.*

2020-10-16 – 2020-10-17 Installation of top layers C3–C14

The installation of blocks above the canister was carried out without interruption. As described in Section 3.1.1 two extra layers were installed to fill out the space up to the tunnel floor (C13 and C14). At the top of the test hole there is a 250 – 300 mm deep slot. The extra two bentonite layers and the slot are considered not to influence on the result of this test. Figure 3-14 illustrates layer C14 and pellets after finished bentonite installation.

2020-10-18 Protection lid

In the final closure design the installed buffer is protected by temporary lids during the installation phase. The lids will be removed when it is time to install backfill over the deposition holes.

In this test a prototype lid was manufactured. To prevent condensation of water, the lid was manufactured with a sandwich layer consisting of two layers of plywood isolated with 50 mm Styrofoam between them. The lid was perforated with openings that allowed measuring the height of each block in the top layer. This was made with a levelling instrument. The openings in the lid are illustrated in Figure 3-15.

***Figure 3-14.** All blocks, pellets and instrumentation installed.*

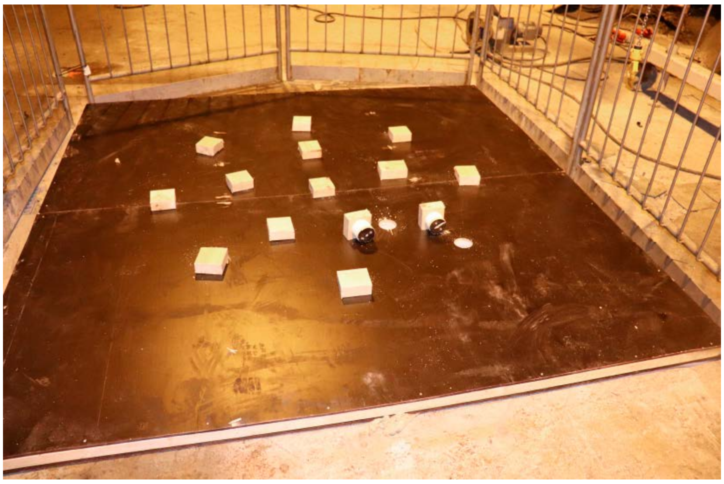

Figure 3-15. *Protective lid with openings for measuring rod.*

2020-10-18 Start of canister heaters

When the installation was finished and the protection lid was in place, the canister heaters were turned on.

3.4.1 Installed weight

The total weight of installed block was 27.386 kg

Total weight of installed blocks, excluding layer C14 was 26 336 kg. The reason for excluding layer C14 from evaluation is explained in Section 3.6.2.

Total weight of installed pellets was 2 680 kg.

3.5 Running of test

This section presents data from the applied heat power, data from installed sensors, both relative humidity sensors and temperature sensors, together with the measured buffer heave. The relative humidity sensors were installed in the buffer while the temperature sensors were installed both in the buffer on the casing surface and in the surrounding rock. Sensor positions are documented in Appendix 1. The test was running for about 90 days and after this period sampling of the buffer took place.

3.5.1 Heating power

The power applied to the heating elements placed in the canister is shown in Figure 3-16. A power of 1 700 W was applied to the heating elements, with small variations, during the whole test period.

3.5.2 Canister and rock temperatures

The temperature measurements made on the canister surface are shown in Figure 3-17. The thermocouples were installed in two directions (B and C) close to the bottom, at mid height and close to the top of the canister. The figure shows that the maximum measured temperature was about 77 °C at mid height of the canister. Furthermore, the maximum temperature at the top and bottom of the canister was about 4 °C lower than the maximum temperature. The temperature on the canister was, as expected, independent of the direction (B and C).

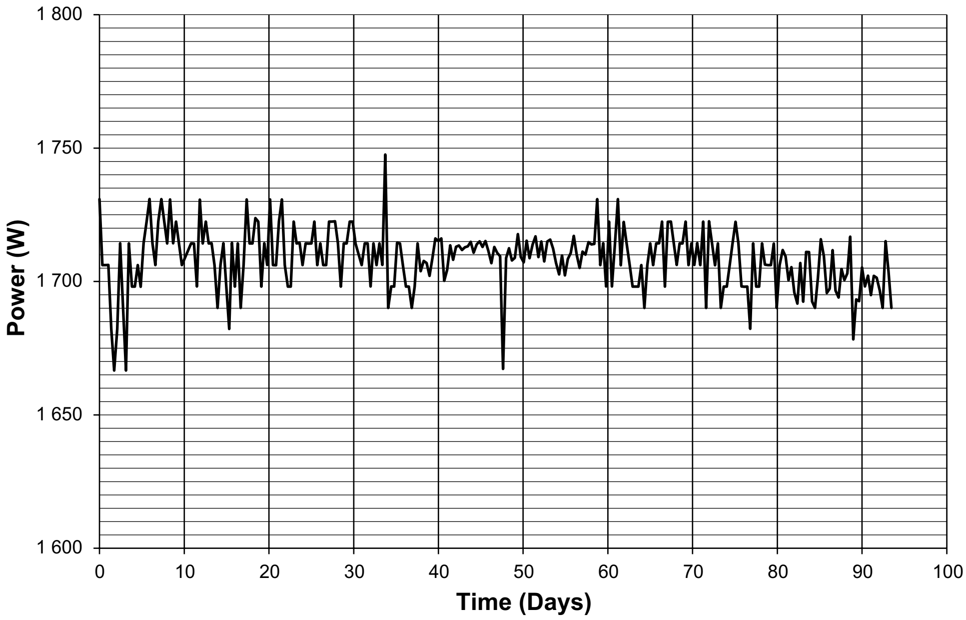

Figure 3-16. *The applied power on the heaters in the canister.*

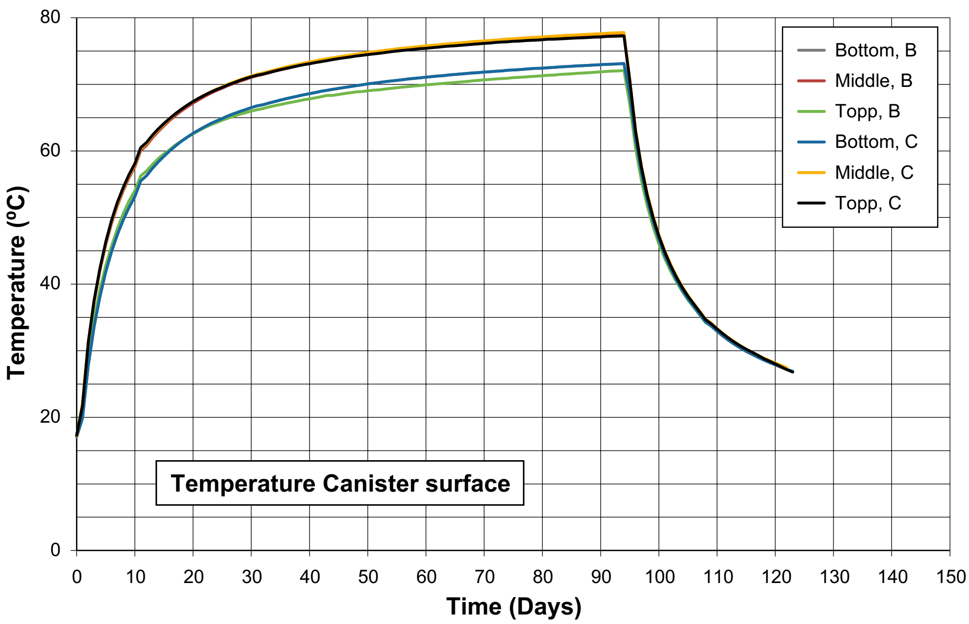

Figure 3-17. *The temperature evolution on the canister surface as function of time. The thermocouples are placed at the bottom, at mid height and at the top of the canister in two directions B and C.*

Also, measurements of the temperature were made in the rock inside the deposition hole. This was done at three levels in the deposition hole, namely 400 mm, 2 900 mm and 4 900 mm from the bottom. The sensors were installed in two directions at each level. Furthermore, sensors were installed about 50 mm into the rock i.e. at a radius of 925 mm and with an installation depth from the surface of 150 mm, corresponding to a radius of 1 025 mm. Data from the measurements at the three levels are presented in Figure 3-18. As expected, the highest temperature was measured the level of 2 900 mm i.e. close to mid height of the canister, while the lowest temperature was measured close to the bottom of the deposition hole, see Figure 3-18. Furthermore, the plots are also indicating that the temperature was higher towards the left wall of the tunnel, i.e. in direction B. The maximum temperature measured on the rock surface was about 42 °C.

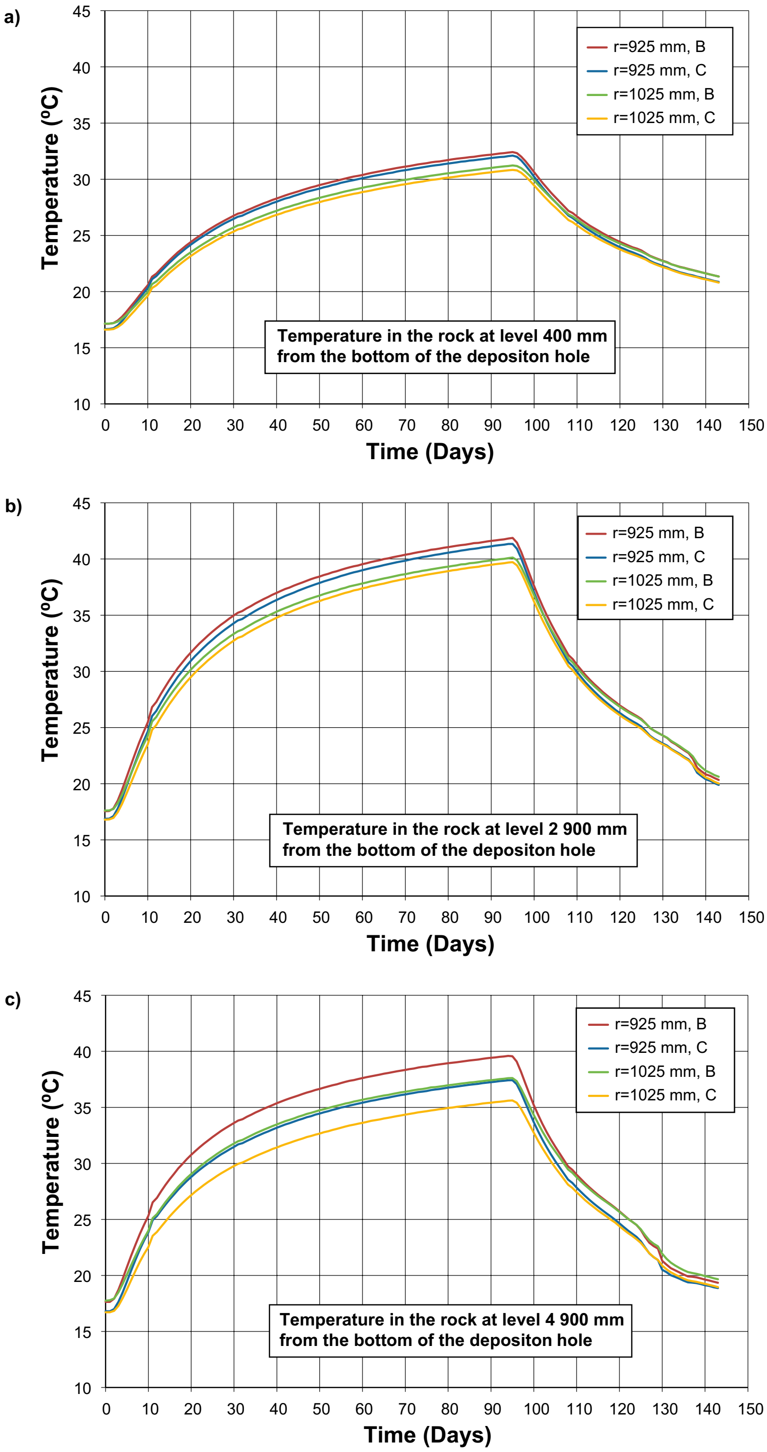

Figure 3-18. *The temperature evolution in the surrounding rock at three different levels in the deposition hole a) 400 mm b) 2 900 mm and c) 4 900 mm from the bottom.*

3.5.3 Buffer temperatures

The temperature in the buffer was measured with thermocouples but also with the RH-sensors. Data from all sensors are shown in Appendix 3. In Figure 3-19 the temperature measurements in buffer block R10 are plotted, showing that the maximum temperature in the buffer was about 68.5 °C. This was measured on the inside surface of the buffer blocks placed around the canister. Furthermore, the figure shows that the temperature drops over the inner gap i.e. between the canister surface and the inner surface of the buffer block was about 9–11 °C, the temperature drops over the buffer block was about 16–17 °C and finally the temperature drops over the pellets filled outer gap was about 9–10 °C.

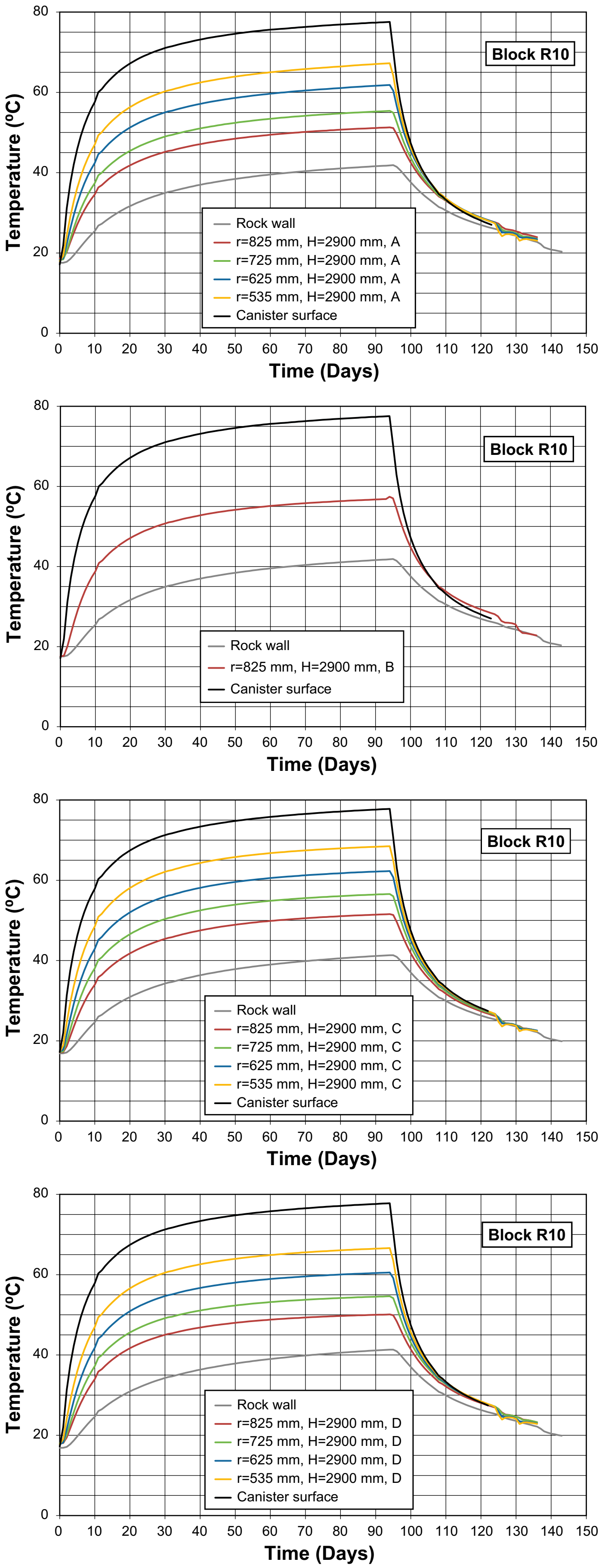

Figure 3-19. *The temperature evolution in buffer block layer R10. The measurements are made in the four directions A, B, C and D.*

3.5.4 Relative humidity

In total, 10 relative humidity sensors were installed in the buffer, one below the canister in layer C2, one above the canister top in layer C4 and the rest in the ring shaped block layers around the canister in layers R6, R10, R14 and R18 respectively. The purpose with measurement of relative humidity is to follow the water uptake of the buffer at different locations within the buffer. A measured relative humidity is always reflecting the water content of the buffer material although the measuring value is depending on the type of bentonite but also whether the buffer is absorbing water or drying out. The readings from the installed sensors are shown in Figure 3-20. Two sensors (R10, r=815) and (R18, r=815) were clearly indicating a slow water uptake. Both these two sensors were placed close to the outer radius of the blocks i.e. close to the pellets filled outer gap. The readings of the sensors are probably reflecting the slow water uptake from the surrounding rock. Five sensors are first indicating a water uptake and then a drying of the buffer. This evolution is most pronounced for the sensor (R10, r=545) which is placed at mid height of the canister and very close to the inner slot between the buffer and canister. A reasonable interpretation of the readings from this sensor is that there is first an increase of the water content caused by the heat from the canister forcing the water towards the wall of the deposition hole. This water movement results in an increase in water content at the sensor position followed by drying of the bentonite caused by the heat from the canister.

At the dismantling of the test, samples were taken of the bentonite close to the installed sensors. On these samples the water content and the dry density were determined, see Section 4.3 regarding the method used. In Figure 3-20 the data from the water content analysis is plotted as function of the readings from the installed relative humidity sensors at the time for the dismantling of the test, i.e. the last readings in Figure 3-21. The figure is indicating a strong correlation between the readings from the sensors and the determined water content.

3.5.5 Buffer heave and condensation

The displacement of the buffer in axial direction was measured with the use of a levelling instrument. This was made at least once a week in 14 positions of the top layer, see Figure 3-22. The results from the measurements are shown in the figure where positive displacement means that the block has moved upwards. The following conclusions can be made from the measurements:

- The maximum average displacement was reached at the end of test period, about 40 mm.
- The displacement velocity was somewhat decreasing with time.
- The displacement of the surfaces varied between 30 and 65 mm.
- The largest displacement was observed in direction A–D which implies that the surface of the top layer was inclined.

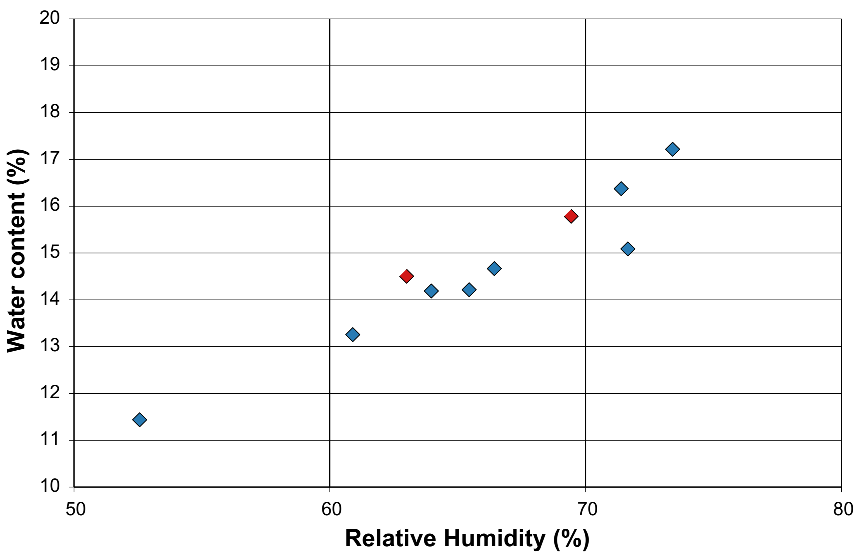

Figure 3-20. *The determined water content as function of the measured relative humidity in different part of the installed test. Note that the red dots are representing water contents on samples taken close to the positions of the sensors.*

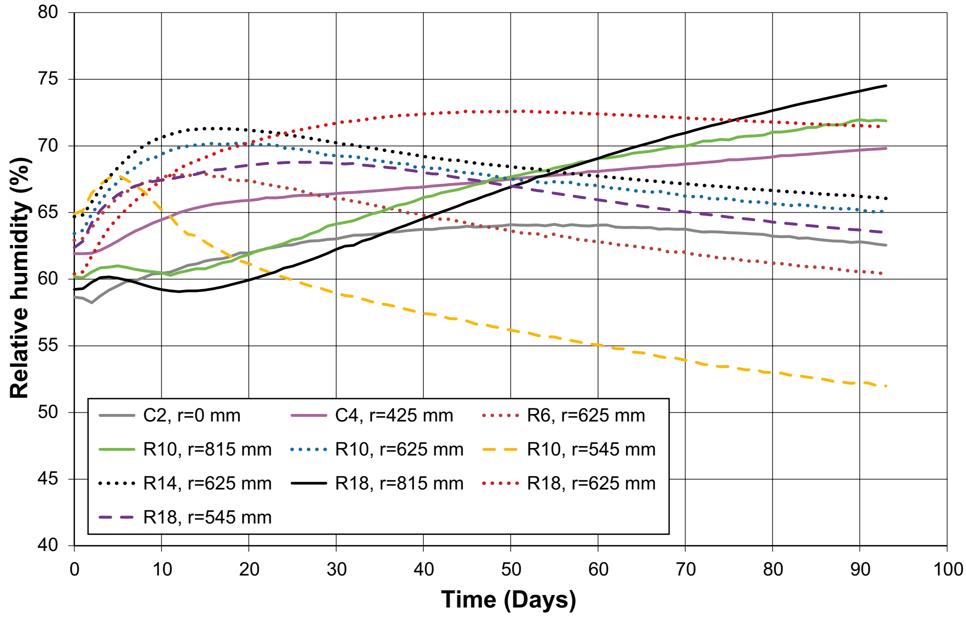

***Figure 3-21.** The readings from the installed relative humidity sensors as function of start of the test. The labels for the curves are describing in which block they were installed and the radial distance from the centre of the block.*

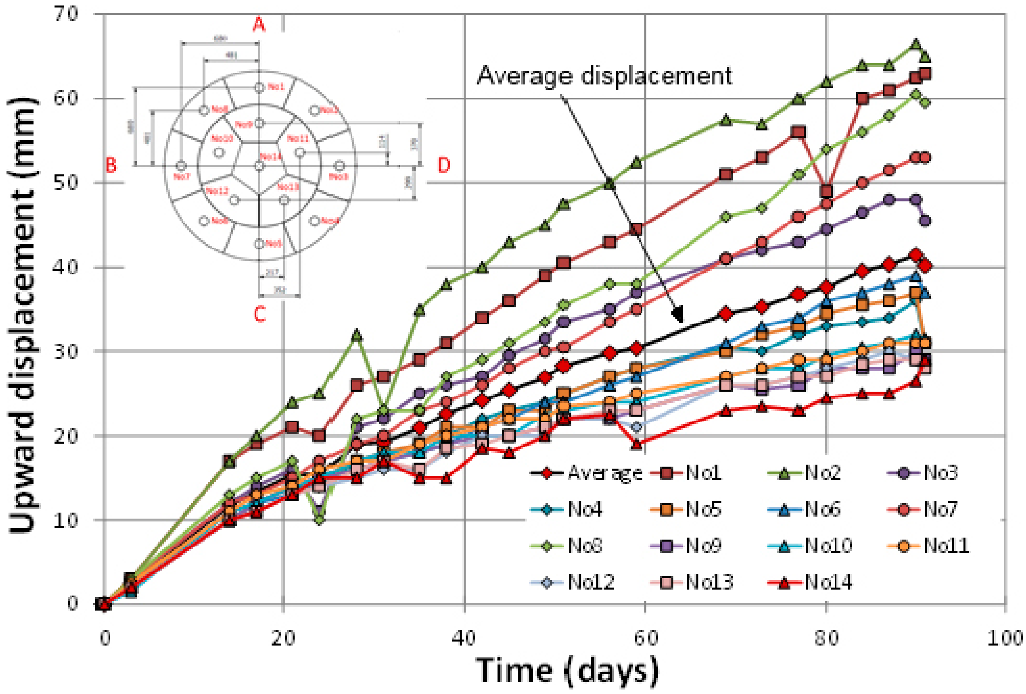

***Figure 3-22.** The upward displacement of the top layer of blocks. The measurements were made in 14 positions. The average of the displacement is also given.*

3.6 Dismantling and analysis

3.6.1 Sampling strategy

The strategy for sampling was to collect bentonite for water content and density analyses. The sampling should cover the buffer in both axial and radial direction. In radial direction: the sampling pattern are illustrated in Figure 3-23 (a). In axial direction: one sample was collected from the middle of each block in every radial position as illustrated in Figure 3-23 (b). Direction A and C are placed in the tunnel's axial direction with A pointing towards the end of the tunnel.

The sampling was be performed by core drilling. Sampling of pellets was done by hand. Directly after core drilling the samples were protected by sealing them in marked plastic bags.

It was expected that there would be an increased accumulation of water in the bentonite closest to the capsule top. For this reason, extra samples were taken from two of the highest ring blocks, R20: 1 and R20: 5. The sampling pattern for these blocks is shown in Figure 3-24.

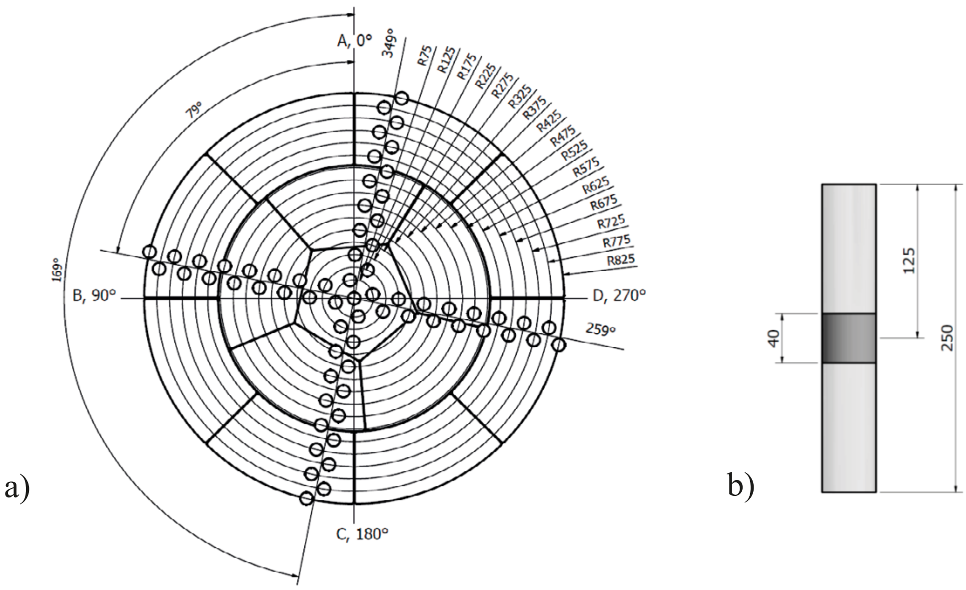

Figure 3-23. *a) radial sampling pattern, b) axial core drilled sample from one block in one position.*

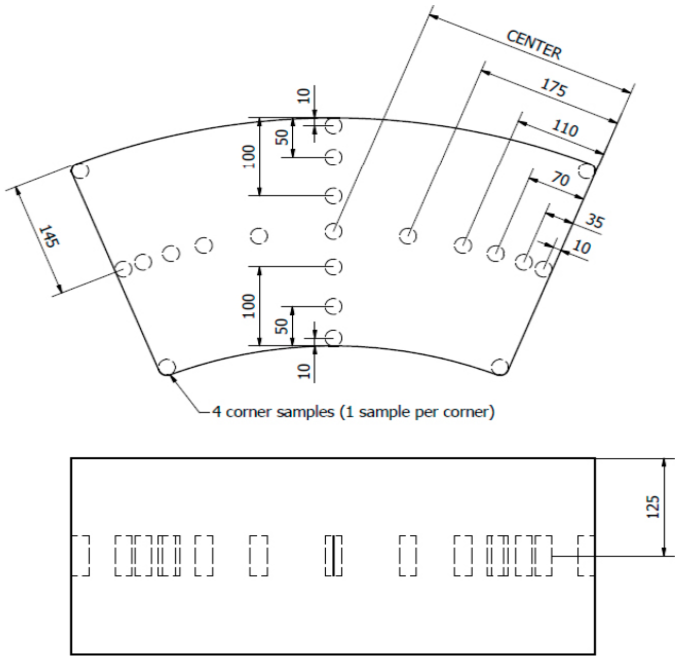

Figure 3-24. *Sampling pattern for R20:1 and R20:5.*

3.6.2 Dismantling and sampling (field activities)

In this section the field activities from dismantling and sampling are reported. Results from analysis of the samples are reported in Chapter 4.

As described in Section 3.6.1, the sampling plan was to core drill in four directions. Besides of core drilling, samples in the pellet slot between the outer blocks and the rock were collected by hand.

A template made of plywood was used as guide when core drilling, as illustrated in Figure 3-25.

To fill up the used test hole, C13 and C14 were added as extra top layers. Layer C14 did not have support from the surrounding rock or pellets as illustrated in Figure 3-26. For this reason, it was decided that layer C14 should be dismantled without sampling.

The dismantling and sampling were performed Monday to Friday 8 hours per day by two persons.

202-01-20 Removal of protection lid

As can be seen in Figure 3-26 there were some major cracks in the top layer C14. The orientation of the damaged area was towards the end of the tunnel (A direction). The outer rings have moved upwards more than the inner rings due to the redistribution of water in the buffer.

Figure 3-25. *Left: Wood template used when core drilling. Right: Core drill.*

Figure 3-26. *Layer C14 after removal of the protection lid. Note that the top surface was even when the test started.*

2020-01-22 – 2020-02-14: Dismantling and sampling of layer C13–C3

Figure 3-27 and 3-28 illustrates some examples from dismantling and sampling of layers above the canister.

2020-02-18: Dismantling and sampling of layer R20

The canister was exposed after removing the special centre blocks from layer R20 as illustrated in Figure 3-29. The height of these centre blocks was adjusted during installation to fill the gap between the upper surface of layer R20 and the top of the canister. Before preparing the canister for lifting, also the outer blocks of layer R20 were removed. As described in Section 3.6.1, block R20:1 and R20:5 was stored for extra sampling, illustrated in Figure 3-30. The sampling of these two blocks was performed 2020-03-25.

Figure 3-27. *Left: Block from layer C12. Right: Sampling of pellets in layer C12.*

Figure 3-28. *Left: Sampling of layer C7. Right: Layer C3.*

Figure 3-29. *Layer R20 after the special centre blocks are removed.*

Figure 3-30. *Core drilling of R20:1 and R20:5.*

2020-02-19: Removal of the canister

The canister was removed with the same machine as used during installation. The removal of the canister is illustrated in Figure 3-31.

2020-02-20 – 2020-03-11 Dismantling and sampling of R19–R1

Figure 3-32 and 3-33 Shows photos from dismantling and sampling of ring segments.

2020-03-19 – 2020-03-17: Dismantling and sampling of C2–C1

Figure 3-34 Shows photos from dismantling and sampling of bottom blocks.

Figure 3-31. *Pictures from removal of the canister.*

Figure 3-32. *Left: Layer R17. Right: Layer R11.*

Figure 3-33. *Left: Layer R5 and R4. Right: Layer R2.*

Figure 3-34. *Left: Layer C2. Right: Layer C1.*

3.6.3 Observed cracks in the buffer

At the dismantling of the test, cracks in the buffer blocks were observed in practically all parts of the buffer. An example of observed cracks in the buffer around the canister is shown in Figure 3-35. Most of these cracks went through the whole blocks i.e. from the inner surface of the blocks towards the pellets filled outer gap. It is not clear whether the cracks were caused by drying of the inner part of the buffer blocks, by water uptake of the buffer from the rock surface in the deposition hole or of both, see Section 3.6.4 concerning the redistribution of the water in the buffer blocks. Although the observed cracks were in some cases quite wide, they are not likely to have affected the redistribution of the water in the buffer as the gaps between the individual blocks were much wider and thus affected this process to a greater extent.

For the cracks observed in the blocks above the canister top it is most likely that these were caused by water uptake from the surrounding rock, see Figure 3-36. The cracks were located at the periphery of the blocks and at spots were water obviously was flowing into the deposition hole. Furthermore, this water uptake also caused variation in height of the different blocks within a layer, see Figure 3-36 b.

a)

b)

c)

d)

Figure 3-35. *Observed cracks in the buffer blocks surrounding the canister a) in layer R1, b) in layer R3, c) in layer R10 and d) in layer R18.*

a)

b)

Figure 3-36. *Observed cracks in the buffer blocks above the canister a) in layer C12 and, b) in layer C13.*

3.6.4 Position of the individual buffer blocks

Measurements of the vertical coordinate for the individual block layers were made both at installation and at dismantling of the test. The measurements were made at 8 locations on top of each block layer. From these data it was possible to determine an average vertical coordinate for each layer and from this data calculate the average height of the layers both at the start and after the test. By comparing these two data sets it was possible to calculate the changes in position for each individual section, see Figure 3-37. A positive value implies a displacement upwards of the block layer. The plot is indicating that small displacements were observed up to mid height of the canister i.e. at the level of the block layer R10 while above that level positive displacements were observed. The displacements are caused by the redistribution of water in the buffer.

3.6.5 Water content and dry density analysis

On each sample taken out from the test the bulk density (ρ_{bulk}) and water content (w) were determined. The bulk density was determined by weighing a sample both in air and submerged in paraffin oil with known density and the water content was determined by drying a sample in an oven at a temperature of 105 °C for 24 hours. Both the determinations of the bulk density and the water content were made in accordance with standard methods developed by SKB and described in Kronberg (2019a, b). With the known density and water content the dry density (ρ_d) was calculated, see Equation 3-1 below. The water content is calculated according to equation 3-2

The data from the water content and bulk density analyses together with the sampling positions were used to evaluate the buffer state after the test.

$$\rho_{dry} = \frac{\rho_{bulk}}{(1+w)} \qquad \text{Equation 3-1}$$

$$w = \frac{m_{water}}{m_{dry}} \qquad \text{Equation 3-2}$$

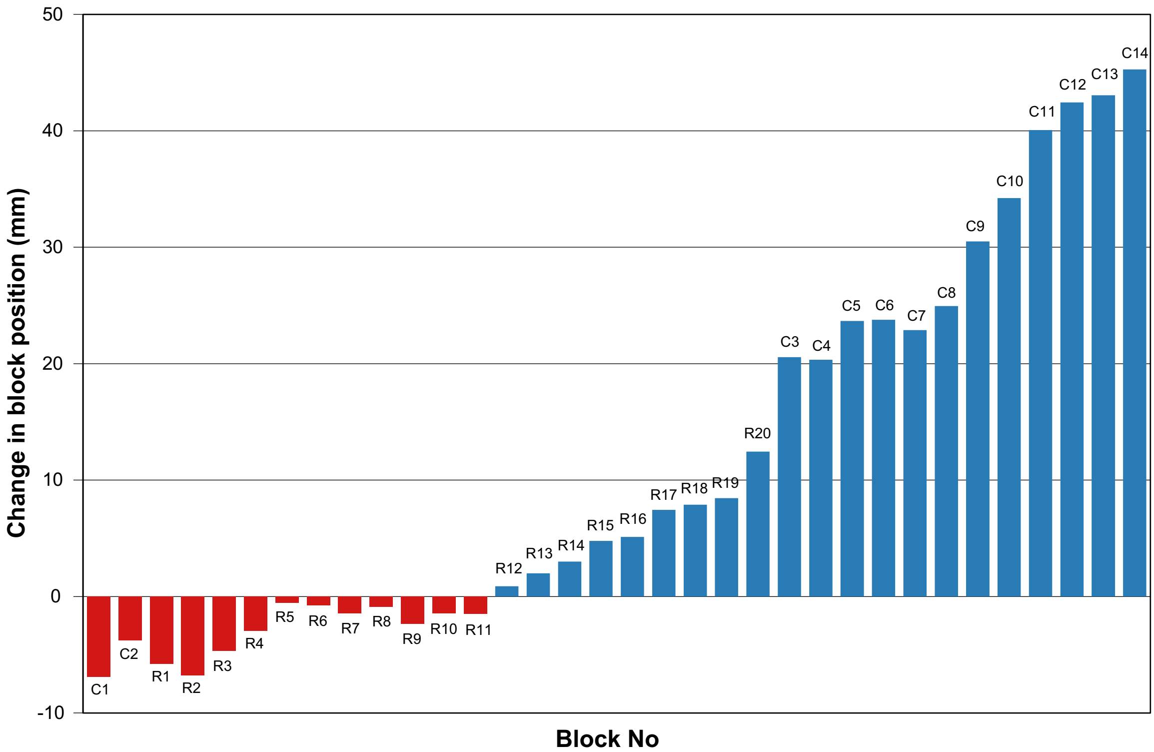

Figure 3-37. *The average displacement of the different block layers. The measurements were made in 8 positions.*

Pellet filling

The analysis of the water content of the pellet filling in the outer slot are summarized in Figure 3-38. The figure is showing the following:

- All parts of the filling had taken up water since the initial water content of the pellets was 12%, see section.
- The water content of the pellet filling varied between 13 and 67 %.
- The highest water content values were observed around a band going from direction B at the top of the filling (90°) towards direction D–A (320°) at the bottom of the deposition hole.
- The figure is indicating that water in the filling entered the deposition hole from water bearing fractures in the wall since the highest water content values were very local.
- It cannot be ruled out that some of the increase in water content of the filling was caused by redistribution of the water in the buffer blocks due to the heating from the canister surface.

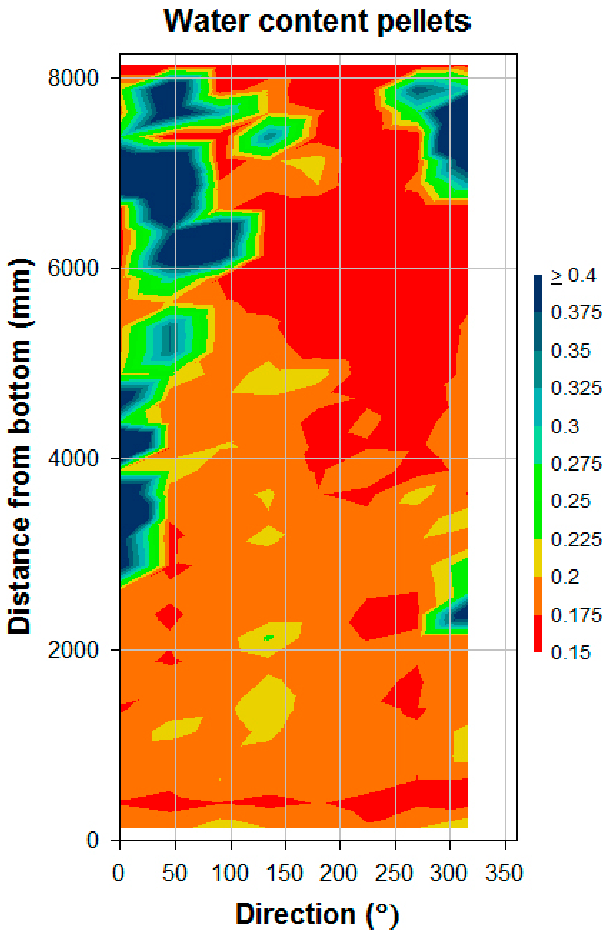

Figure 3-38. *Water content in the pellet filling after the test.*

Above the canister

The water content and the density in the buffer were determined in four profiles in each block layer. In Figure 3-39, the densities and the water contents are plotted in four profiles in block layer C3 as a function of the distance from the centre of the deposition hole. The figure shows that the water content at the centre of the block was higher than the initial water content by about 2%. Close to the outer diameter of the block section the plot is indicating a water content close to the initial. For the pellet filling the water content was increased from the initial value of 12 to up to 18%. Furthermore, there was a decrease in the dry density of the centre block. Thus, the plot is indicating that in the central part of the block layer a water uptake occurred, causing a decrease in dry density. Furthermore, water uptake in the pellets was observed. Corresponding plots for the rest of the investigated sections of the solid blocks above the canister are shown in Appendix 4.

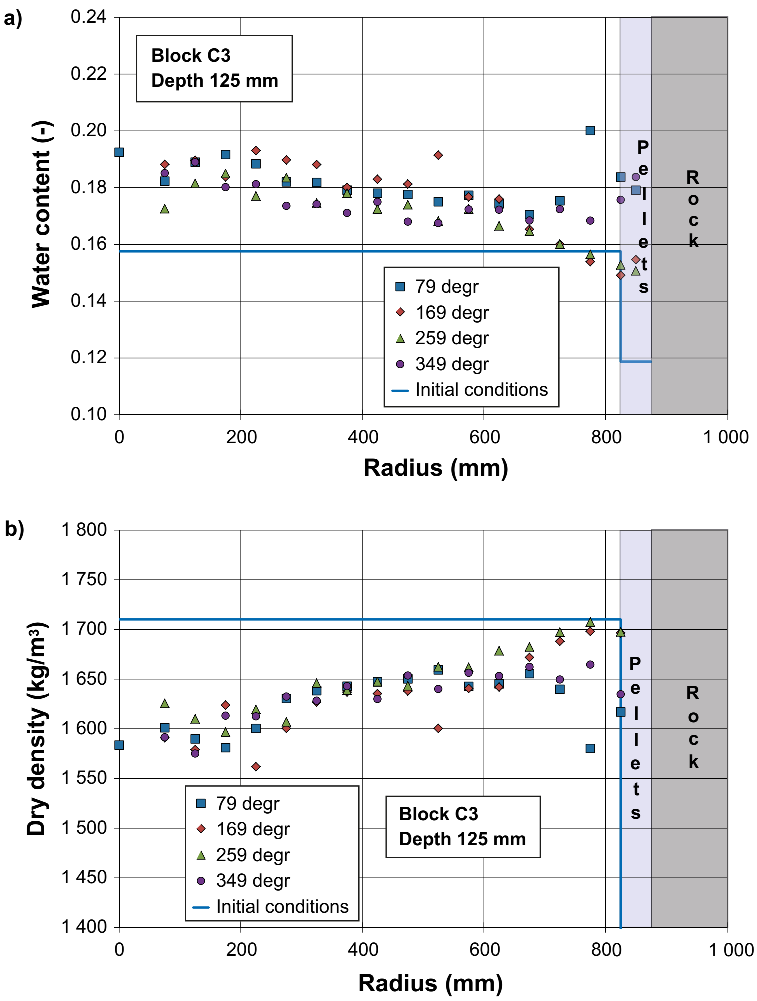

Figure 3-39. *Analysis of a) water content and b) dry density of the bentonite in block layer C3 as function of distance from the centre of the deposition hole. The analysis are made at the depth 125 mm depth from the upper surface of the block layer.*

Around the canister

In Figure 3-40, the densities and the water contents are plotted in four profiles in block layer R10. The figure is indicating drying of the part of the buffer close to canister, compared to the initial conditions, resulting in an increase of the dry density. For the part of the buffer close to the wall of the deposition hole a water uptake can be observed, especially for the pellets filling causing a decrease in dry density. This was valid for the buffer at mid height of the canister. Corresponding plots for all of the investigated sections are shown in Appendix4.

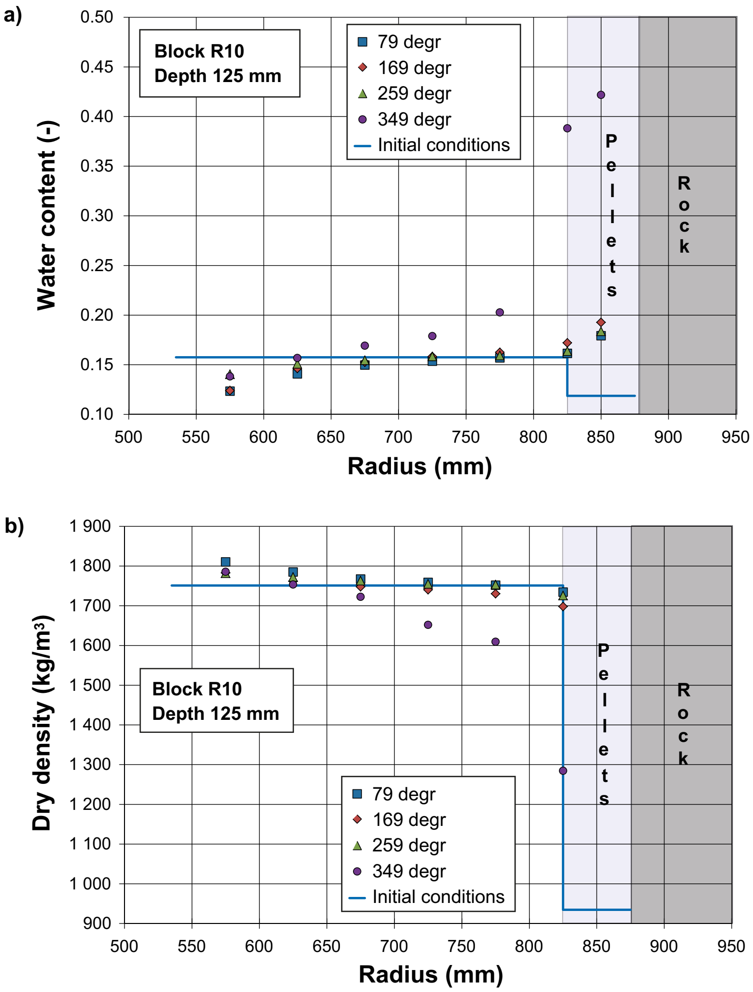

Figure 3-40. *Analysis of a) water content and b) dry density of the bentonite in block layer R10 as function of distance from the centre of the deposition hole. The analysis are made at four different directions at the depth of 125 mm from the upper surface of the block layer.*

Below the canister

In Figure 3-41, the densities and the water contents are plotted in four profiles in block layer C2. The canister was standing on this block layer. The figure shows that the water content at the centre block was almost the same as the initial. From the centre of the block layers towards the radial surface of the canister i.e. at the radius of 525 mm there was a decrease in water content followed by an increasing water content towards the wall of the deposition hole. In most of the block layer, the water content decreased compared to the initial conditions, resulting in an increase in dry density. However, the pellet filling had an increased water content compared to its initial conditions. Corresponding plots for the rest of the investigated sections of the solid blocks below the canister are shown in Appendix 4.

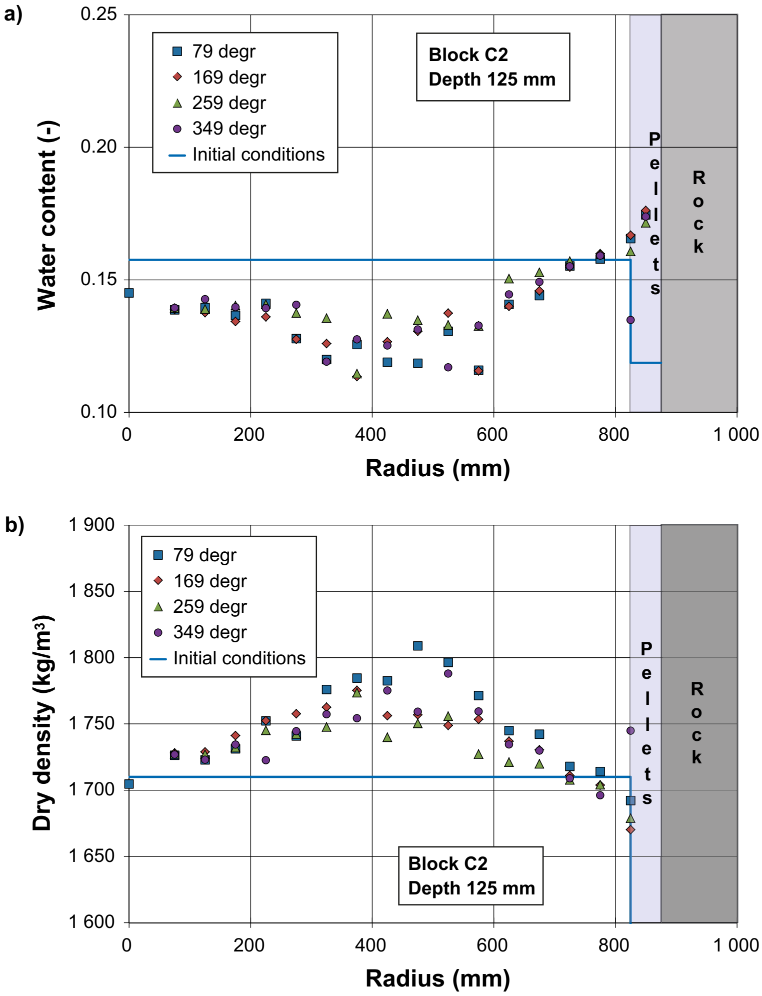

Figure 3-41. *Analysis of a) water content and b) dry density of the bentonite in block layer C2 as function of distance from the centre of the deposition hole. The analysis are made at four different directions at the depth of 125 mm from the upper surface of the block layer.*

The density and water content of the whole buffer

A summary of data from all the analysis of the water content and density in the four directions (079, 169, 259 and 349 respectively) are shown in Figure 3-42 and Figure 3-43. The initial water content of the buffer blocks was about 16% and for the pellets filling 12%. The dry density for the block sections around the canister was at the installation about 1 751 kg/m^3. For the block sections above and below the canister the corresponding dry density was about 1 710 kg/m^3.

The figures indicate that the water uptake was relatively axisymmetric. There was an increase of the water content close to the top of the canister which indicates that there has been a condensation of water at that region of the buffer. Furthermore, there was a drying of the buffer close to the canister surface from about 500 mm below the top of the canister to the bottom of the canister. This is also valid for the block section on which the canister is standing. As described in above all parts of the pellets filling had taken up water.

The plots of the density are indicating decreases in the dry density of the buffer at locations of water uptake and an increase of the dry density at those parts of the buffer where a drying has occurred.

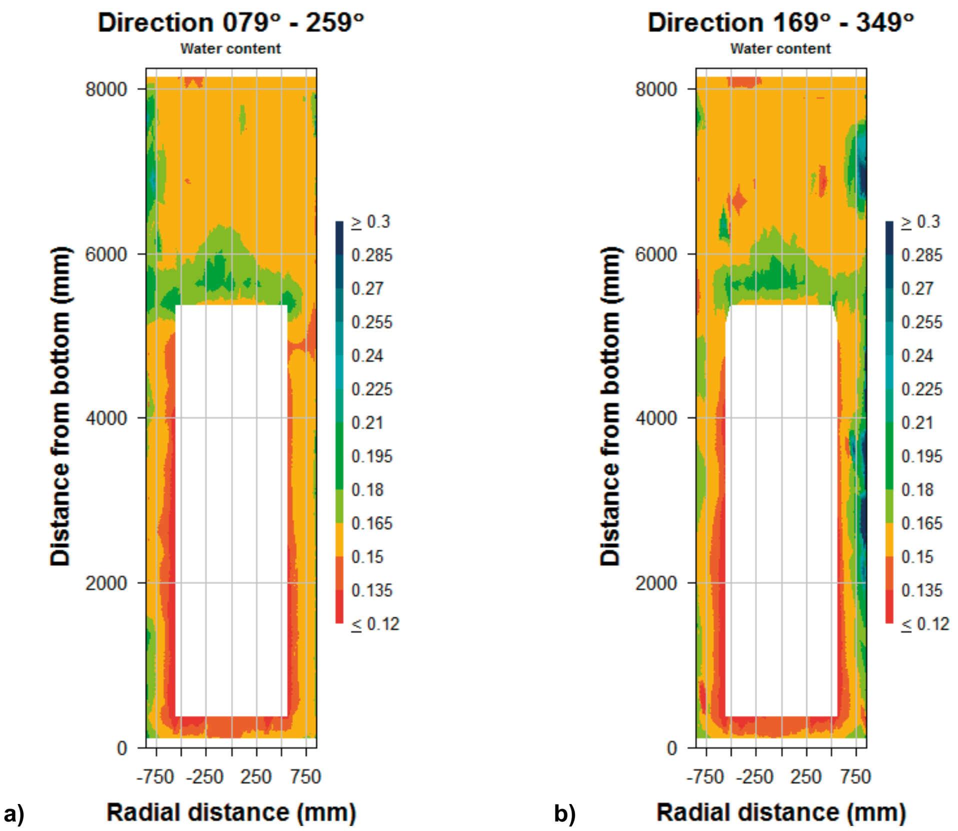

Figure 3-42. *Water content for the buffer a) in section 079°–259° and b) in section 169°–349°.*

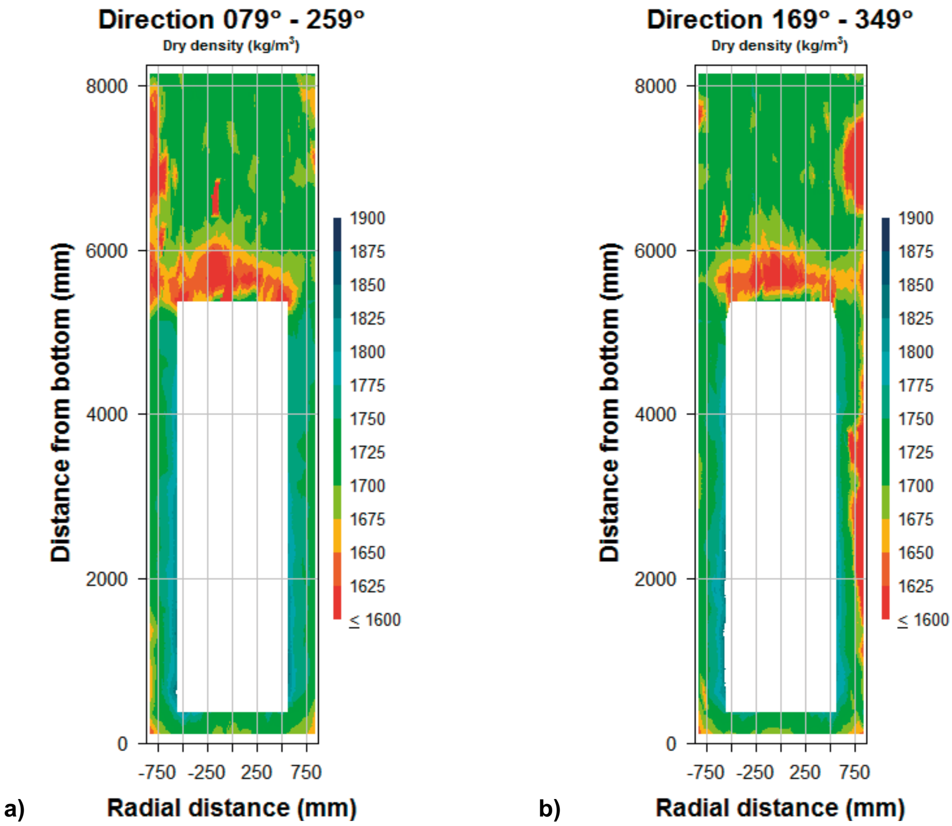

Figure 3-43. *Dry density for the buffer a) in section 079°–259° and b) in section 169°–349°.*

4 Evaluation

4.1 Overview and strategy of the evaluation

The test in this report had the purpose to find out how a buffer with segmented blocks behaves in the short term during the installation period before the backfill is installed on top of the buffer. Since this test, hereafter called Test 2, has been done with segmented blocks, which has more air-filled gaps than the previous reference design, very little experience of the THM (Thermal-Hydraulic-Mechanical) behaviour is available. A test made on the reference design, hereafter called Test 1, is reported in Luterkort et al. (2017), was used to compare the design for segmented buffer with the reference design (ring shaped and cylindrical blocks). The reference design is shown in Figure 4-1 where it is compared to the design with segmented blocks. The major difference between the reference design and the design with the segmented blocks is the introduction of gaps between the blocks. It is known that air filled gaps can transport a lot of water and accelerate drying (Luterkort et al. 2017). This drying will affect the thermal conductivity and the swelling of the buffer, especially in the short term. Even though it is known on a conceptual level how the processes work there is a large uncertainty in how big influence the gaps will have. Therefore, a full-scale test was needed to find out both how large the actual gaps would be during installation and to what extent the gaps would affect the performance of the buffer during the short term. Short term in this case is defined as the installation phase until the backfill is placed on top of the buffer. This time is expected to be at maximum 60 days but the test is running for an extra 30 days to have some margin to the expected installation time.

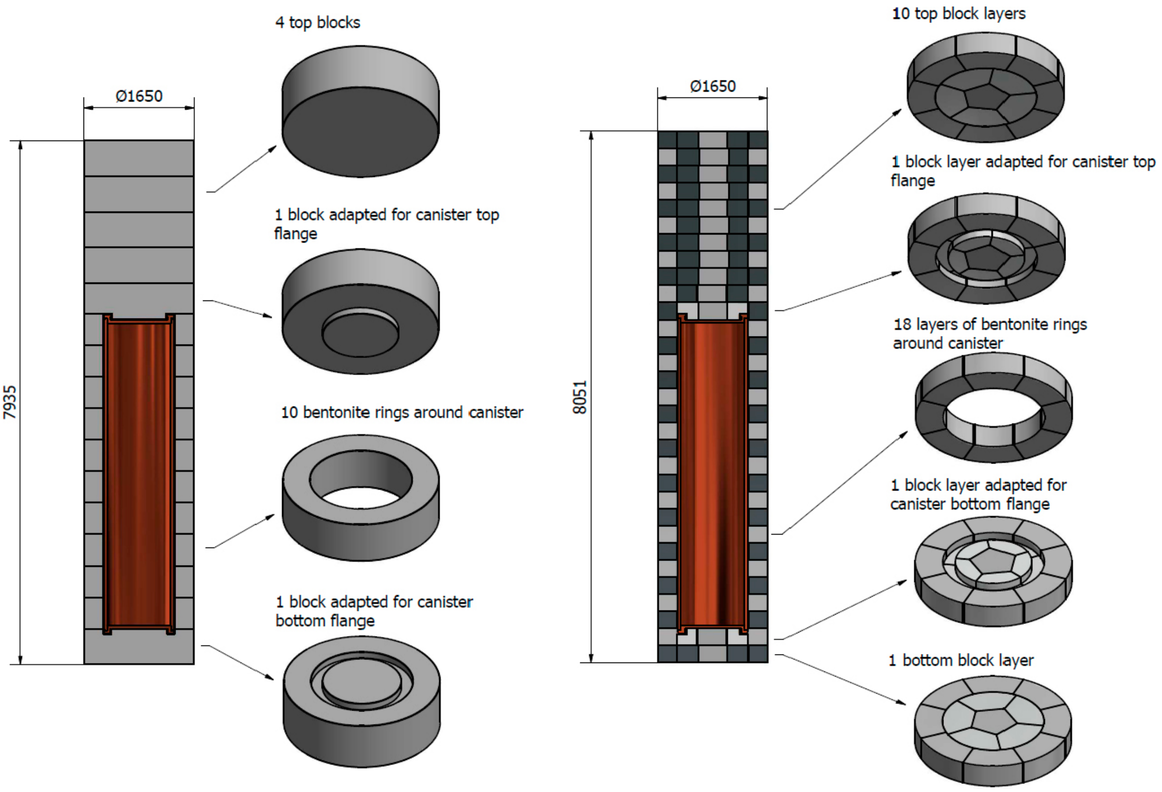

Figure 4-1. *Illustration of the differences between the two designs.*

The focus of this evaluation will mainly be to do a qualitative comparison between the tests and describe the differences between the two tests and how the gaps between the blocks affect the system and if this could in any significant way affect the requirement fulfilment. For a more detailed understanding of the processes a deeper analysis needs to be done which might need to include modelling of the system. Since there are some differences between the two tests that are being compared there could be some uncertainties. The differences between the tests and what the expected affect from these differences are described in the following chapters. The comparison will be kept relatively general and will not include any detailed analysis. The most important purpose with this comparison is to show that the buffer with segmented blocks do not differ too much from current reference design on a deposition hole scale.

4.2 Boundary conditions and differences between the tests

The boundary conditions of the test affect the development of the redistribution of water and heat in the buffer. In this case the two main thermal boundary conditions are the thermal power applied in the canister and the rock wall. The top boundary of the test also affects the system but is not expected to have a large effect, mainly because the temperature decreased before it reaches the top of the test due to that the heat mainly leaves through the rock wall. Hydraulic boundaries are similar for both of the tests because they were done in the same deposition hole. The top hydraulic boundary condition is different between the tests as well. Upper boundary was more sealed for vapour transport in the case of the test with the reference design, Test 1. The most important boundary conditions are:

- Hydraulic boundaries, the inflow of water from the rock.
- Temperature of the rock wall.
- Thermal power in the canister.

A general illustration of the test setups is shown in Figure 4-2. From Figure 4-2 the differences between the tests can be seen. The segmented blocks have a lot of air-filled gaps between the blocks which can transport water vapour between the blocks. However, it is difficult to quantify how much vapour will be transported in the gaps between the blocks because all gap widths between blocks are different. This unevenness in the gap width between the blocks could also make the redistribution of water more unsymmetrical and harder to predict. It is likely that the air flow between the blocks can be described with Poiseuille flow which suggests that the flow will be proportional to the cube of gap width.

Another difference between the tests is the upper part of the buffer. In Test 1 two concrete blocks were placed at the top of the test. Therefore, vapour could only leave the deposition hole through the pellet filled slot between buffer blocks and the rock wall. The test with segmented blocks is slightly higher than it would be in a real deposition hole. This is because the deposition hole is slightly deeper than planned for the spent fuel repository so to avoid a large air-filled space were the humidity could be high the buffer was extended upwards with approximately 500 mm (layers C13 and C14).

Below, the most important differences in the test compared with the design for segmented block, Figure 4-1, are listed:

- The test hole at Äspö is 8 624 mm deep. To fill up the extra space 4 extra layers will be installed, making it a total of 14 block layers above the canister.
- The average diameter of the selected deposition hole is 1 762 m. This causes the pellet-filled outer gap to be nominally 6 mm wider than the reference design.
- The test deposition hole lacks the bevel in the upper part.
- The canister will have an extra lid on the top of the canister that protects the cables from the heaters. This means that the canister in the experiment will be about 150 mm higher than the reference design. This also means that the buffer blocks around the canister are correspondingly 150 mm higher to match the height of the canister.

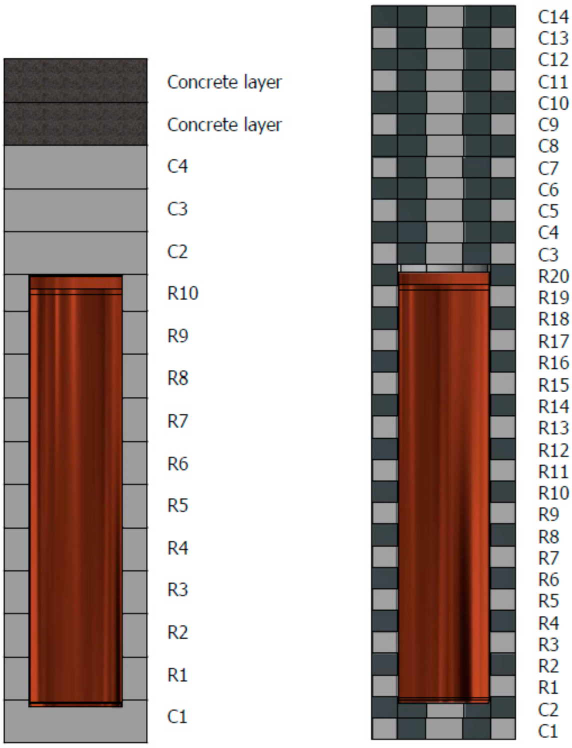

Figure 4-2. *Illustration of the differences between the two test designs.*

4.2.1 Thermal boundaries

As mentioned earlier there are three thermal boundaries in the test: the rock wall; the thermal power inside the canister and the boundary at the top of the buffer. The two first are considered to be the most important ones. The top boundary is located quite far from the canister and since the thermal conductivity in the rock is larger than in the bentonite, the heat is predicted to be transported out to the rock and then further out in the rock mass. This is supported by modelling done in Luterkort et al. (2017).

The two main boundaries (rock wall and canister) have been instrumented in the same positions in both tests and can thus be compared. Regarding the thermal power in the canister the goal value was 1 700 W. In Figure 4-3 the thermal power is plotted for the two tests. In Test 1 heater power was reduced by 50 % for a short period between approximately day 78 to day 88 due to a problem with a fuse. However, this short loss in heater power was judged to not influence the test very much. The average power for the test with segmented blocks was 1 708 W and for Test 1 it was 1 702 W during the first 78 days. Therefore, it can be concluded that the heating power is comparable in the two tests.

The other important boundary condition is the temperature of the rock wall. Both Test 1 and Test 2 with segmented blocks were performed in the same deposition hole and the heating power is basically the same. Therefore, the temperature on the rock wall should be the same. However, there could be redistribution of heat flow which would change the temperature in some positions. The temperature in the rock wall was measured in two directions and the result from the two different tests is shown in Figure 4-4 and Figure 4-5. The result shows that the temperatures are very similar. The only difference that could be seen is that the temperatures just above the canister, at the height 4 900 mm, are slightly higher for the segmented blocks. One reason could be that the airflow between the blocks can transport heat through convection. That means that hot air close to the canister can be transported out to the pellet filling through the gaps in-between the block due to convection. If this is the case hot air would be transported along the canister and at the top it flows out between the blocks to the pellet filled slot between the buffer blocks and the rock wall and therefore heat the rock at that position.

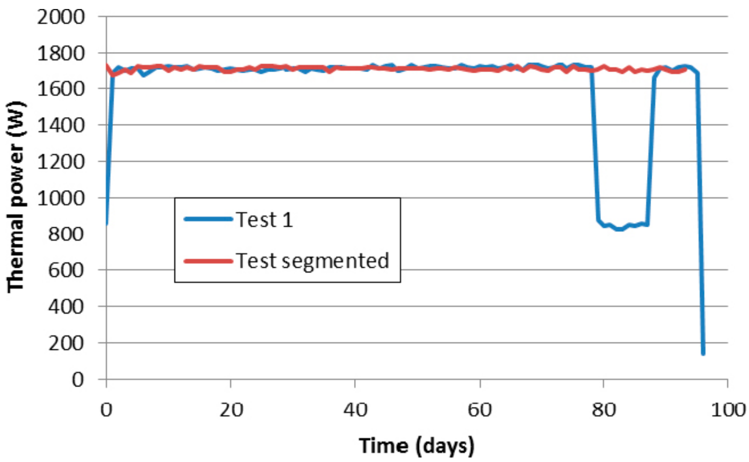

Figure 4-3. *The thermal power applied at the heaters in the canister for the test with segmented blocks and with form the test with reference design, Test 1.*

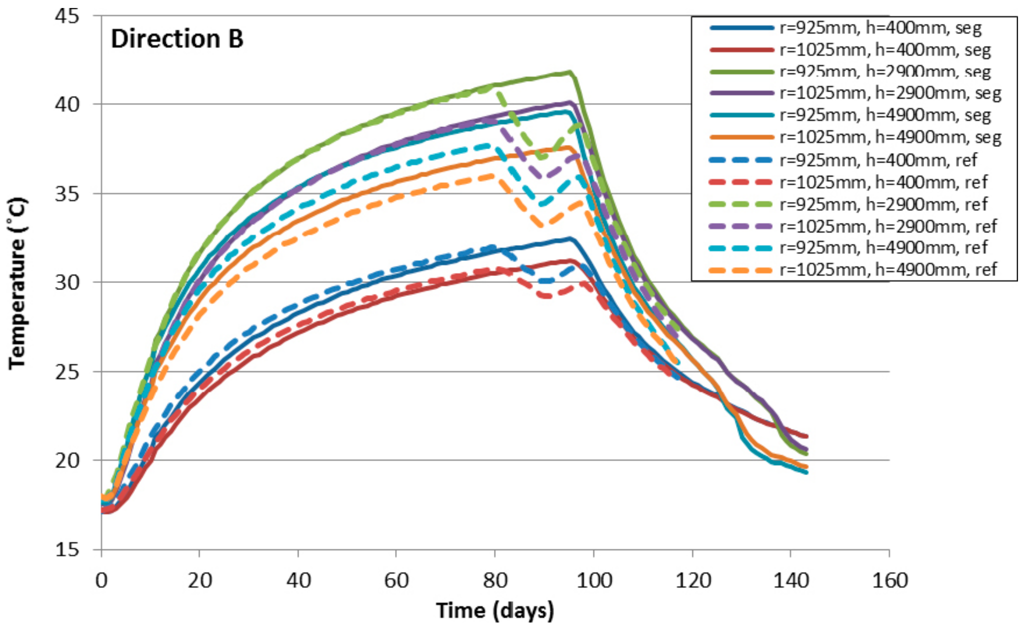

Figure 4-4. *Comparison of the rock wall temperatures for the test with segmented blocks (Test 2) and Ttest1 with the reference design in the B direction. Dashed lines are data from Test1.*

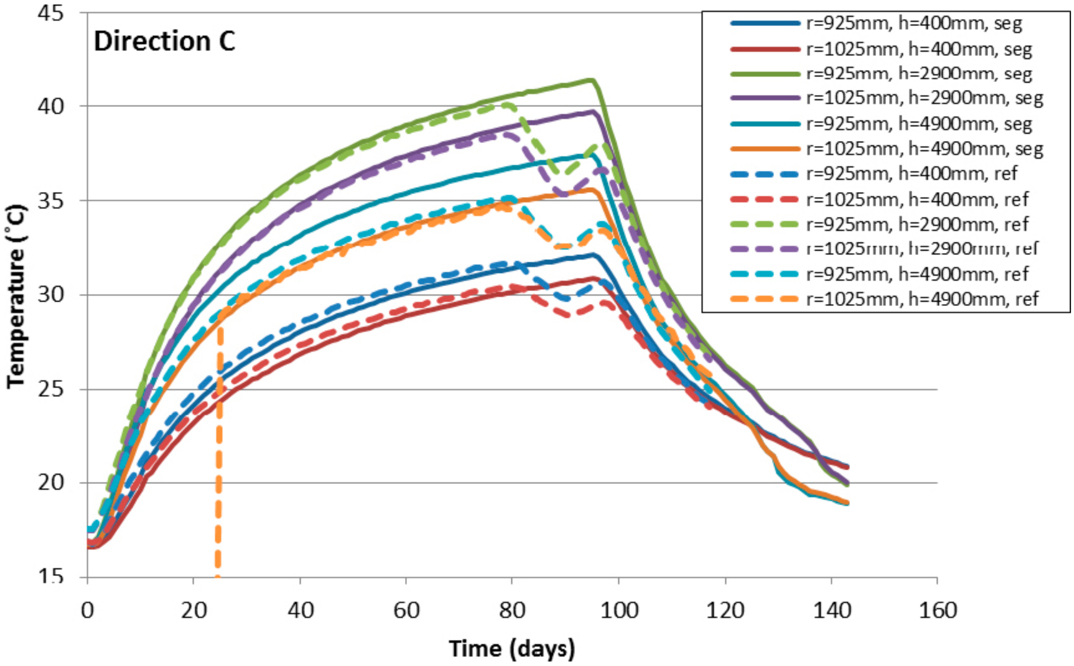

Figure 4-5. *Comparison of the rock wall temperatures for the test with segmented blocks (Test 2) and Test1 with the reference design in the C direction. Dashed lines are data from Test1.*

4.2.2 Hydraulic boundaries

Since the same deposition hole was used in both tests it is likely that the water inflow should be similar. The water inflow was measured in before test 1 to 8e−4 l/min. After the test with segmented blocks it was measured to 7.2e−4 l/min which suggests that the inflow has not changed or changed very little between the two tests. The inflow seems to mainly originate from a vertical crack in the upper half of the deposition hole. The similarity in the two tests can also be seen in the water content measurements in the pellet filling which is shown in Figure 4-8.

4.3 Water content and density distribution

4.3.1 Water content

The comparison of the water content distribution between the two tests is important because most of the properties of bentonite are dependent on the water content, for example thermal conductivity and mechanical properties. Since the thermal and hydraulic boundaries were very similar in the two tests it should be possible to see what affect the gaps between the blocks have on the overall transport properties of moisture. The two tests were sampled in two perpendicular directions. The results are shown in Figure 4-6 and Figure 4-7. Due to practical reasons the two tests were not sampled in the same angles. Therefore, the outer part of the buffer closest to the pellet filled slot cannot be directly compared. This is because the wetting of the pellet slot is not symmetric, but by comparing with the water content in the pellet, Figure 4-8, the wet areas can be identified and they correlate with wet areas at the outer part of the buffer blocks. The two tests seem to behave in the same way with a drying to a water content of approximately 12% closest to the canister.

The main difference between the tests is that the segmented blocks have a wetted area in top of the canister which is probably caused by moisture transport in the gaps between the blocks due to convection. There is also a tendency to have an increased drying in the lower part of the buffer. It should also be noted that the initial water content of the pellets is slightly different between the tests. The initial water content of the pellets in Test 1 was 15% and for the segmented block it was approximately 11%.

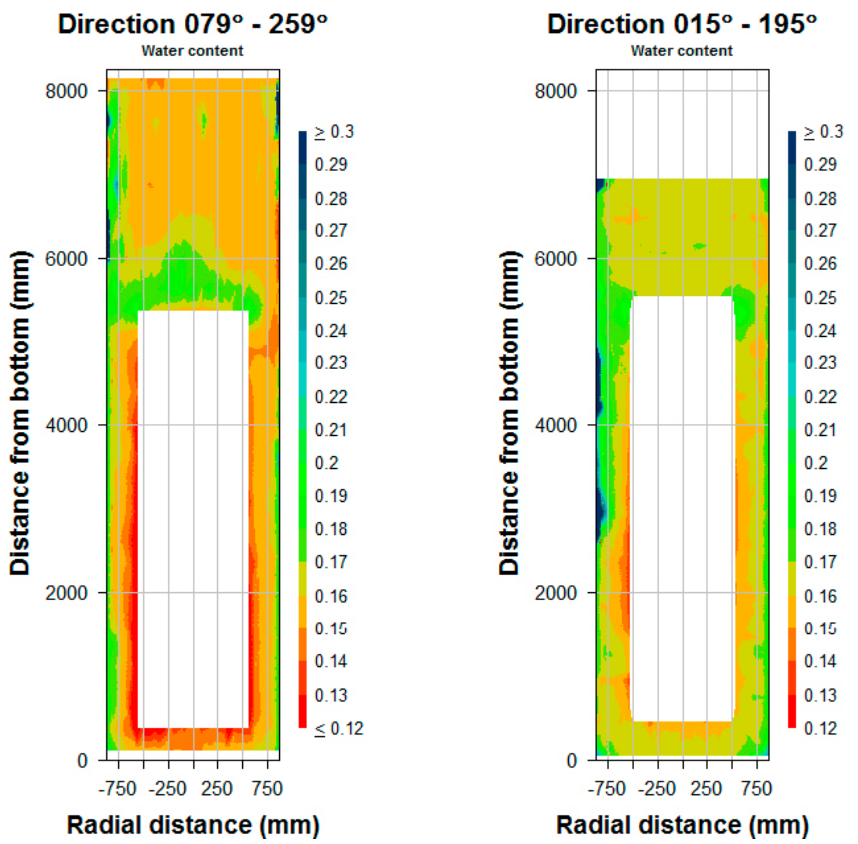

Figure 4-6. *Water content distribution in the buffer blocks between the two tests. The segmented blocks to the left.*

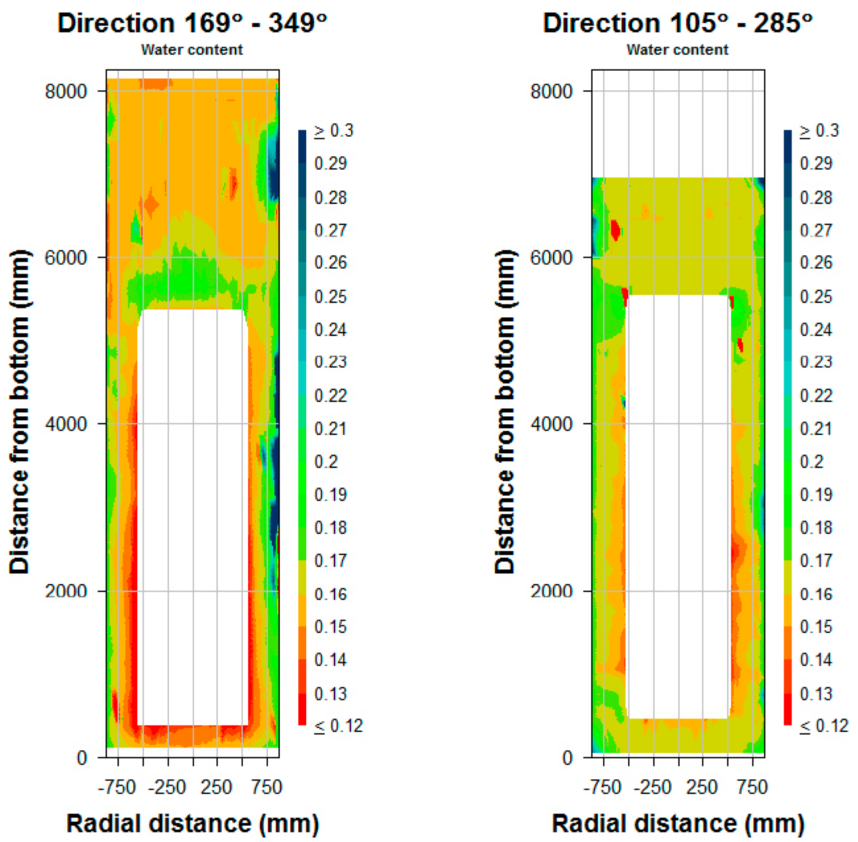

Figure 4-7. *Water content distribution in the buffer blocks between the two tests. The segmented blocks to the left.*

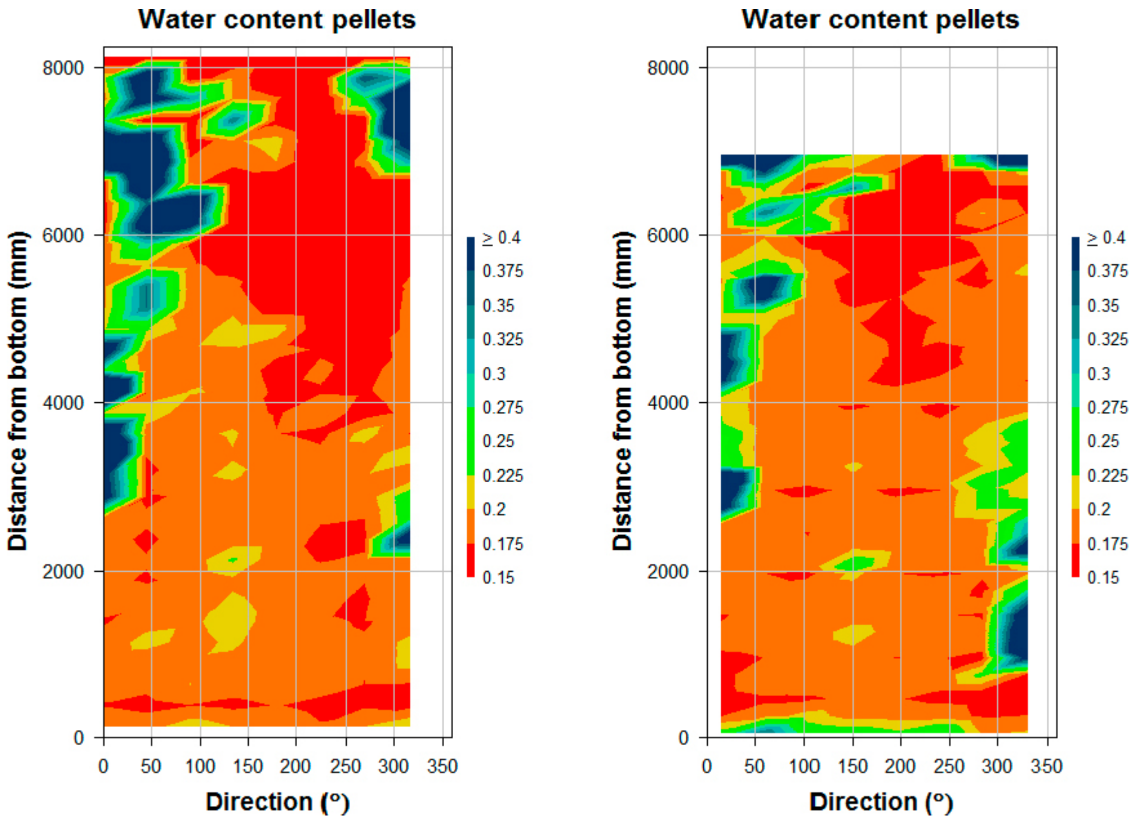

Figure 4-8. *Comparison between the water content measurements in the pellet filling. The wetted area correspond to a crack In the deposition hole which is the main inflow. The segmented blocks to the left.*

4.3.2 Dry density

The dry density in the tests is basically a function of water content for the two tests because there is very little confining pressure. The result can be seen in Figure 4-9 and Figure 4-10. The confining pressure in the tests is small and very little compaction of the bentonite takes place. The initial dry densities of the blocks are slightly different between the tests. The blocks in the layers on top and below the canister had an initial dry density of 1 717 kg/m^3 and the blocks around the canister had the initial dry density of 1 752 kg/m^3. The corresponding dry densities for Test1 are: 1 698 kg/m^3 and 1 758 kg/m^3 respectively.

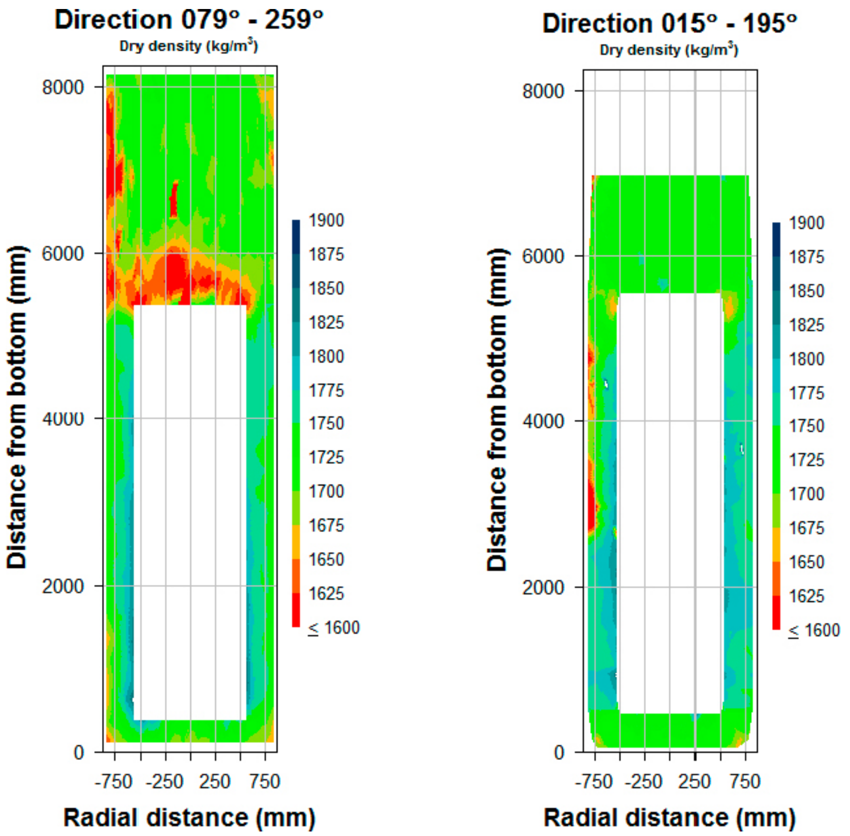

Figure 4-9. *Dry density distribution comparison between the two tests. The segmented blocks to the left.*

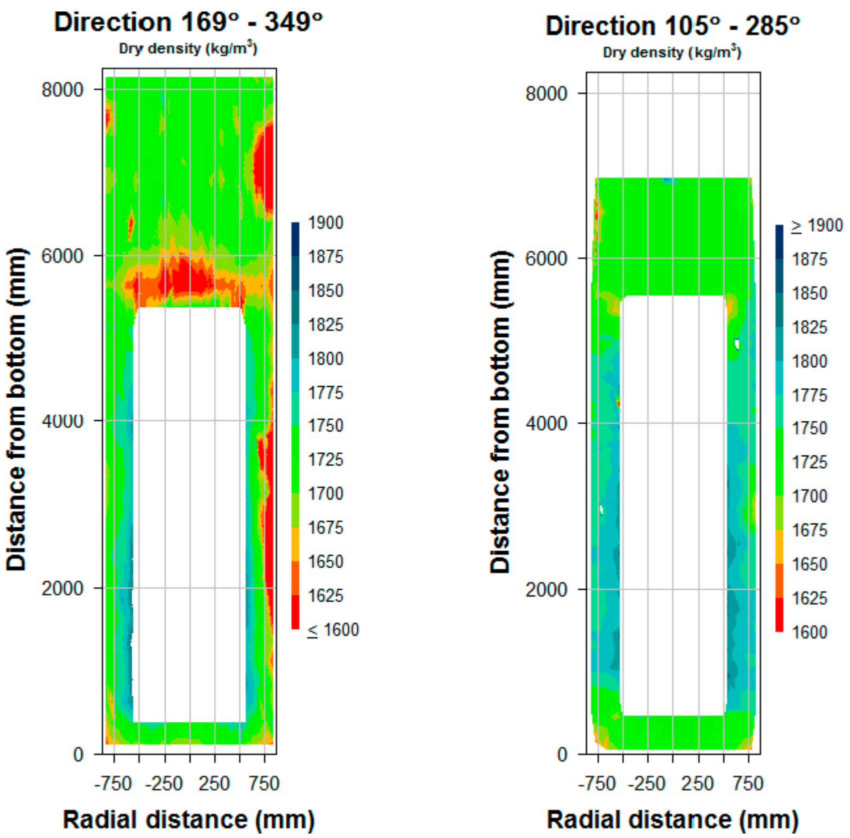

Figure 4-10. *Dry density distribution comparison between the two tests, segmented blocks to the left.*

4.4 Thermal conditions

One important property is the thermal conductivity of the buffer since it determines the maximum temperature of the buffer which is set to 100 °C in the technical design requirements. There has been an uncertainty on the thermal conductivity of the segmented blocks. This is because of two main reasons; one is that an increase of gaps between the blocks which could act as isolating layers which would reduce the overall thermal conductivity. However, the main heat transport is expected to be in the radial direction and therefore these gaps around the canister are parallel to the heat flow direction which would reduce the influence from them. The air flow in-between the blocks can also transport heat due to convection. However, this effect is likely to be small due to the low flow velocities.

The second reason why the segmented blocks could have a different thermal conductivity is that the water content distribution is different. This is because bentonite with higher water content has higher thermal conductivity and if the blocks would dry faster the effective thermal conductivity could decrease. To compare if there is a difference in effective thermal conductivity between the tests the temperature of the canister can compared. This can be done since the thermal boundary conditions are the same for the two tests. The two tests both have a thermal power in the canister of approximately 1 700 W and the rock wall temperature is similar. If the temperature of the canister is the same in the two tests, the effective thermal conductivity of the buffer would be the same.

In Figure 4-11 the temperature of the canisters in the two tests are compared and the result suggests that there is no difference in the effective thermal conductivity. One measurement diverges slightly between the two tests, the top in direction C which is higher than in the reference Test 1. However, that could be an effect of the canister being placed eccentrically, and thereby have a larger isolating slot or by convection in the gaps between the blocks which could transport hotter air towards the top in the inner slot between the canister and the buffer blocks.

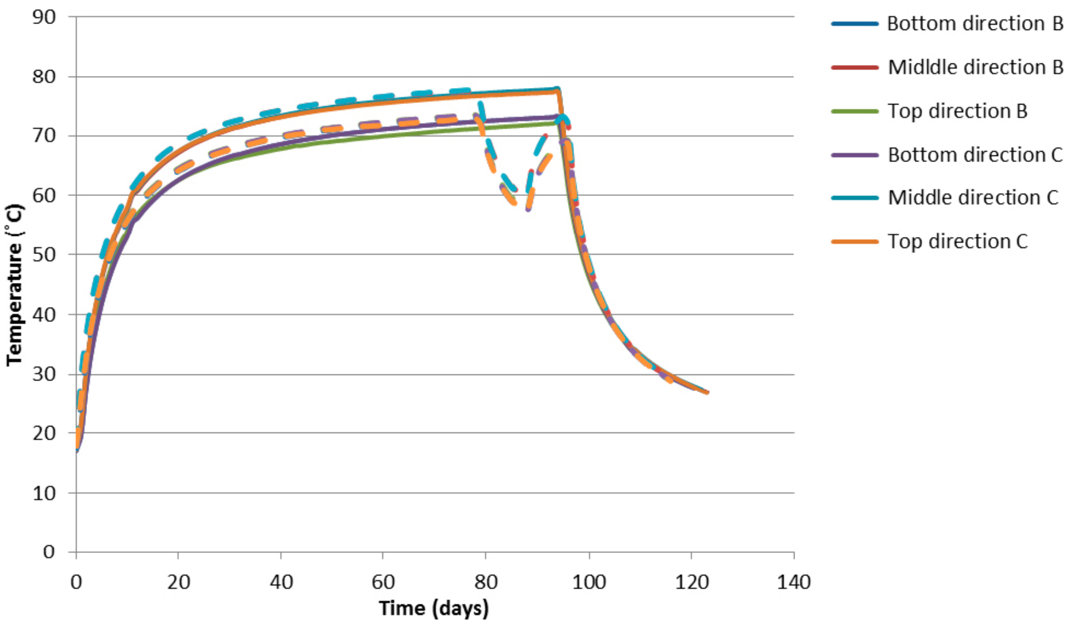

Figure 4-11. *Comparison between canister temperatures between the two tests. Dashed lines are data from test 1. Note that the results are so similar that the graphs are on top of each other. One value is not consistent with the other which is Top direction C which gives a higher value than the other top and bottom temperatures. The temperature in the top direction C is comparable to the mid canister temperature.*

4.5 Buffer movements

The average movement of the blocks at the top of the two tests in are compared in Figure 4-12. The average upwards movement are similar in the two tests, but there is a larger spread in between maximum and minimum upwards movement. However, the comparison is slightly more complicated because the buffer height is larger for the segmented blocks, approximately 14% larger. Also, a lot of the water inflow is located in the top of the test. This would suggest that the most of the swelling takes place in the top. When the movement of the individual blocks is compared between the two tests, see Figure 3-37 and Figure 4-13, it can be seen that the blocks below mid height of the canister has moved downwards while the blocks above mid height of the canister has moved upwards in the test with segmented blocks. In the Test 1, Figure 4-13 it can be seen that almost all blocks have moved upwards. If the two tests would have been the same height the test with the segmented blocks would only have been up to layer C8 which has an average upwards movement of approximately 25–30 mm. It cannot be excluded that the segmented blocks swell less than in Test1. However, more analysis on especially the water inflow would be needed to fully compare the upwards movement of the blocks as most of the inflow seem to be located in the top of the deposition hole.

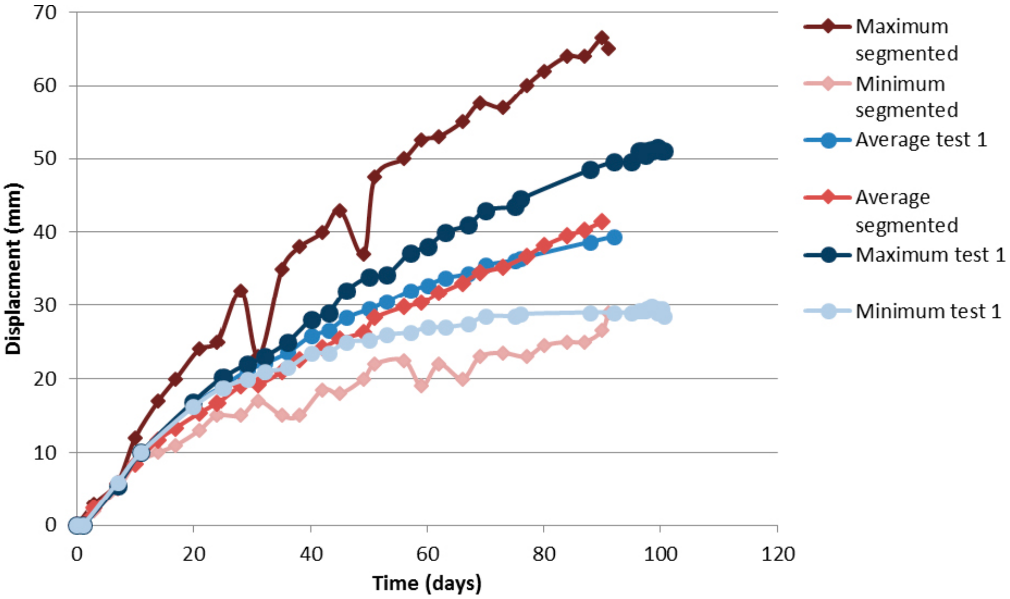

Figure 4-12. Comparison between the movements of the top surface of Test 2 with segmented blocks and Test1.

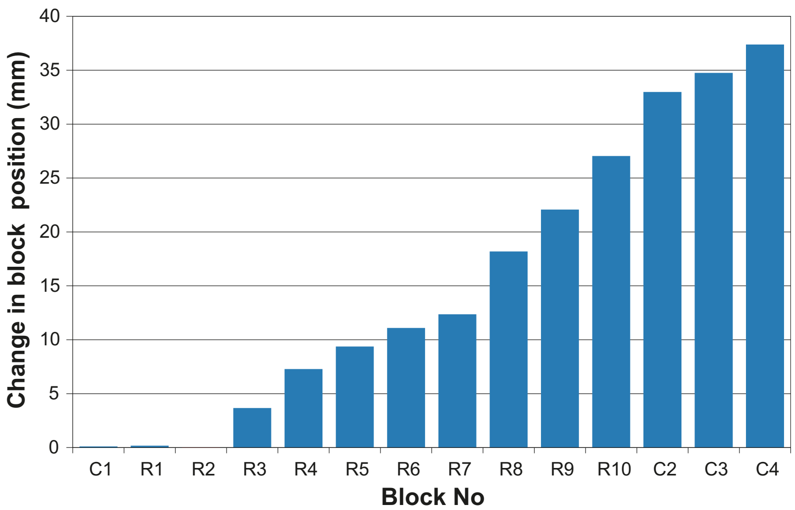

Figure 4-13. Accumulated swelling of the blocks in Test 1 which shows how much each block layer has moved upwards. C4 here is at the same height as C8 in the test with segmented blocks. The result for the same measurements for segmented blocks can be seen in Figure 3-37.

4.6 Gaps between blocks

The gap widths in vertical direction were measured during the installation of the test in the blocks surrounding the canister (R1–R20). The results are shown in Appendix 2. The horizontal gaps between the blocks were considered to be very small due to relatively good manufacturing tolerances and these gaps were too small to be measured.

If it is assumed that the flow rate of air in the gaps is low, it could be described as a Poiseuille flow. This means that the air flow would be proportional to the cube of the gap width. Using this assumption an equivalent gap width can be calculated. The equivalent gap width is a width which is equal between all the blocks and that will have equal combined flow rate as Test 2 with segmented blocks. For all the rings around the canister the equivalent gap width is approximately 1.8 mm. The equivalent gap width for each layer is shown in Table 4-1. Larger gaps than this could increase transport of moisture and more analysis, mainly through modelling, would be needed to be able to quantify how large gaps that could be accepted. However, it seems like the gap width in the current setup, 1.8 mm, is acceptable. The average gap width is approximately 1 mm which would suggest that the gaps are only 0.2 % of the total volume of the blocks surrounding the canister. The total amount of gaps in the buffer was calculated by adding the volumes of the different components and removing that from the total volume. This calculation estimates that the gap volume is approximately 1% of the block volume. However, there are large uncertainties in this calculation.

The blocks have also cracked due to the redistribution of water within the block which is caused by the temperature gradient in the system. See Figure 3-35 and Figure 3-36 The cracks would make pathways for air through the blocks. However, the judgement is that the observed cracks in the different parts of the buffer do not affect the performance of the buffer. The blocks in Test 1 did also crack but the width of the cracks was quite small and are judged to have limited influence in the water redistribution.

Table 4-14. The gaps between the block recalculated to an equal size slot width would give the same air flow.

Ring number	Gap width which would give the same flow (mm)
R1	3.1
R2	3.3
R3	2
R4	1.7
R5	1.3
R6	0.9
R7	0.7
R8	0.7
R9	1.3
R10	0.8
R11	1.5
R12	1.6
R13	1.4
R14	1.5
R15	1.5
R16	1.8
R17	1.5
R18	1.3
R19	1.4
R20	1

5 Conclusions

A test has been performed with a buffer made of segmented blocks. The two main goals with this test was to learn more about the early THM development of the buffer and to get experience from manufacturing and installing segmented blocks.

The result has been compared with an earlier test, Test1, that was made using large cylindrical and rings shaped blocks. The two tests were very similar with respect to thermal and hydraulic conditions. One important difference between the tests is that the buffer in the test with segmented blocks was higher. This means that the segmented buffer had more length that could possibility expand. The main water inflow to the deposition hole during the tests was located at the top which would make the expansion even larger in the top blocks which did not exist in Test1 (the two top blocks were made of concrete). Therefore, the upwards movement of the blocks is not be completely comparable between the two tests.

The effective thermal conductivity of the two buffer designs is very similar and no or very small differences could be seen on the canister temperature. It could be suspected that the gaps between the blocks could act as insulating layers and also that the air flow in these gaps can redistribute the water in the buffer and change the thermal conductivity. However, no such effect on the effective or overall thermal conductivity is shown in the test. This does not mean that the thermal conductivity could change locally and due to the gaps, it could also mean that the thermal conductivity is more anisotropic. However, the important property is the effective thermal conductivity, since this determines the maximum temperature in the buffer, and as mentioned earlier no significant difference can be seen in this property.

The water content distribution in the buffer are slightly different between the tests and is most likely dependent on the number of gaps and how wide they are. The main difference between the two tests are that there is an accumulation of water on top of the canister for the segmented blocks which results in a lower dry density and also the buffer seems to be slightly drier in the bottom for the segmented blocks. This is what is expected if convection occurs in the gaps which then will transport water vapour. The amount of gaps in the blocks around the canister were measured during installation and from this data it can be concluded that if an even gap width of 1.8 mm between all the blocks is used the air flow, and therefore also the transport properties of water vapour, should be the same as in the test. It is therefore likely that a 2 mm gap between the blocks could be accepted because this is supported by the test. The gap width could maybe be larger but then more understanding on how the gap width affects the system is needed before the gap width tolerance can be increased.

The upwards movement of the top blocks is a little more complicated since the two tests cannot be directly compared due to the difference in the height of the buffer. The segmented blocks seemed to have a larger upwards movement and a larger spread between the max and min value. However, if the segmented buffer test is evaluated at the height of the top of Test1 the segmented blocks actually shows a lower upwards movement. Due to the differences in the tests, the results are not completely comparable but the segmented blocks do not seem to expand more than the buffer with the ring shaped and cylindrical blocks. This of course assumes that the gap widths between the blocks are larger than in the test. If the gap width is larger than in the test it is not obvious what will happen.

It can also be concluded that the block could be produced according to specification although the block compaction could be optimized to reduce cracks in the blocks originating from the manufacturing.

The main overall conclusion is that there are no major differences between the two types of buffer blocks, segmented or ring shaped/solid blocks, regarding the THM (Thermo-Hydro-Mechanical) behaviour during the installation phase which is approximately 90 days.

Based on experiences from the production of segmented blocks for this test, the blocks held an overall high quality. They were well within specified height and weight requirements without any need of machining after compaction.

The high quality with small differences in height between the individual blocks was a key factor for installing the buffer manually with good precision.

6 Future work and recommendations

Although the test made on segmented buffer shows that it would work, it is still a lot of uncertainties on how the system behaves in other configurations, for example the THM behaviour. One large uncertainty is the influence on gap width. If the gap width gets larger than in the performed test either due to poor precision during installation or due to that the gaps opens up when the canister moves the blocks during installation, it is important to know how this will affect the system. It is probable that if the gap gets to wide, drying will be fast which could open up the gaps even more. An excessive drying could also increase the temperature of the buffer and canister due to reduced thermal conductivity of the buffer.

It is therefore important to get a better understanding how the system works and be able to model it. This increased knowledge could then be used to set tolerances on the gap width to make sure that the buffer behaves as desired.

More work should also be done to examine how the buffer behaves in timescales larger than during installation time. It could be possible for the buffer to dry out due to the increased transport of water vapour at longer times in very dry deposition holes. Although, modelling done in Luterkort et al. (2017) suggests that the vapour would stay in the deposition hole and accumulate in the top of the deposition hole and therefore sealing it off from deposition tunnel, it has not been evaluated if it is likely that this would be the case when vertical gaps in the buffer are present

A third area where more knowledge is needed is regarding how the water inflow in to the deposition hole and the location of it affects the upwards movement of the buffer blocks during installation. This could affect the installation sequence of the buffer. If the upwards movement is to fast it could cause problems for the installation of the backfill.

In addition to the THM behaviour of the system with a segmented buffer it is important to do installation test with adapted installation equipment to get some statistics on how well the blocks can be installed in a more industrial context. Some more data on how large volume of the buffer is taken up by the gaps would help in more accurately choose a density of the blocks so that the total dry density gets correct.

The last issue on which more work is needed is to set tolerances on all parts of the buffer so that no problems will arise during the installation process. If the tolerances are too large the buffer height could be too high which would case problem when the backfill is installed. On the other hand, if the tolerances are too small the requirements on installation and production will be difficult and expensive to achieve.

References

SKB's (Svensk Kärnbränslehantering AB) publications can be found at www.skb.com/publications.
SKBdoc documents will be submitted upon request to document@skb.se.

Andersson C, Johansson Å, 2002. Boring of full-scale deposition holes at the Äspö Hard Rock Laboratory. Operational experiences including boring performance and work time analysis. SKB TR-02-26, Svensk Kärnbränslehantering AB.

Hardenby C, 2002. Äspö Hard Rock Laboratory. Tunnel for the canister retrieval test. Geological mapping of tunnel and deposition holes. SKB IPR-02-49, Svensk Kärnbränslehantering AB.

Kronberg H, 2019a. Bestämning av vattenhalt och vattenkvot i bentonitlera. SKBdoc 1419679 ver 2.0, Svensk Kärnbränslehantering AB. (In Swedish.)

Kronberg H, 2019b. Bestämning av skrym- och torrdensitet för bentonitlera. SKBdoc 1431662 ver 2.0, Svensk Kärnbränslehantering AB. (In Swedish.)

Kronberg M, Johannesson L-E, Eriksson P, 2020. Strategy, adaptive design and quality control of bentonite materials for a KBS-3 repository. SKB TR-20-03, Svensk Kärnbränslehantering AB.

Lundgren C, Johannesson L-E, 2020. Optimering av buffertpellets för KBS3. Laboratorieförsök på fyra olika pellets. SKB R-19-25, Svensk Kärnbränslehantering AB (In Swedish.)

Luterkort D, Johannesson L-E, Eriksson P, 2017. Buffer design and installation method. Installation report. SKB TR-17-06, Svensk Kärnbränslehantering AB.

SKB, 2010. Design, production and initial state of the buffer. SKB TR-10-15, Svensk Kärnbränslehantering AB.

Svensson D, Eriksson P, Johannesson L-E, Lundgren C, Bladström T, 2019. Development and testing of methods suitable for quality control of bentonite as KBS-3 buffer and backfill. SKB TR-19-25, Svensk Kärnbränslehantering AB.

Positioning of sensors

◈ RH Sensors, type JUMO or Vaisala

○ Temperature sensors

Block C1 and C2

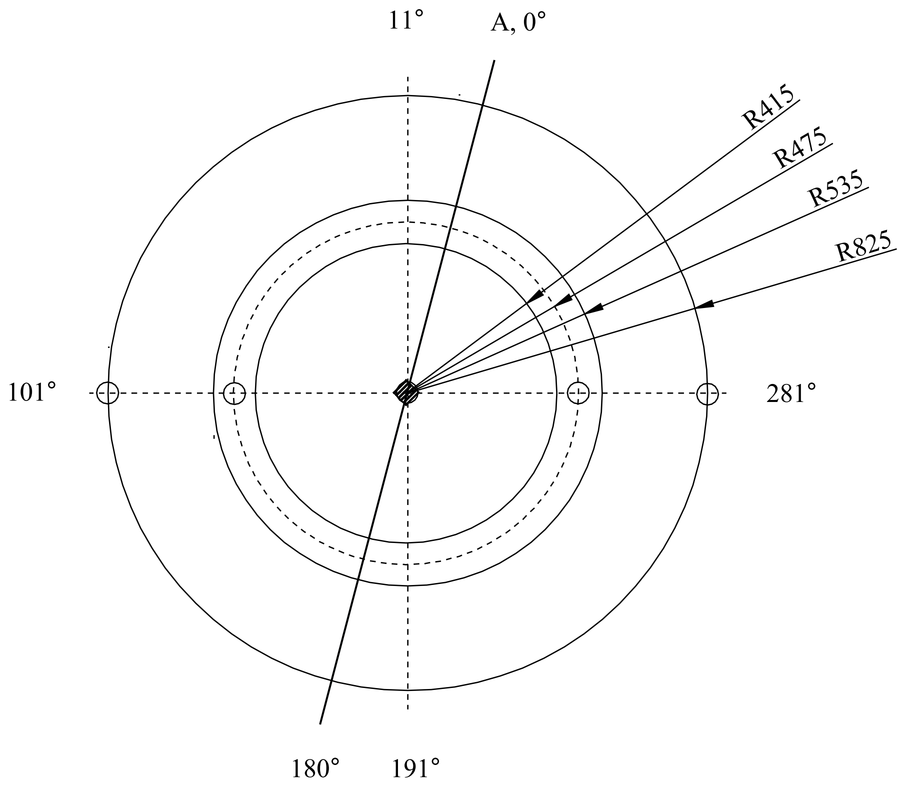

RH sensor type JUMO in block layer C2

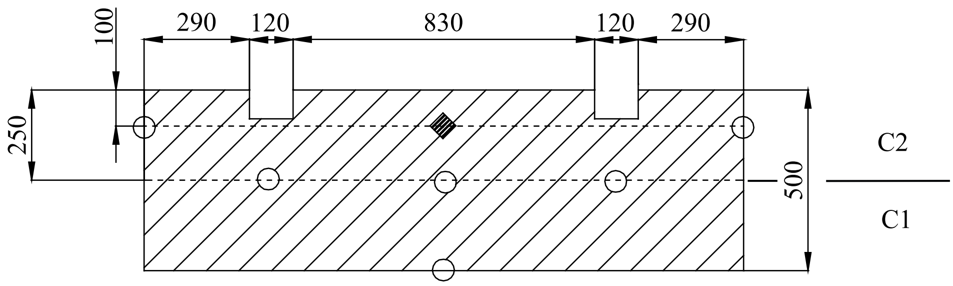

Snitt B-D

Ring R1 och R2

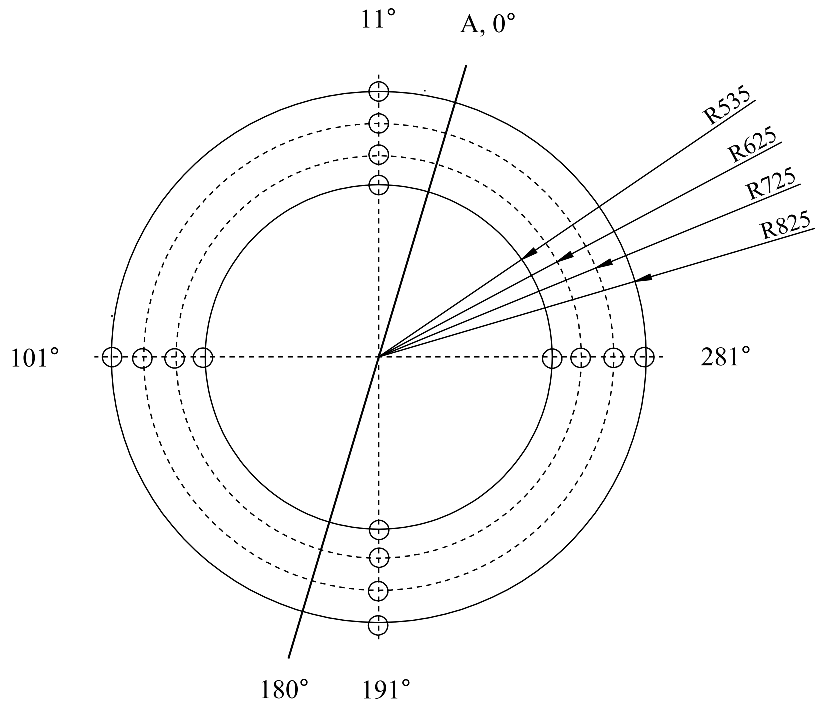

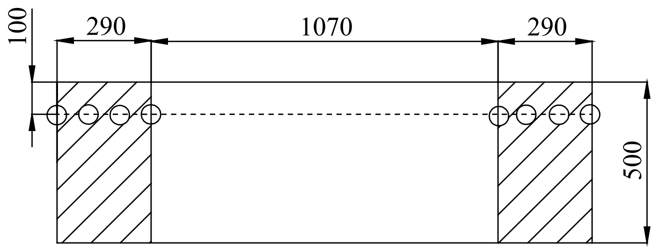

Snitt B-D

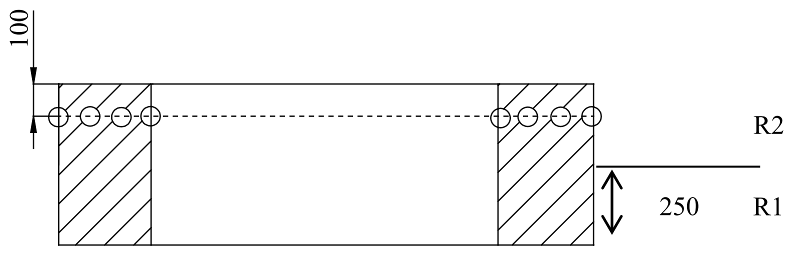

Snitt A-C

Ring R5 och R6. Ring R13 och R14

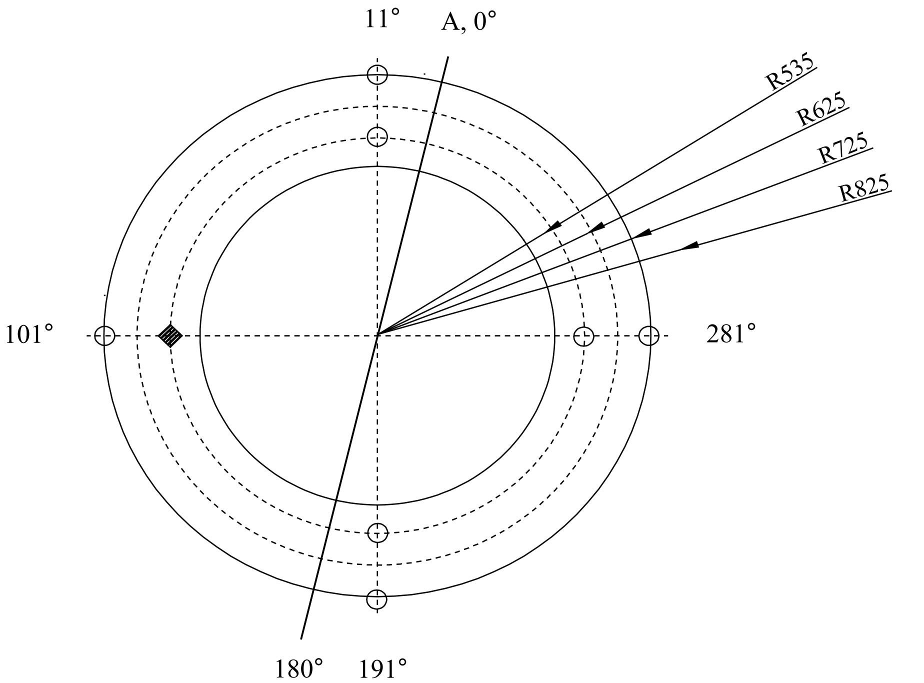

RH givare typ JUMO för R6

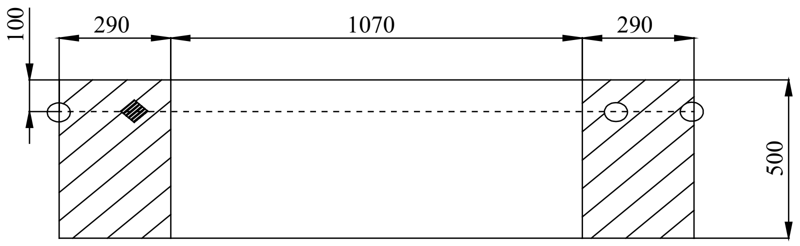

Snitt B-D

RH givare typ Vaisala för R14

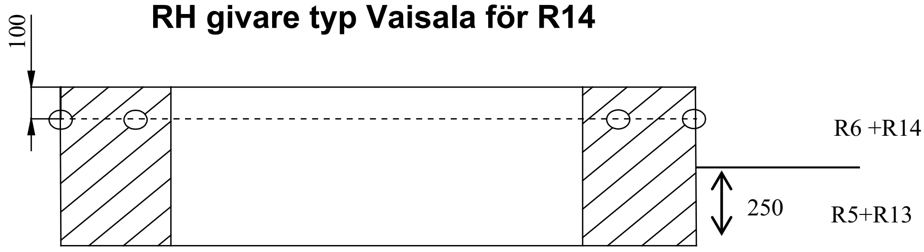

Snitt A-C

Ring R9 och R10. Ring R17 och R18

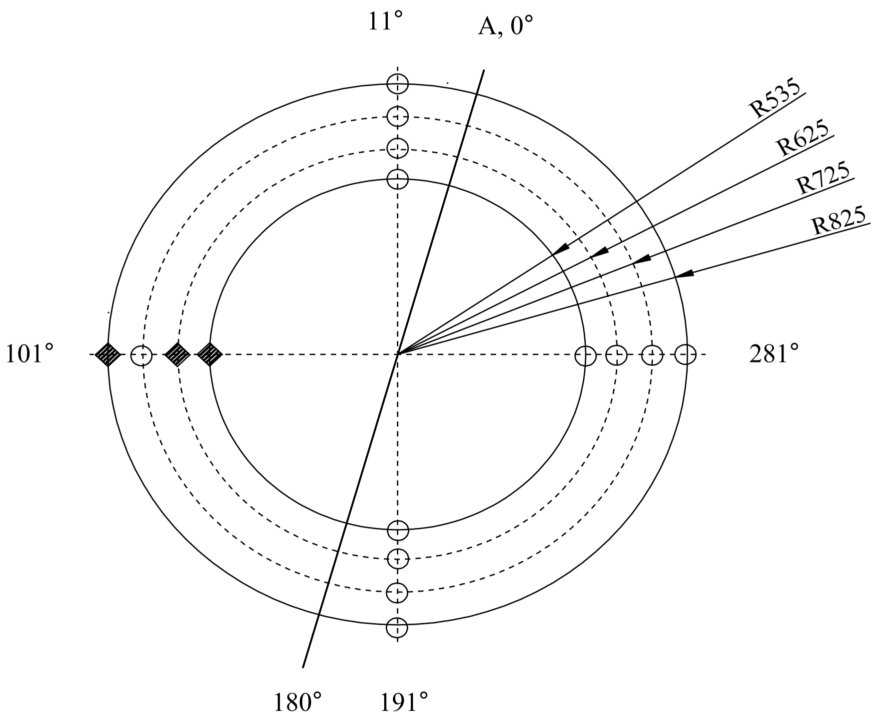

RH givare typ JUMO för R10 3 st

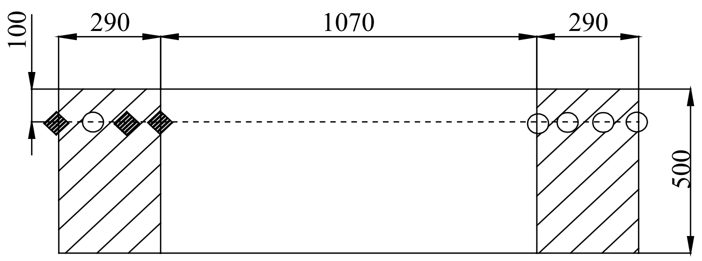

Snitt B-D

RH givare typ Vaisala för R18

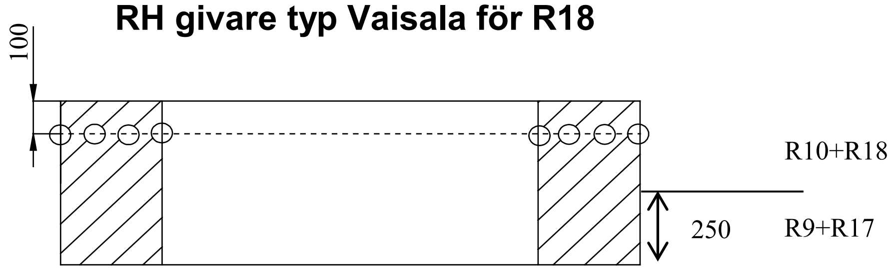

Snitt A-C

Block C3 och C4

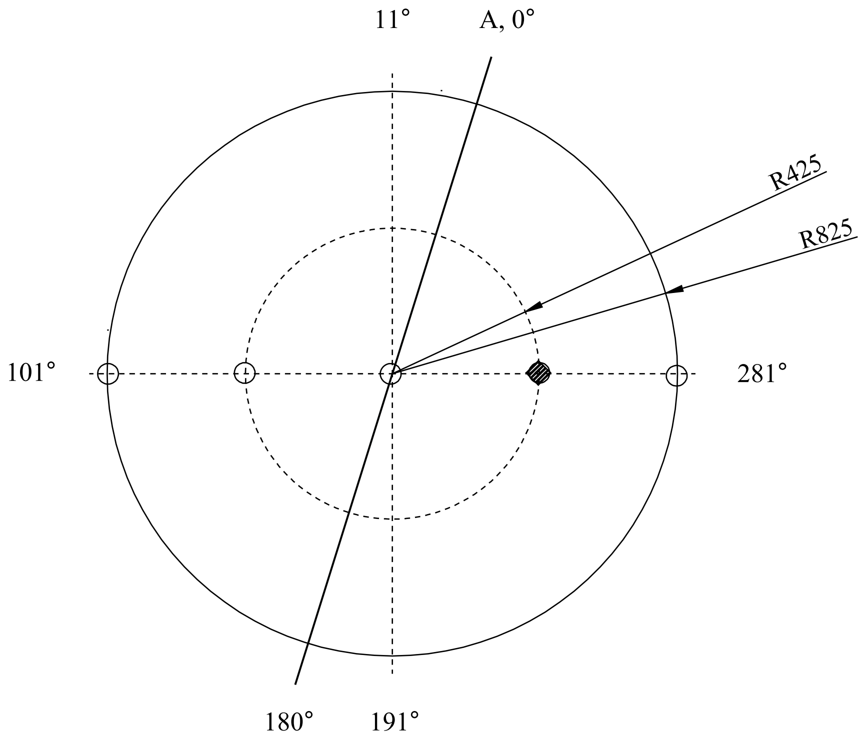

RH givare typ Vaisala för C4

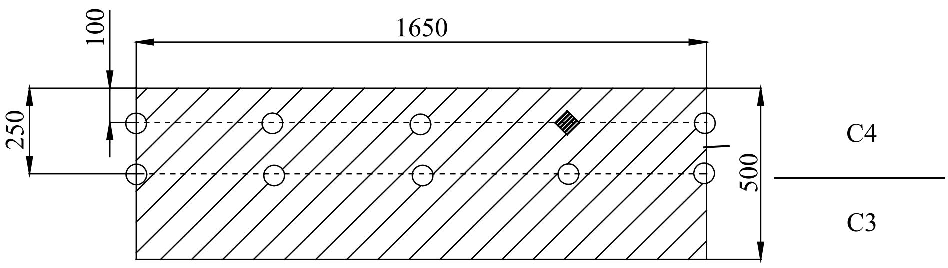

Snitt B-D

Block C5 och C6. Block C7 och C8

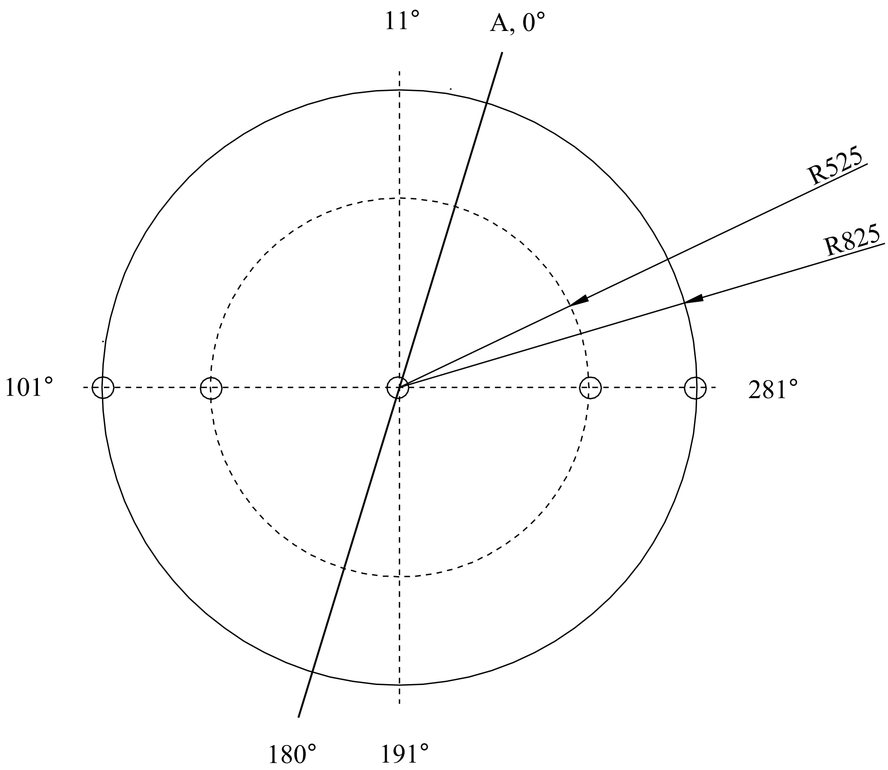

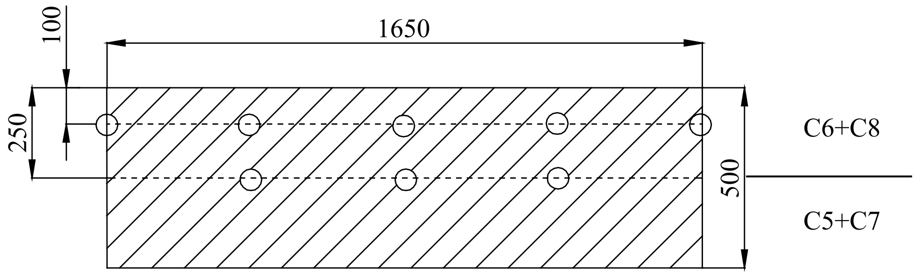

Snitt B-D

Appendix 2

Measurement of gaps between outer blocks, R1–R20 (mm)

Layer	Pos 8–1	Pos 1–2	Pos 2–3	Pos 3–4	Pos 4–5	Pos 5–6	Pos 6–7	Pos 7–8
R1	0	1.5	0	0	0.5	2.5	6.0	0
R2	5.5	0	0.5	0.5	5.0	1.5	1.5	1.0
R3	2.5	2.5	0.5	2.5	1.5	1.5	1.0	2.0
R4	1.5	3.0	0.5	0.5	0	0.5	1.5	2.0
R5	1.0	0	0	0.5	2.5	1.0	0.5	0
R6	1.0	1.0	0	0.5	0.5	1.5	0.5	0
R7	0.5	1.0	0.5	0	1.0	0.5	0.5	0.5
R8	0.5	0.5	0	0.5	1.0	1.0	0.5	0.5
R9	0.5	0.5	0	0.5	1.0	0.5	0.5	2.5
R10	0.5	0.5	0.5	0.5	1.0	1.0	0.5	1.0
R11	1.5	0.5	0	2.5	2.0	1.0	1.0	0.5
R12	0.5	0	0	0	0.5	2.0	2.0	2.5
R13	1.0	1.0	1.0	0	1.5	2.5	0.5	0.5
R14	2.0	0.5	2.0	0.5	2.0	1.0	1.0	0.5
R15	1.5	1.5	0.5	0.5	0.5	2.5	1.5	0.5
R16	0.5	2.0	1.5	1.0	1.0	2.5	2.5	0
R17	1.0	0.5	2.5	2.0	1.0	1.0	0	0.5
R18	0.5	2.0	0.5	1.5	1.0	2.0	0	1.5
R19	0.5	0.5	0.5	2.0	1.0	2.0	1.5	0
R20	0	1.5	0.5	0	1.5	0.5	0.5	0.5

Temperature measurements

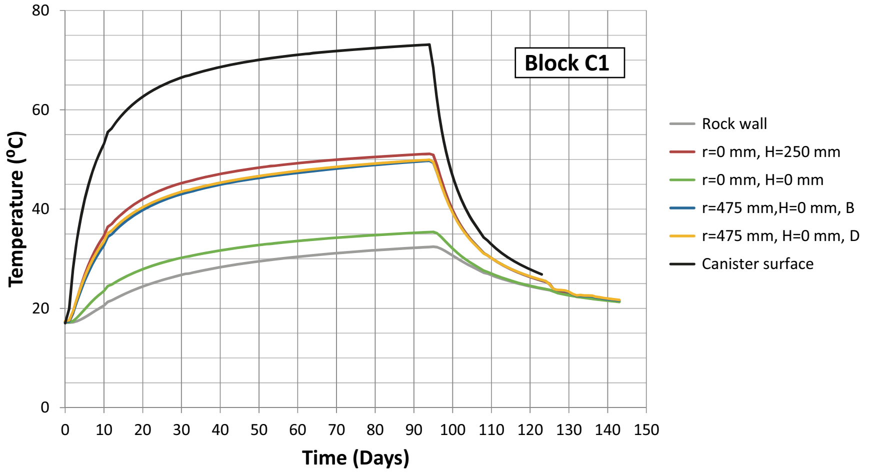

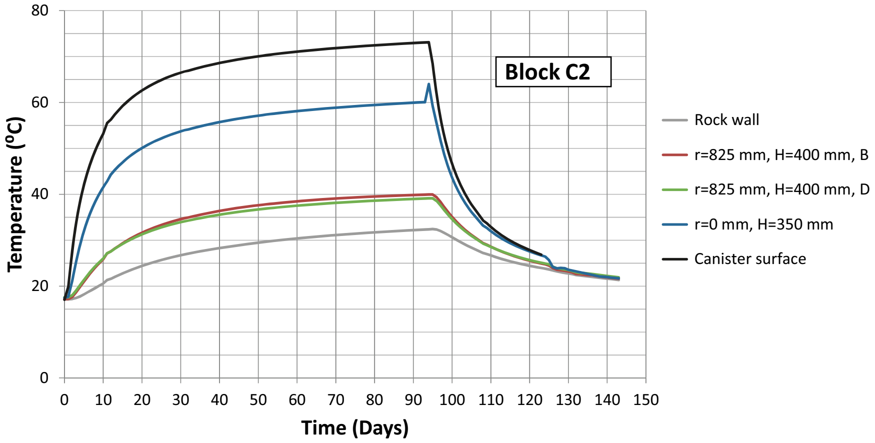

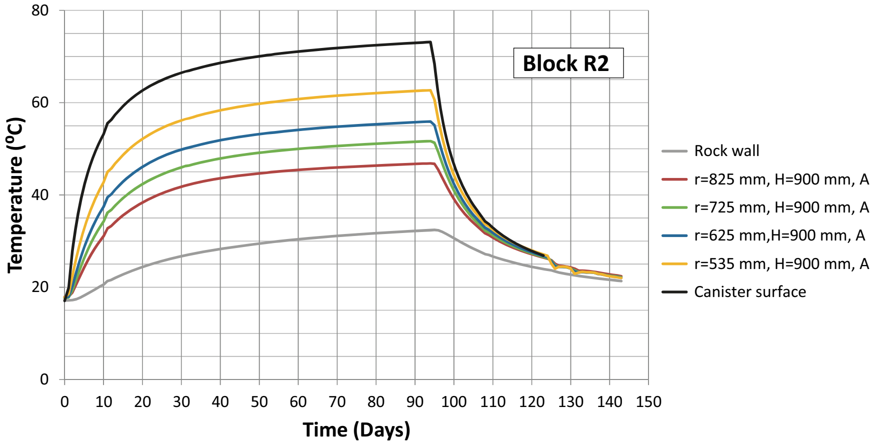

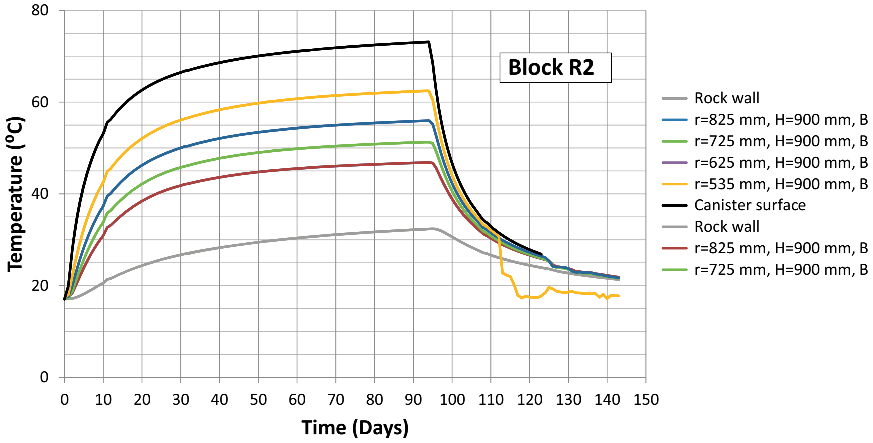
Block R2
Temperature (°C)
Time (Days)
Rock wall
r=825 mm, H=900 mm, B
r=725 mm, H=900 mm, B
r=625 mm, H=900 mm, B
r=535 mm, H=900 mm, B
Canister surface
Rock wall
r=825 mm, H=900 mm, B
r=725 mm, H=900 mm, B

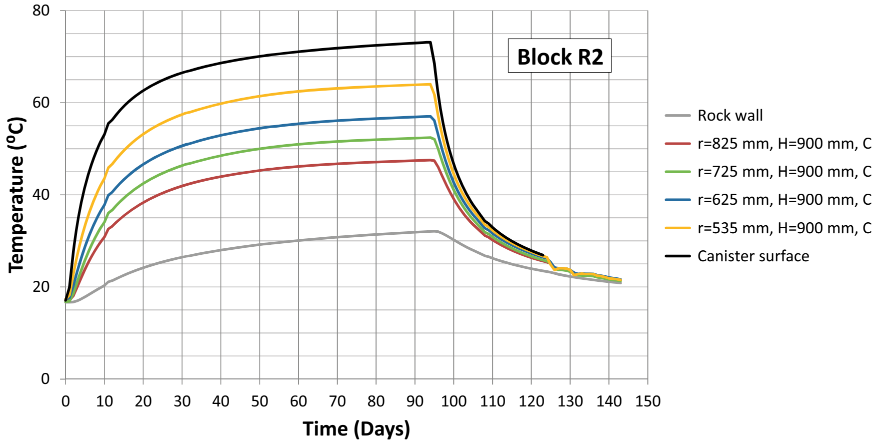
Block R2
Temperature (°C)
Time (Days)
Rock wall
r=825 mm, H=900 mm, C
r=725 mm, H=900 mm, C
r=625 mm, H=900 mm, C
r=535 mm, H=900 mm, C
Canister surface

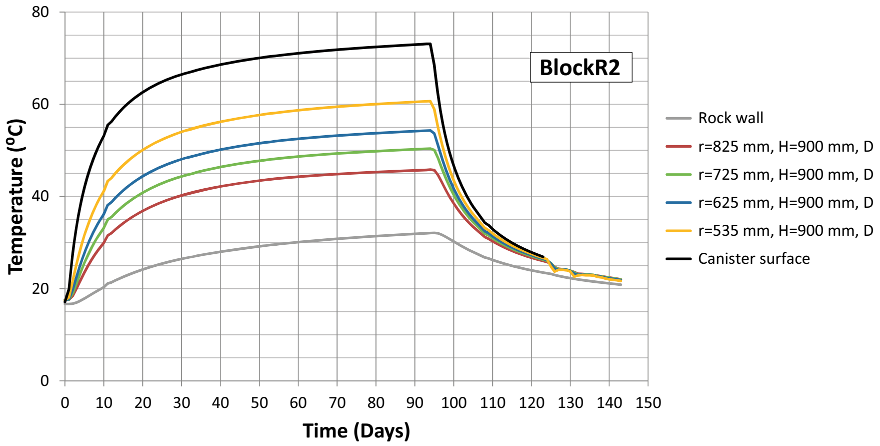
BlockR2
Temperature (°C)
Time (Days)
Rock wall
r=825 mm, H=900 mm, D
r=725 mm, H=900 mm, D
r=625 mm, H=900 mm, D
r=535 mm, H=900 mm, D
Canister surface

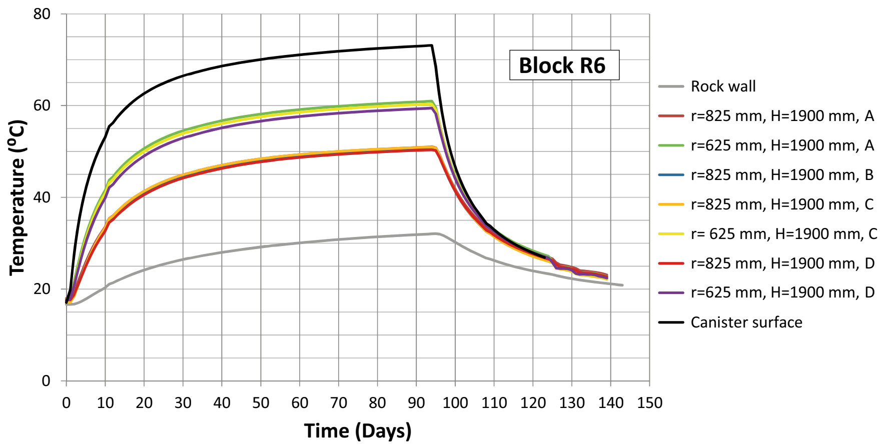
Block R6
Temperature (°C)
Time (Days)
Rock wall
r=825 mm, H=1900 mm, A
r=625 mm, H=1900 mm, A
r=825 mm, H=1900 mm, B
r=825 mm, H=1900 mm, C
r= 625 mm, H=1900 mm, C
r=825 mm, H=1900 mm, D
r=625 mm, H=1900 mm, D
Canister surface

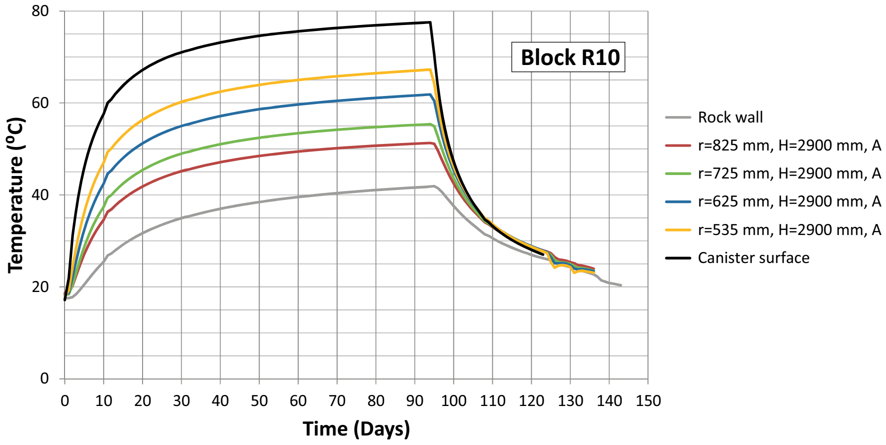
Block R10
Temperature (ºC)
Time (Days)
Rock wall
r=825 mm, H=2900 mm, A
r=725 mm, H=2900 mm, A
r=625 mm, H=2900 mm, A
r=535 mm, H=2900 mm, A
Canister surface

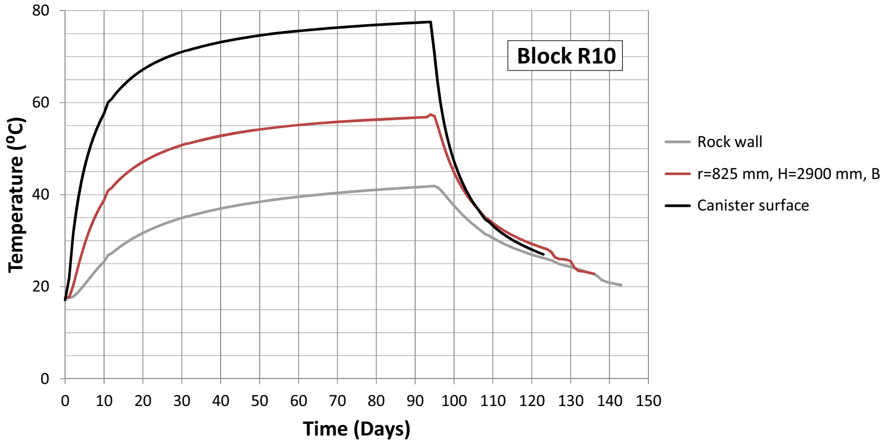
Block R10
Temperature (ºC)
Time (Days)
Rock wall
r=825 mm, H=2900 mm, B
Canister surface

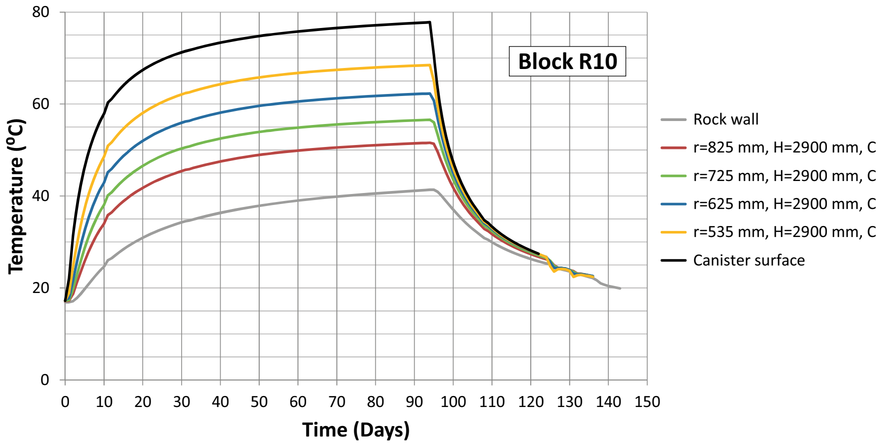
Block R10
Temperature (ºC)
Time (Days)
Rock wall
r=825 mm, H=2900 mm, C
r=725 mm, H=2900 mm, C
r=625 mm, H=2900 mm, C
r=535 mm, H=2900 mm, C
Canister surface

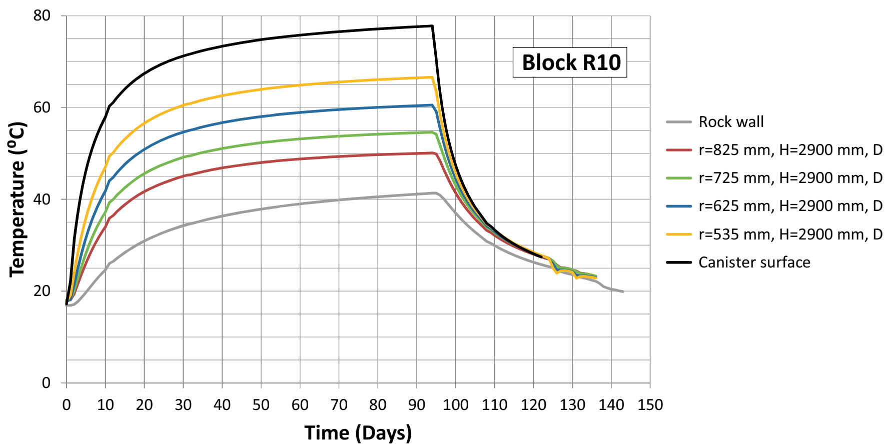
Block R10
Temperature (ºC)
Time (Days)
Rock wall
r=825 mm, H=2900 mm, D
r=725 mm, H=2900 mm, D
r=625 mm, H=2900 mm, D
r=535 mm, H=2900 mm, D
Canister surface

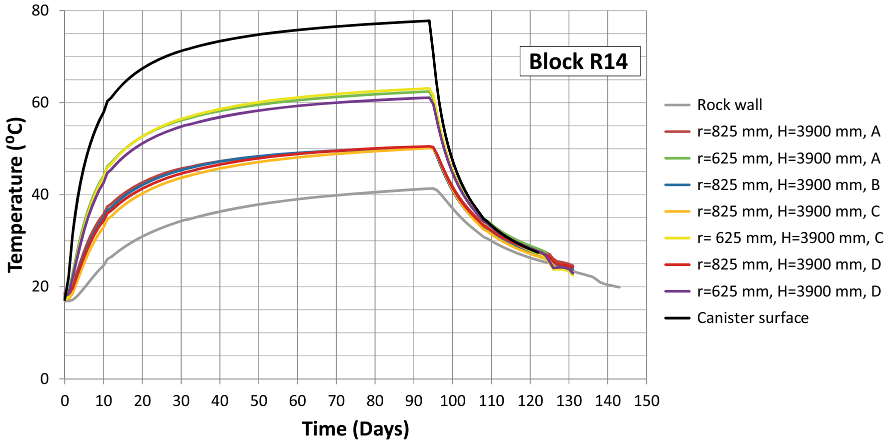
Block R14
Temperature (°C)
Time (Days)
Rock wall
r=825 mm, H=3900 mm, A
r=625 mm, H=3900 mm, A
r=825 mm, H=3900 mm, B
r=825 mm, H=3900 mm, C
r= 625 mm, H=3900 mm, C
r=825 mm, H=3900 mm, D
r=625 mm, H=3900 mm, D
Canister surface

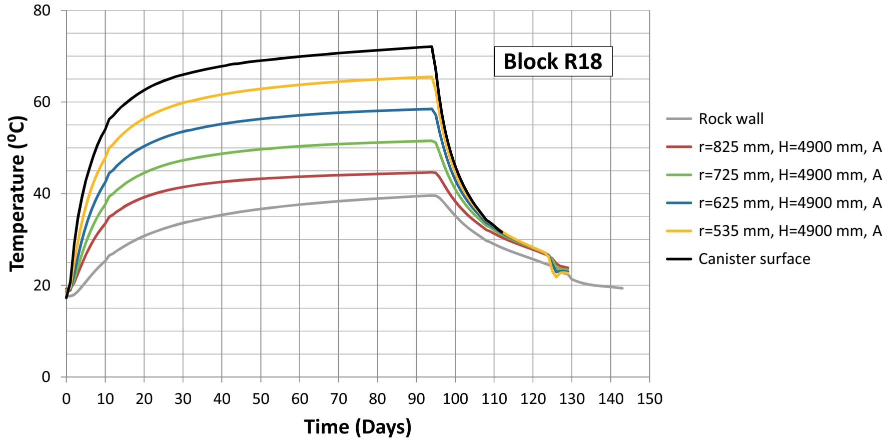
Block R18
Temperature (°C)
Time (Days)
Rock wall
r=825 mm, H=4900 mm, A
r=725 mm, H=4900 mm, A
r=625 mm, H=4900 mm, A
r=535 mm, H=4900 mm, A
Canister surface

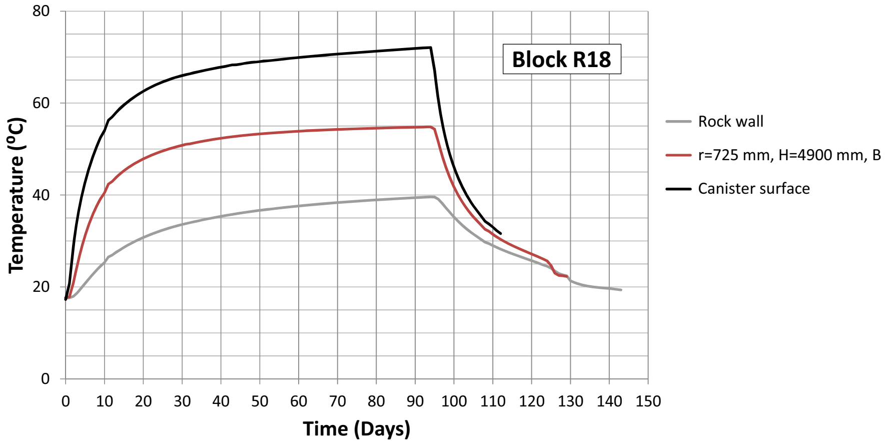
Block R18
Temperature (°C)
Time (Days)
Rock wall
r=725 mm, H=4900 mm, B
Canister surface

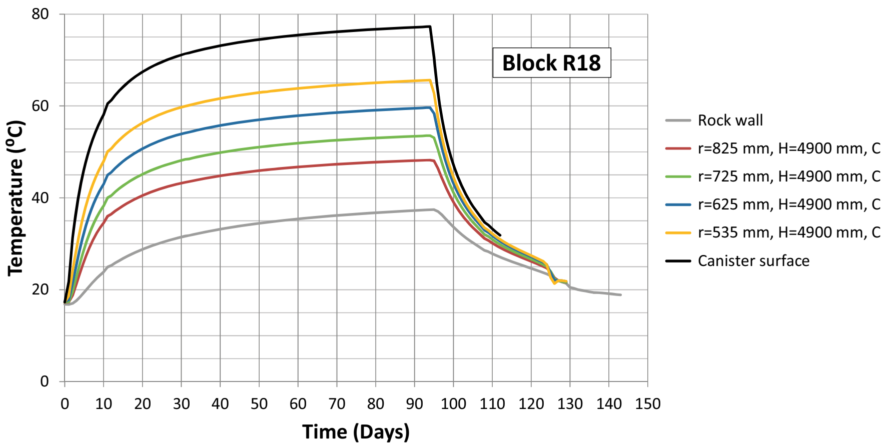
Block R18
Temperature (°C)
Time (Days)
Rock wall
r=825 mm, H=4900 mm, C
r=725 mm, H=4900 mm, C
r=625 mm, H=4900 mm, C
r=535 mm, H=4900 mm, C
Canister surface

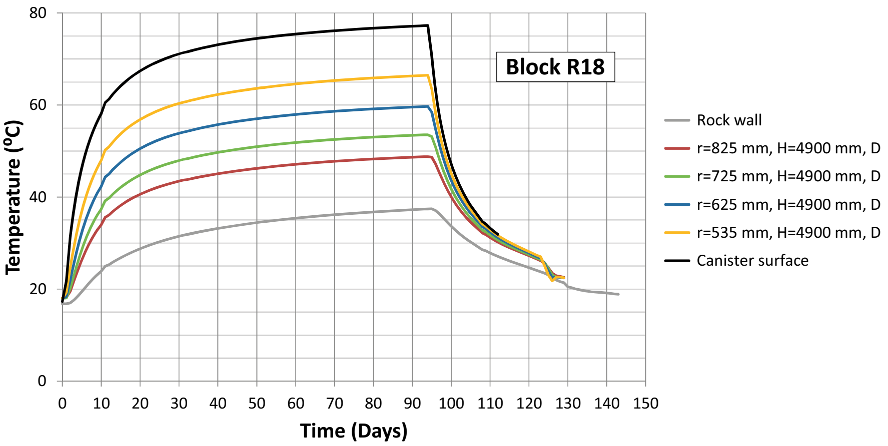
Block R18
Temperature (ºC)
Time (Days)
Rock wall
r=825 mm, H=4900 mm, D
r=725 mm, H=4900 mm, D
r=625 mm, H=4900 mm, D
r=535 mm, H=4900 mm, D
Canister surface

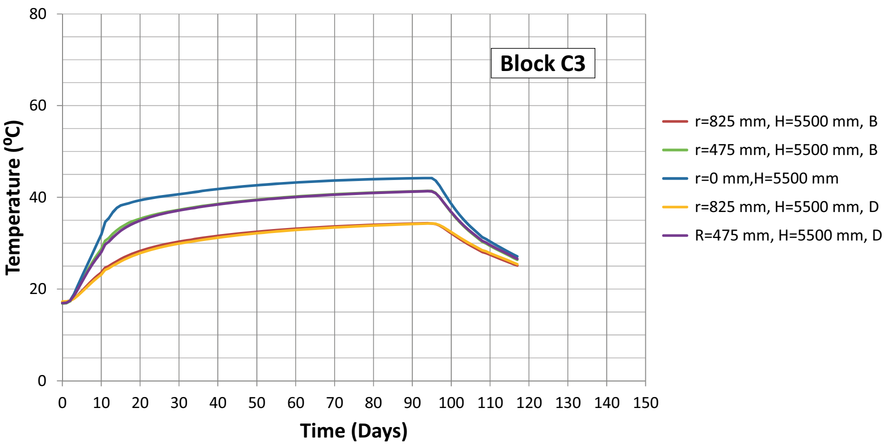
Block C3
Temperature (ºC)
Time (Days)
r=825 mm, H=5500 mm, B
r=475 mm, H=5500 mm, B
r=0 mm,H=5500 mm
r=825 mm, H=5500 mm, D
R=475 mm, H=5500 mm, D

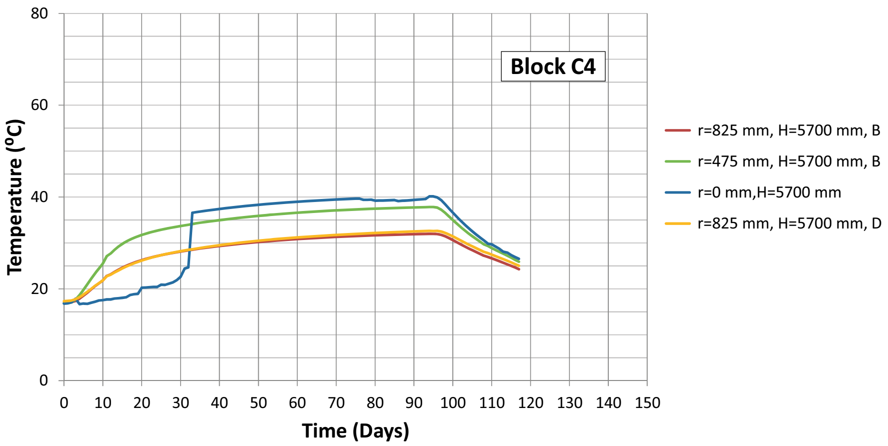
Block C4
Temperature (ºC)
Time (Days)
r=825 mm, H=5700 mm, B
r=475 mm, H=5700 mm, B
r=0 mm,H=5700 mm
r=825 mm, H=5700 mm, D

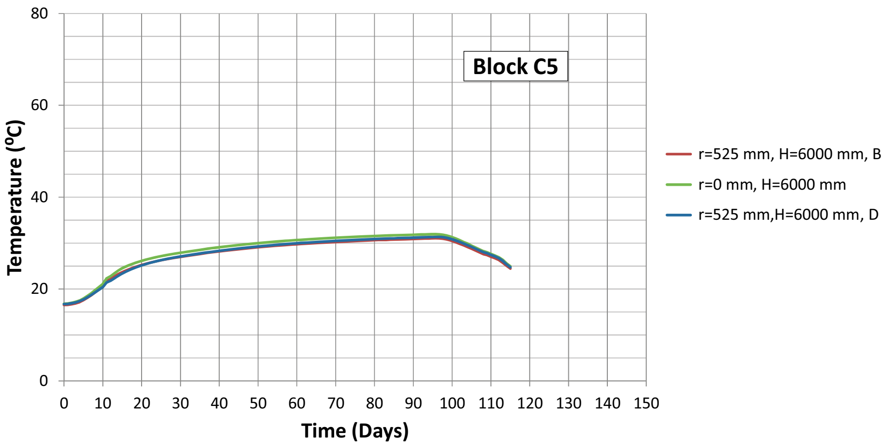
Block C5
Temperature (ºC)
Time (Days)
r=525 mm, H=6000 mm, B
r=0 mm, H=6000 mm
r=525 mm,H=6000 mm, D

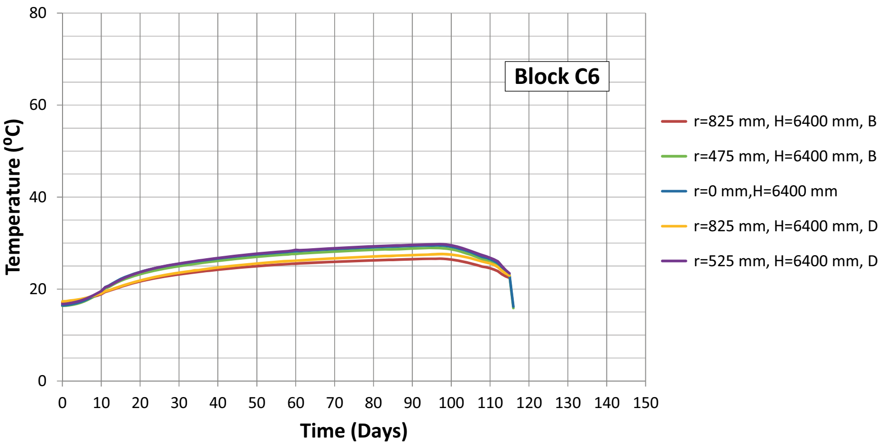
Block C6
Temperature (ºC)
Time (Days)
0
20
40
60
80
0
10
20
30
40
50
60
70
80
90
100
110
120
130
140
150
r=825 mm, H=6400 mm, B
r=475 mm, H=6400 mm, B
r=0 mm,H=6400 mm
r=825 mm, H=6400 mm, D
r=525 mm, H=6400 mm, D

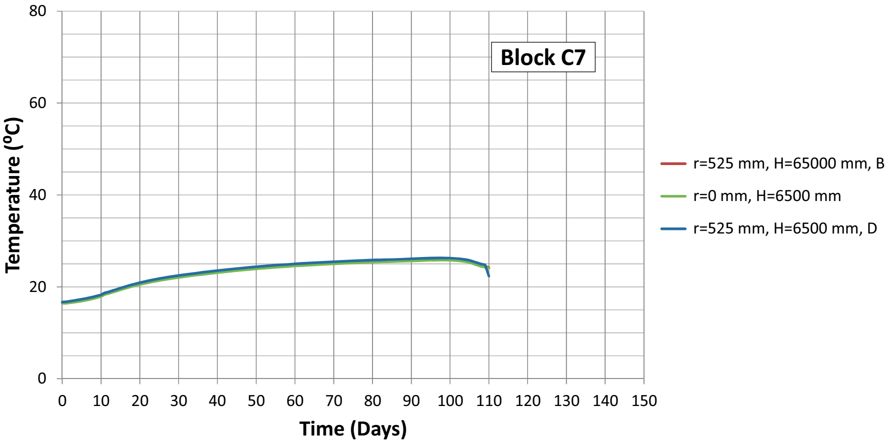
Block C7
Temperature (ºC)
Time (Days)
0
20
40
60
80
0
10
20
30
40
50
60
70
80
90
100
110
120
130
140
150
r=525 mm, H=65000 mm, B
r=0 mm, H=6500 mm
r=525 mm, H=6500 mm, D

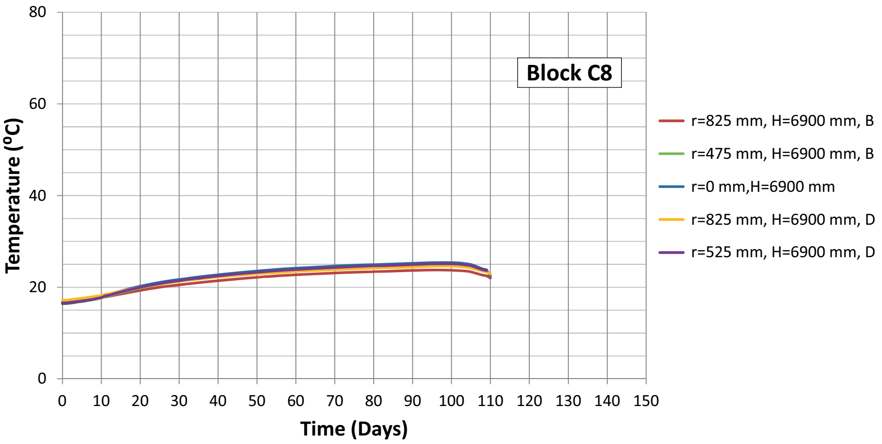
Block C8
Temperature (ºC)
Time (Days)
0
20
40
60
80
0
10
20
30
40
50
60
70
80
90
100
110
120
130
140
150
r=825 mm, H=6900 mm, B
r=475 mm, H=6900 mm, B
r=0 mm,H=6900 mm
r=825 mm, H=6900 mm, D
r=525 mm, H=6900 mm, D

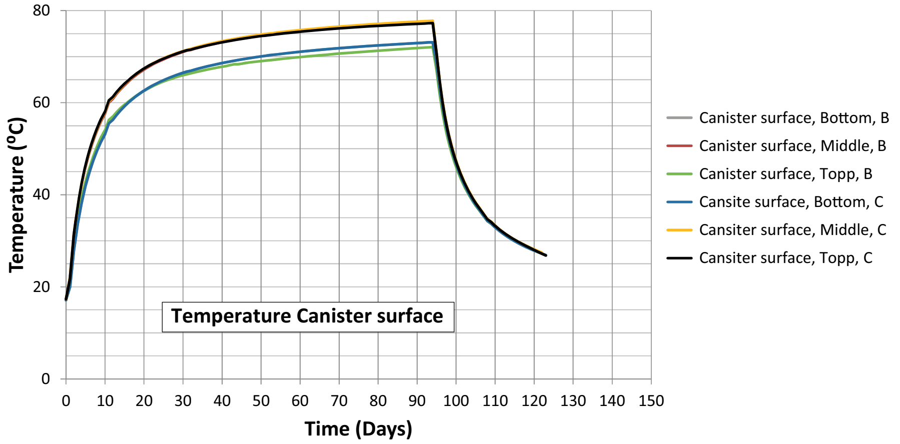
Temperature (ºC)
0
20
40
60
80
0 10 20 30 40 50 60 70 80 90 100 110 120 130 140 150
Time (Days)
Temperature Canister surface
Canister surface, Bottom, B
Canister surface, Middle, B
Canister surface, Topp, B
Cansite surface, Bottom, C
Cansiter surface, Middle, C
Cansiter surface, Topp, C

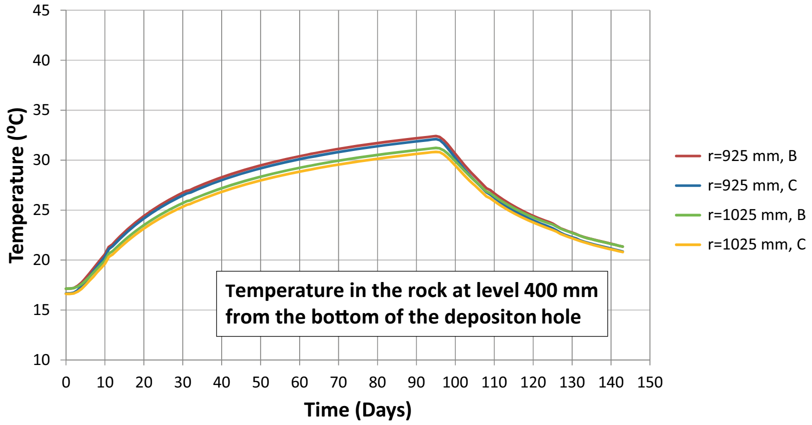
Temperature (ºC)
10
15
20
25
30
35
40
45
0 10 20 30 40 50 60 70 80 90 100 110 120 130 140 150
Time (Days)
Temperature in the rock at level 400 mm
from the bottom of the depositon hole
r=925 mm, B
r=925 mm, C
r=1025 mm, B
r=1025 mm, C

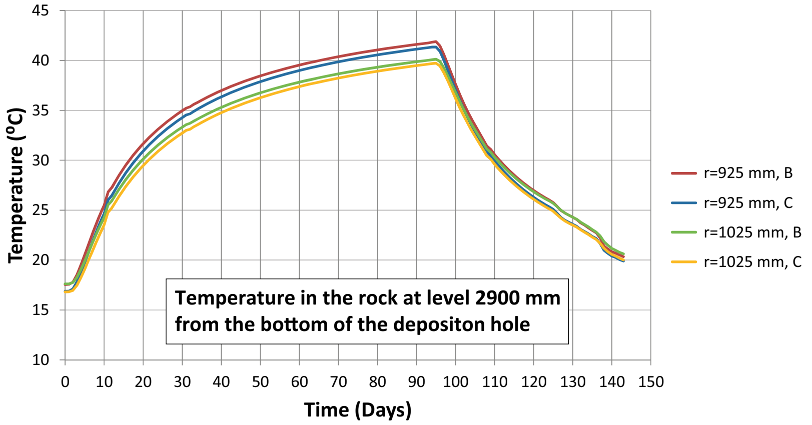
Temperature (ºC)
10
15
20
25
30
35
40
45
0 10 20 30 40 50 60 70 80 90 100 110 120 130 140 150
Time (Days)
Temperature in the rock at level 2900 mm
from the bottom of the depositon hole
r=925 mm, B
r=925 mm, C
r=1025 mm, B
r=1025 mm, C

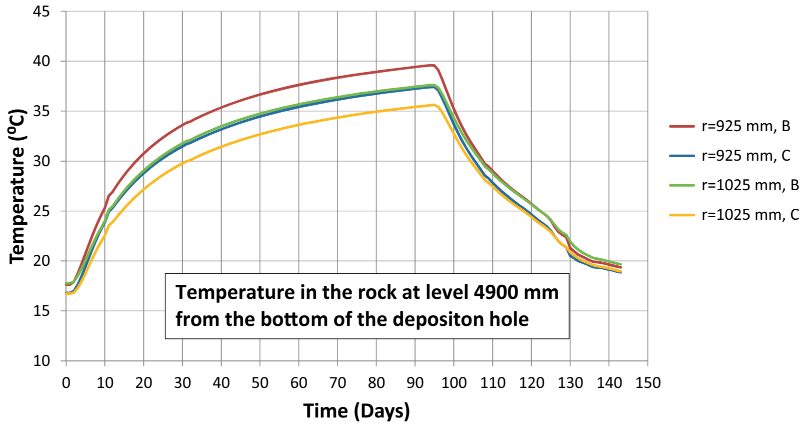
Temperature (ºC)
10
15
20
25
30
35
40
45
0 10 20 30 40 50 60 70 80 90 100 110 120 130 140 150
Time (Days)
Temperature in the rock at level 4900 mm
from the bottom of the depositon hole
r=925 mm, B
r=925 mm, C
r=1025 mm, B
r=1025 mm, C

Water content and density

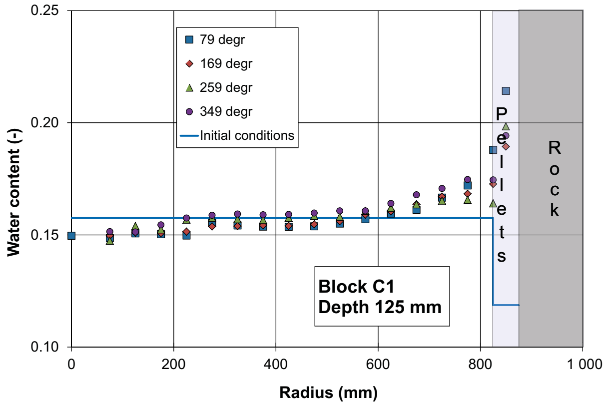

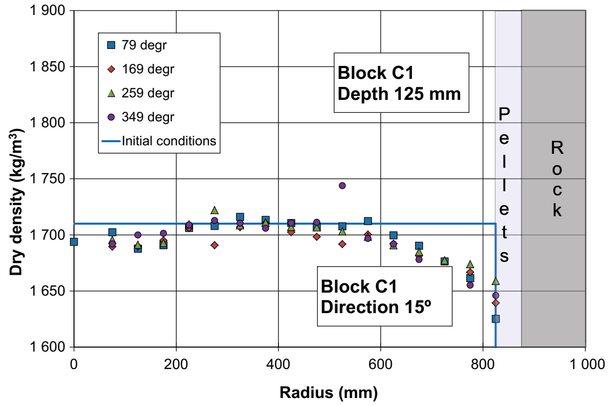

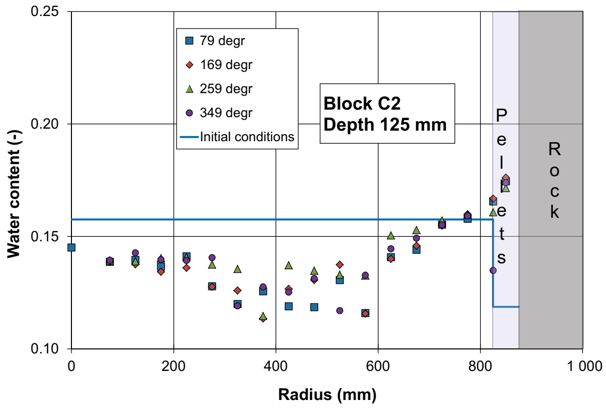

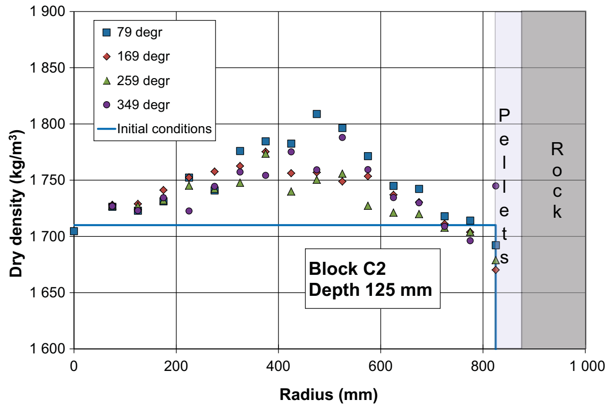

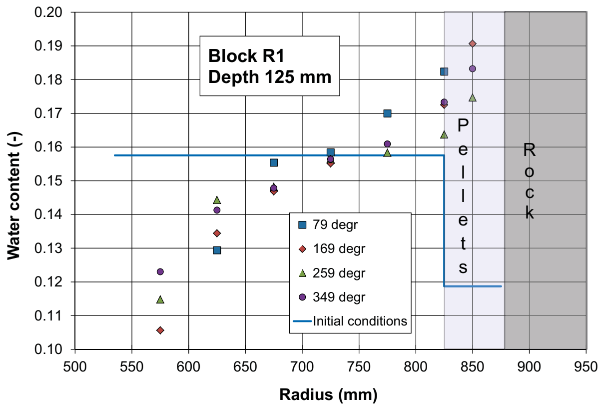

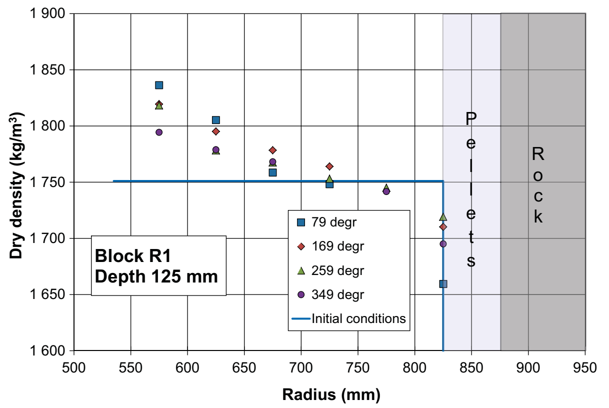

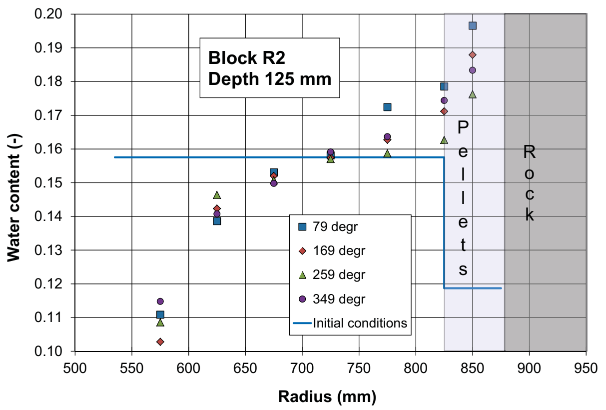

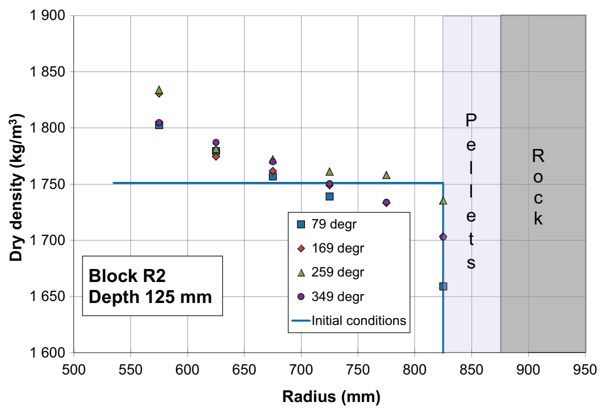

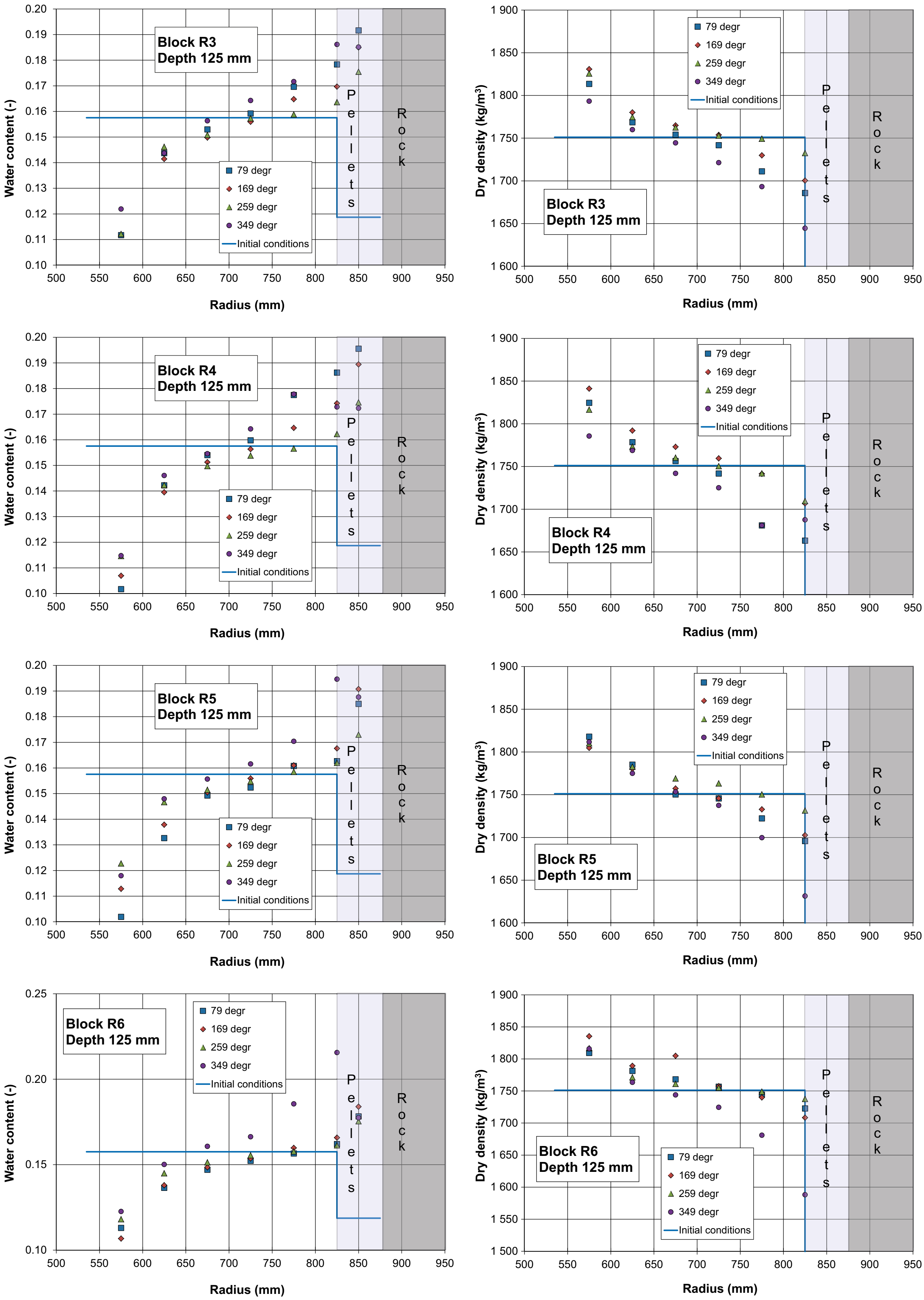
Block R3
Depth 125 mm
Block R4
Depth 125 mm
Block R5
Depth 125 mm
Block R6
Depth 125 mm
Water content (-)
Dry density (kg/m³)
Radius (mm)
79 degr
169 degr
259 degr
349 degr
Initial conditions
Pellets
Rock

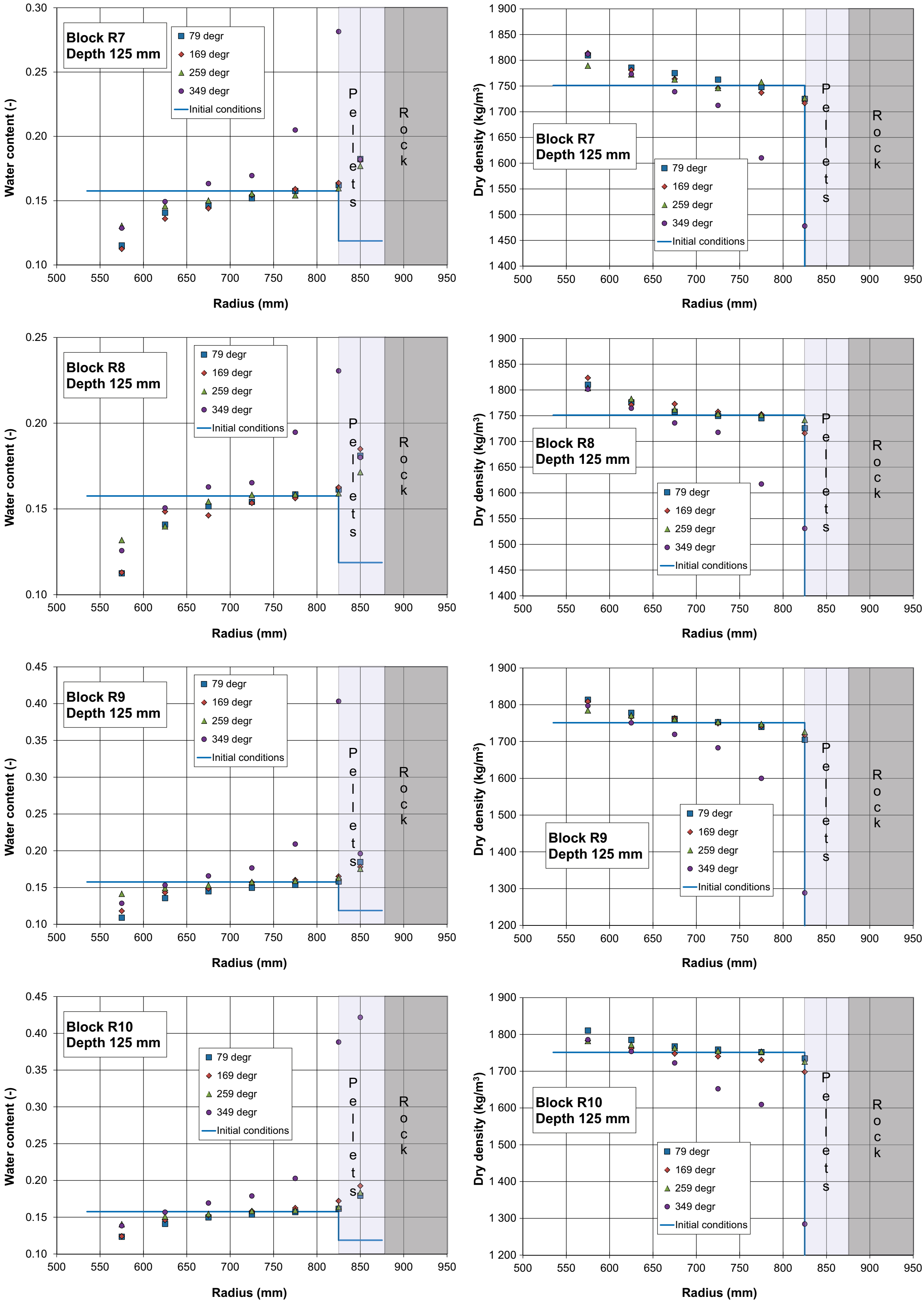
Block R7
Depth 125 mm
Block R8
Depth 125 mm
Block R9
Depth 125 mm
Block R10
Depth 125 mm
79 degr
169 degr
259 degr
349 degr
Initial conditions
Pellets
Rock
Water content (-)
Dry density (kg/m³)
Radius (mm)

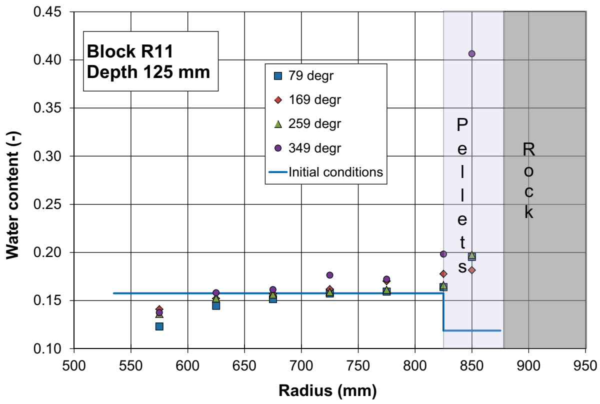
Block R11
Depth 125 mm
79 degr
169 degr
259 degr
349 degr
Initial conditions
Pellets
Rock
Water content (-)
Radius (mm)

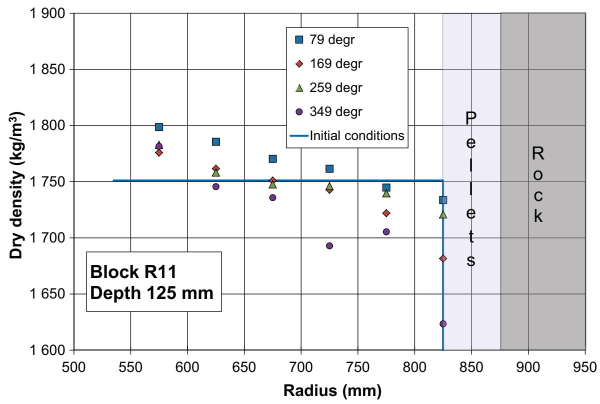
Block R11
Depth 125 mm
79 degr
169 degr
259 degr
349 degr
Initial conditions
Pellets
Rock
Dry density (kg/m³)
Radius (mm)

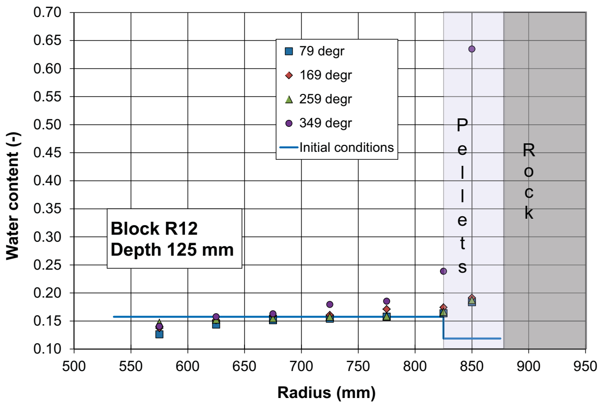
Block R12
Depth 125 mm
79 degr
169 degr
259 degr
349 degr
Initial conditions
Pellets
Rock
Water content (-)
Radius (mm)

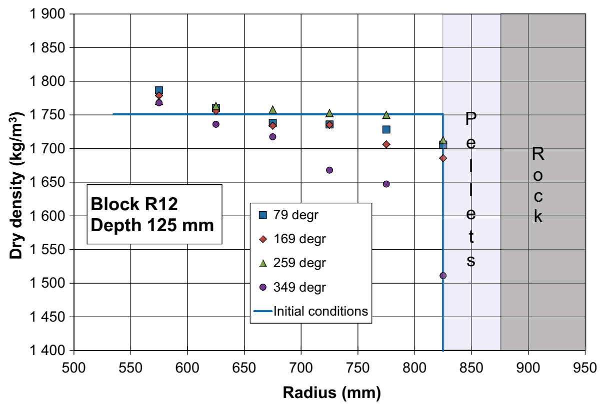
Block R12
Depth 125 mm
79 degr
169 degr
259 degr
349 degr
Initial conditions
Pellets
Rock
Dry density (kg/m³)
Radius (mm)

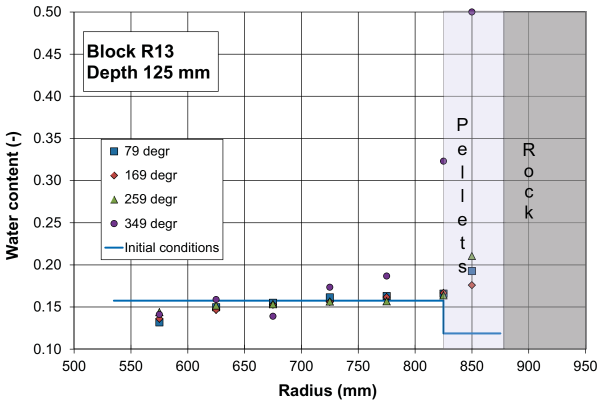
Block R13
Depth 125 mm
79 degr
169 degr
259 degr
349 degr
Initial conditions
Pellets
Rock
Water content (-)
Radius (mm)

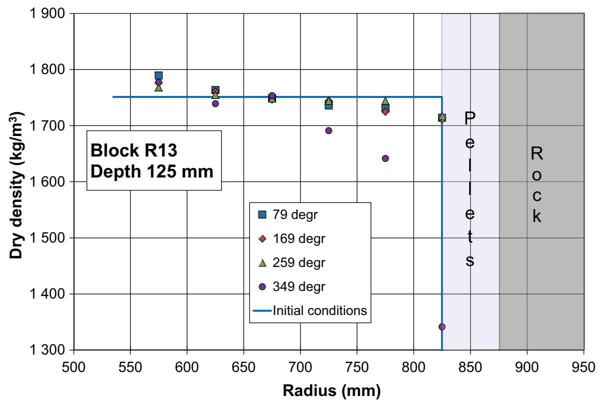
Block R13
Depth 125 mm
79 degr
169 degr
259 degr
349 degr
Initial conditions
Pellets
Rock
Dry density (kg/m³)
Radius (mm)

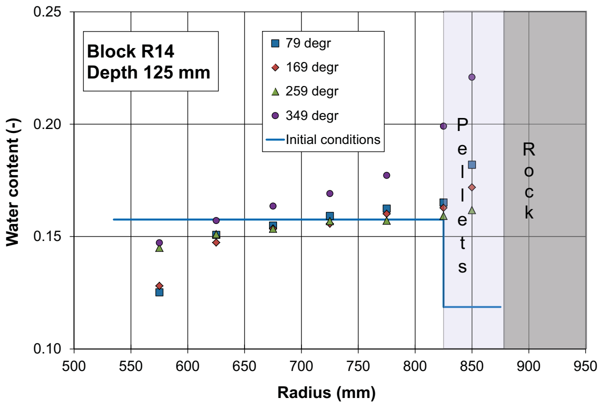
Block R14
Depth 125 mm
79 degr
169 degr
259 degr
349 degr
Initial conditions
Pellets
Rock
Water content (-)
Radius (mm)

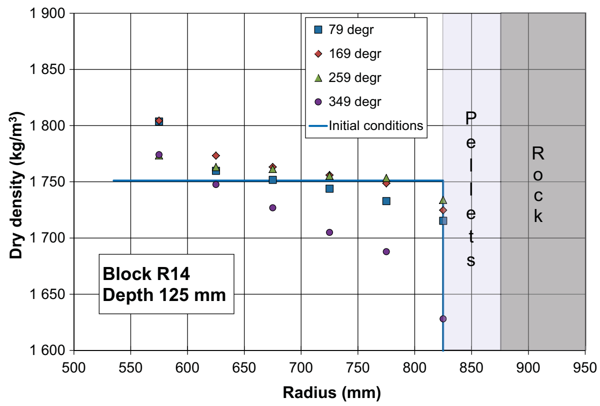
Block R14
Depth 125 mm
79 degr
169 degr
259 degr
349 degr
Initial conditions
Pellets
Rock
Dry density (kg/m³)
Radius (mm)

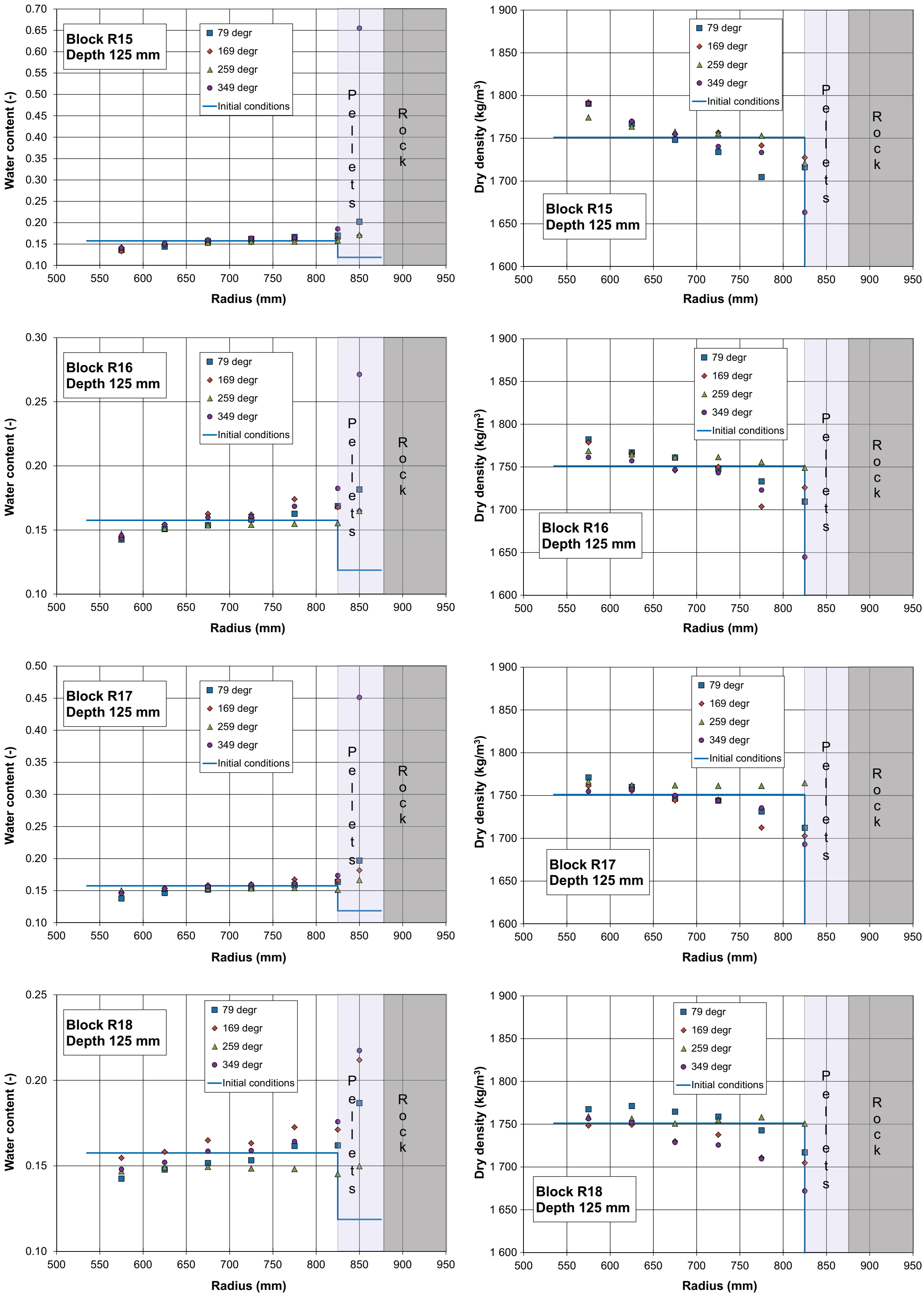
Block R15
Depth 125 mm
Block R16
Depth 125 mm
Block R17
Depth 125 mm
Block R18
Depth 125 mm
79 degr
169 degr
259 degr
349 degr
Initial conditions
Pellets
Rock
Water content (-)
Dry density (kg/m³)
Radius (mm)

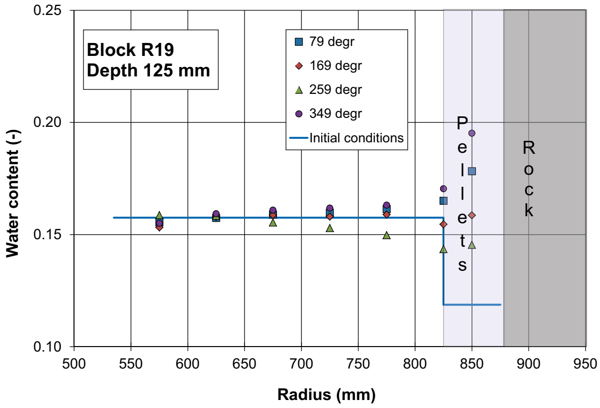
Block R19
Depth 125 mm
79 degr
169 degr
259 degr
349 degr
Initial conditions
Pellets
Rock
Water content (-)
Radius (mm)
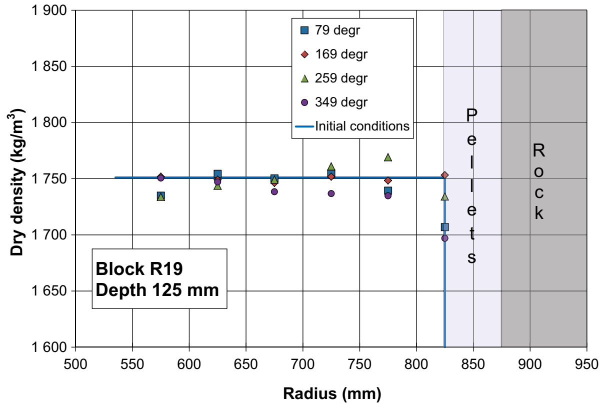
Block R19
Depth 125 mm
79 degr
169 degr
259 degr
349 degr
Initial conditions
Pellets
Rock
Dry density (kg/m3)
Radius (mm)
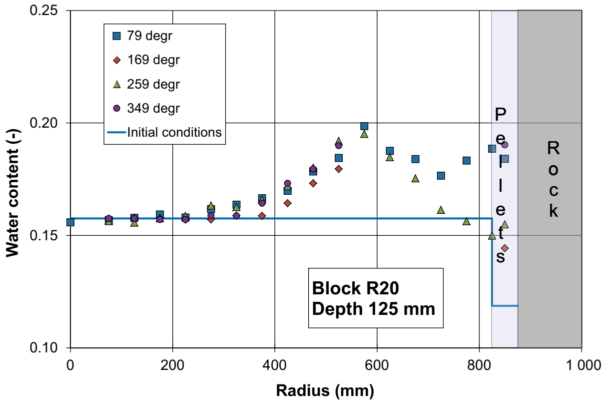
Block R20
Depth 125 mm
79 degr
169 degr
259 degr
349 degr
Initial conditions
Pellets
Rock
Water content (-)
Radius (mm)
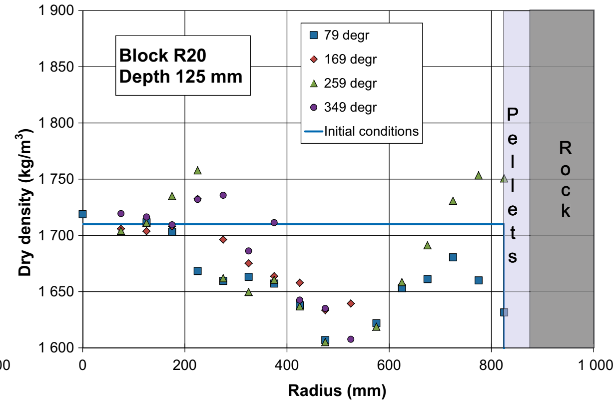
Block R20
Depth 125 mm
79 degr
169 degr
259 degr
349 degr
Initial conditions
Pellets
Rock
Dry density (kg/m3)
Radius (mm)
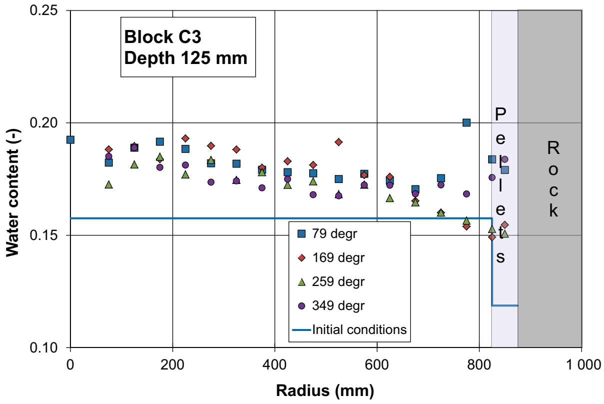
Block C3
Depth 125 mm
79 degr
169 degr
259 degr
349 degr
Initial conditions
Pellets
Rock
Water content (-)
Radius (mm)
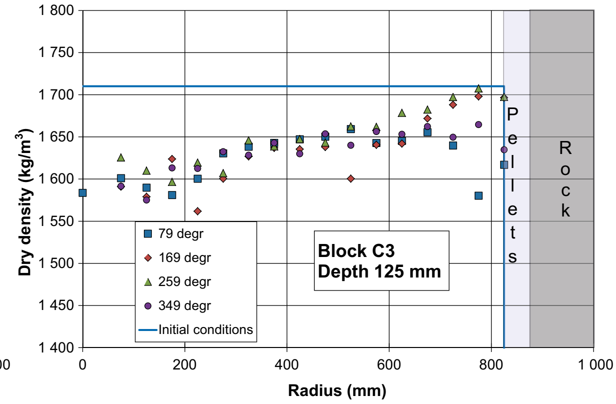
Block C3
Depth 125 mm
79 degr
169 degr
259 degr
349 degr
Initial conditions
Pellets
Rock
Dry density (kg/m3)
Radius (mm)
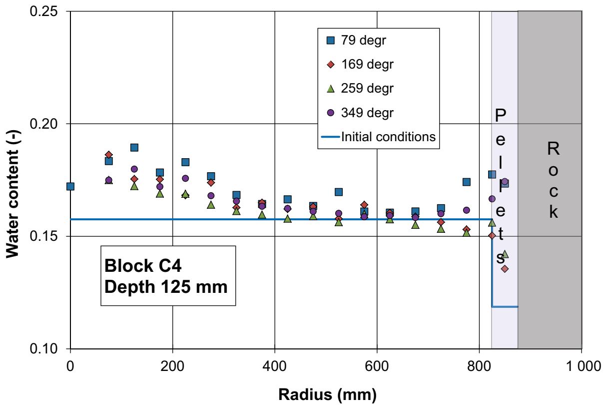
Block C4
Depth 125 mm
79 degr
169 degr
259 degr
349 degr
Initial conditions
Pellets
Rock
Water content (-)
Radius (mm)
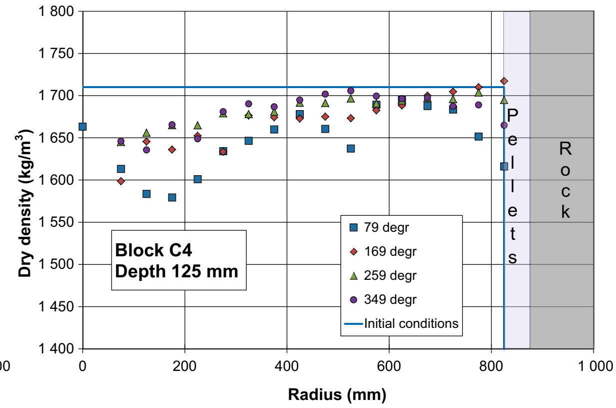
Block C4
Depth 125 mm
79 degr
169 degr
259 degr
349 degr
Initial conditions
Pellets
Rock
Dry density (kg/m3)
Radius (mm)

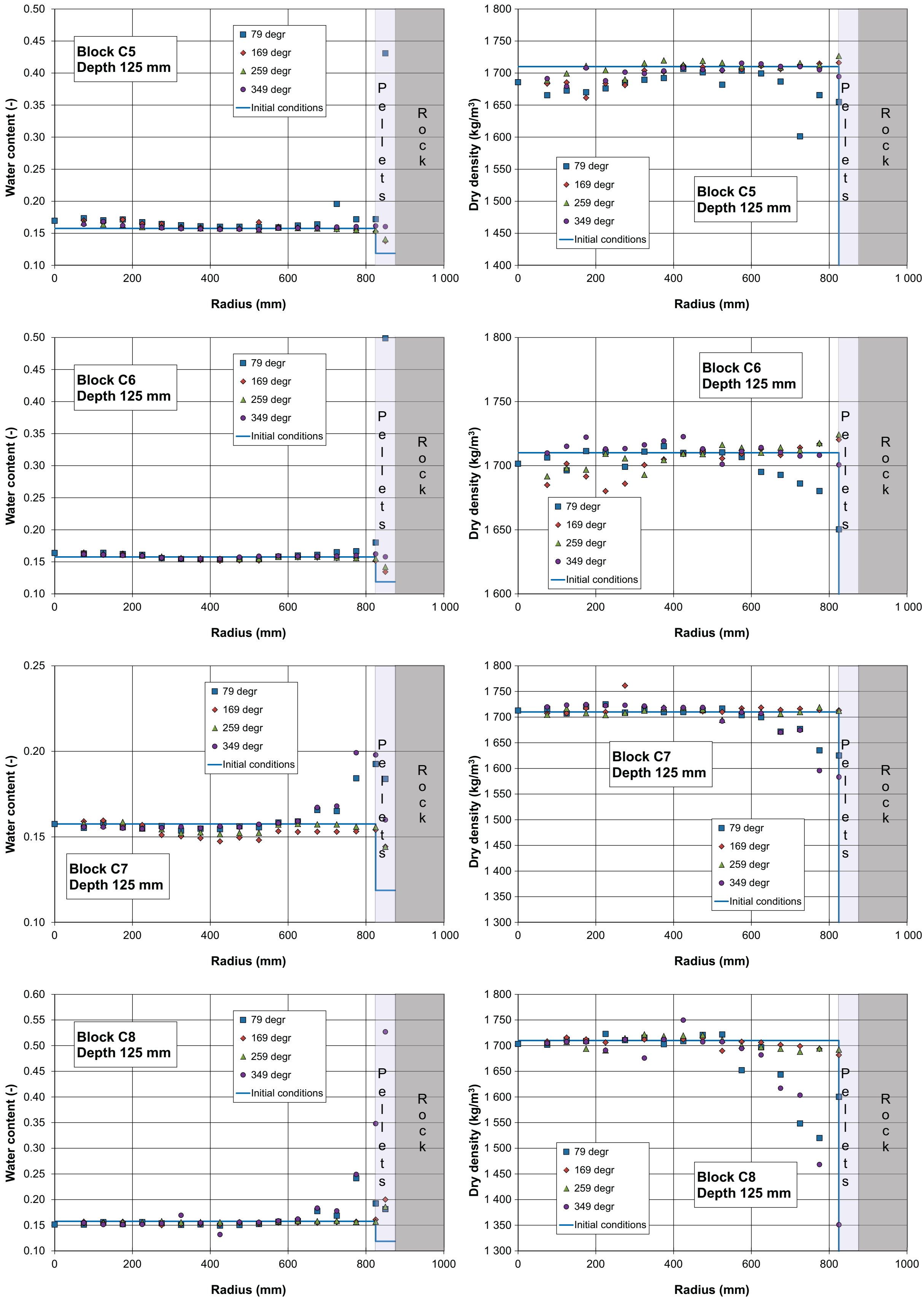
Block C5
Depth 125 mm
Block C6
Depth 125 mm
Block C7
Depth 125 mm
Block C8
Depth 125 mm
79 degr
169 degr
259 degr
349 degr
Initial conditions
Pellets
Rock
Water content (-)
Dry density (kg/m³)
Radius (mm)

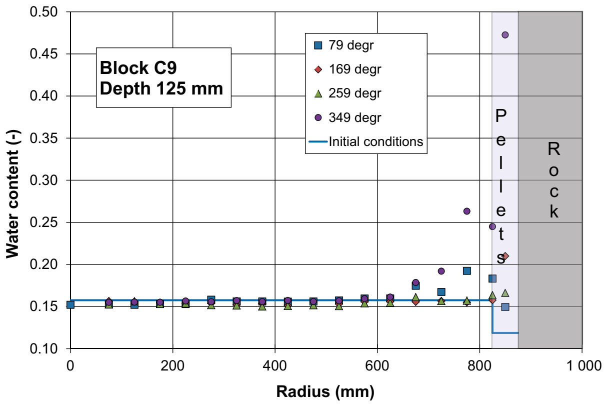

Block C9
Depth 125 mm
79 degr
169 degr
259 degr
349 degr
Initial conditions
Pellets
Rock
Water content (-)
Radius (mm)

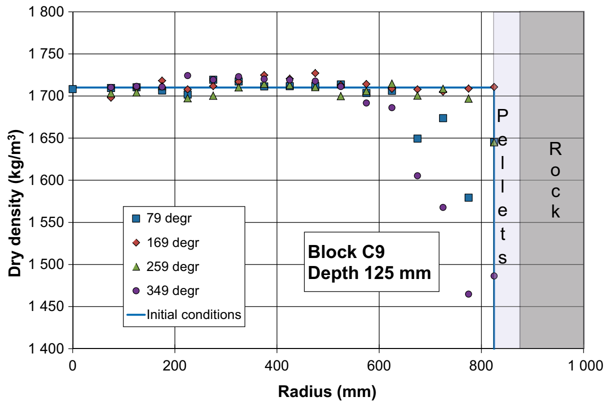

Block C9
Depth 125 mm
79 degr
169 degr
259 degr
349 degr
Initial conditions
Pellets
Rock
Dry density (kg/m³)
Radius (mm)

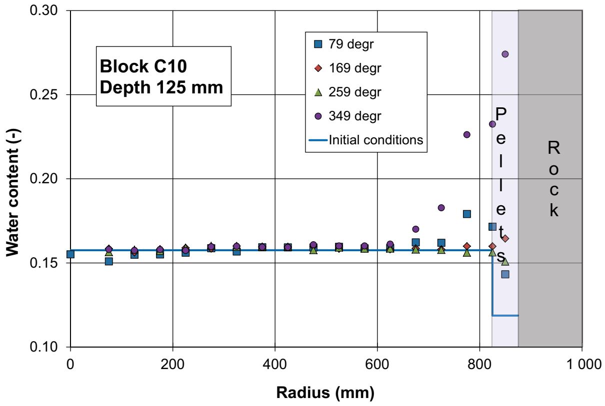

Block C10
Depth 125 mm
79 degr
169 degr
259 degr
349 degr
Initial conditions
Pellets
Rock
Water content (-)
Radius (mm)

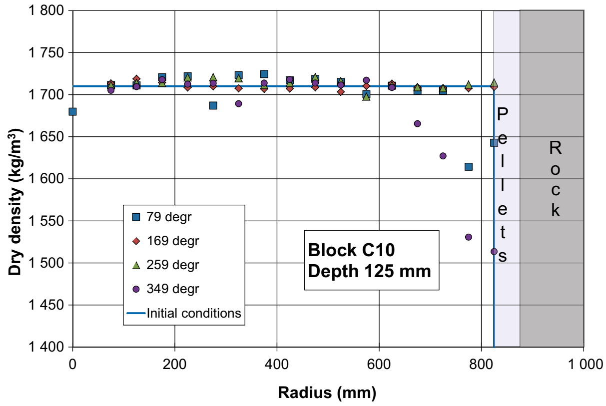

Block C10
Depth 125 mm
79 degr
169 degr
259 degr
349 degr
Initial conditions
Pellets
Rock
Dry density (kg/m³)
Radius (mm)

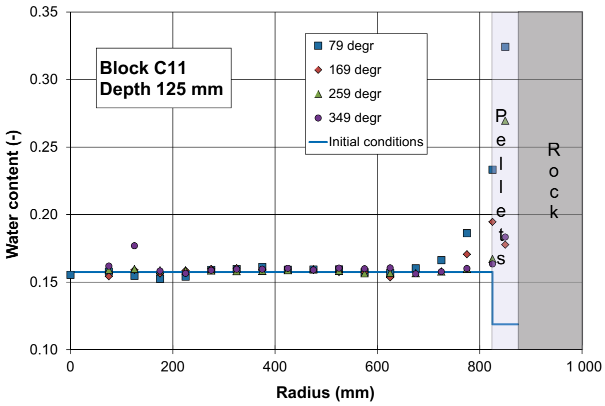

Block C11
Depth 125 mm
79 degr
169 degr
259 degr
349 degr
Initial conditions
Pellets
Rock
Water content (-)
Radius (mm)

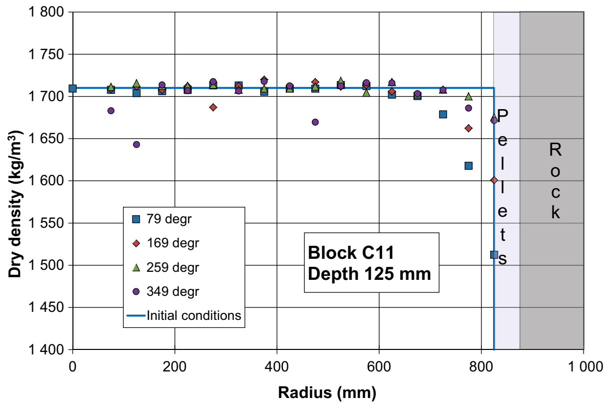

Block C11
Depth 125 mm
79 degr
169 degr
259 degr
349 degr
Initial conditions
Pellets
Rock
Dry density (kg/m³)
Radius (mm)

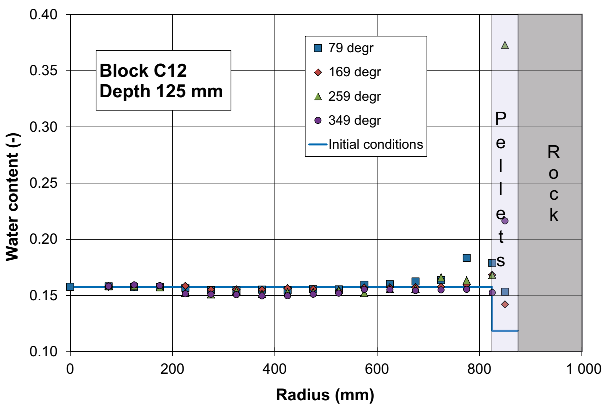

Block C12
Depth 125 mm
79 degr
169 degr
259 degr
349 degr
Initial conditions
Pellets
Rock
Water content (-)
Radius (mm)

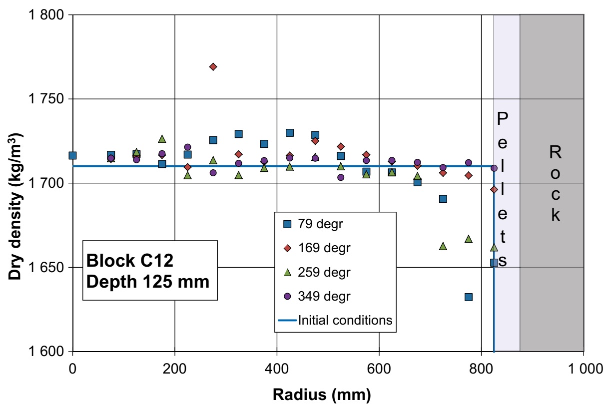

Block C12
Depth 125 mm
79 degr
169 degr
259 degr
349 degr
Initial conditions
Pellets
Rock
Dry density (kg/m³)
Radius (mm)

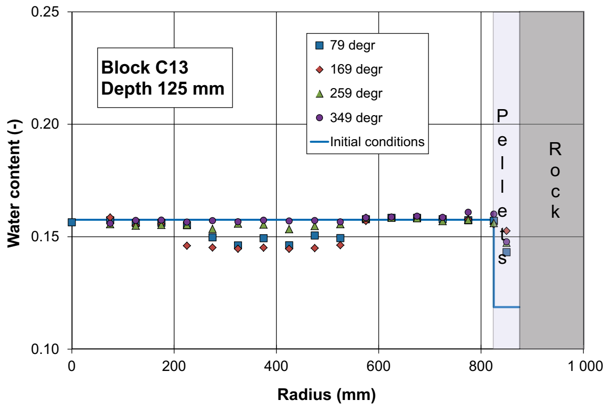
Block C13
Depth 125 mm
79 degr
169 degr
259 degr
349 degr
Initial conditions
Pellets
Rock
Water content (-)
Radius (mm)

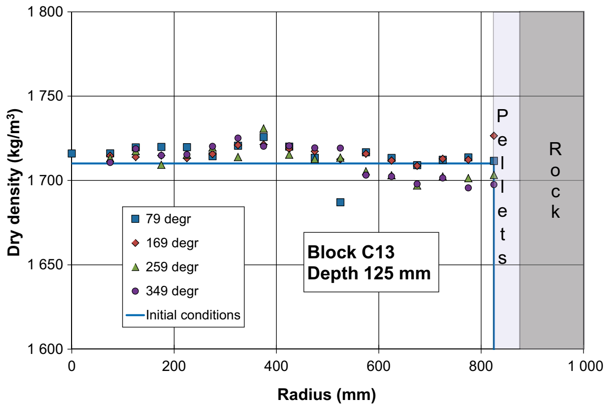
Block C13
Depth 125 mm
79 degr
169 degr
259 degr
349 degr
Initial conditions
Pellets
Rock
Dry density (kg/m³)
Radius (mm)

Arkitektkopia AB, Bromma, 2020

SKB is responsible for managing spent nuclear fuel and radioactive waste produced by the Swedish nuclear power plants such that man and the environment are protected in the near and distant future.

skb.se